University of Windsor
Scholarship at UWindsor

Electronic Theses and Dissertations | Theses, Dissertations, and Major Papers

2014

Regulation of chromosome segregation in Drosophila meiosis

Zhi Hao Guo
University of Windsor

Follow this and additional works at: https://scholar.uwindsor.ca/etd

Part of the Cell Biology Commons, Genetics Commons, and the Molecular Biology Commons

Recommended Citation

Guo, Zhi Hao, "Regulation of chromosome segregation in Drosophila meiosis" (2014). *Electronic Theses and Dissertations*. 5716.
https://scholar.uwindsor.ca/etd/5716

This online database contains the full-text of PhD dissertations and Masters' theses of University of Windsor students from 1954 forward. These documents are made available for personal study and research purposes only, in accordance with the Canadian Copyright Act and the Creative Commons license—CC BY-NC-ND (Attribution, Non-Commercial, No Derivative Works). Under this license, works must always be attributed to the copyright holder (original author), cannot be used for any commercial purposes, and may not be altered. Any other use would require the permission of the copyright holder. Students may inquire about withdrawing their dissertation and/or thesis from this database. For additional inquiries, please contact the repository administrator via email (scholarship@uwindsor.ca) or by telephone at 519-253-3000ext. 3208.

Regulation of chromosome segregation in *Drosophila* meiosis

By

Zhi Hao Guo

A Thesis
Submitted to the Faculty of Graduate Studies
through the Department of Biological Sciences
in Partial Fulfillment of the Requirements for
the Degree of Master of Science
at the University of Windsor

Windsor, Ontario, Canada

2015

© 2015 Zhi Hao Guo

Regulation of chromosome segregation in *Drosophila* meiosis

by

Zhi Hao Guo

APPROVED BY:

_____

S. Ananvoranich
Department of Chemistry and Biochemistry

_____

A. H. Warner
Department of Biological Sciences

_____

A. Swan, Advisor
Department of Biological Sciences

January 12, 2015

DECLARATION OF PREVIOUS PUBLICATION

This thesis includes 1 original papers that have been previously published/submitted for publication in peer reviewed journals, as follows:

Thesis Chapter	Publication title/full citation	Publication status
Chapter 3	*Distinct Roles for Securin, Separase and the cohesin complex in female meiosis, polar body formation and syncytial mitotic divisions of Drosophila*	*submitted*

I certify that I have obtained a written permission from the copyright owner(s) to include the above published material(s) in my thesis. I certify that the above material describes work completed during my registration as graduate student at the University of Windsor.

I declare that, to the best of my knowledge, my thesis does not infringe upon anyone's copyright nor violate any proprietary rights and that any ideas, techniques, quotations, or any other material from the work of other people included in my thesis, published or otherwise, are fully acknowledged in accordance with the standard referencing practices. Furthermore, to the extent that I have included copyrighted material that surpasses the bounds of fair dealing within the meaning of the Canada Copyright Act, I certify that I have obtained a written permission from the copyright owner(s) to include such material(s) in my thesis.

I declare that this is a true copy of my thesis, including any final revisions, as approved by my thesis committee and the Graduate Studies office, and that this thesis has not been submitted for a higher degree to any other University or Institution.

ABSTRACT

Sister-chromatid cohesion is maintained by Cohesin complex. Separase releases the cohesion through the cleavage of the kleisin subunit of Cohesin complex. Separase is regulated by its inhibitor, Securin/Pim. These processes are well studied in mitosis but little is known for meiosis. I found that Separase is required for the proper separation of homologous chromosomes and sister chromatids in *Drosophila* meiosis. Its function is inhibited by Securin/Pim during the process. I showed that the common kleisin subunit, Rad21, is not likely to be the meiotic target of Separase and that Rad21 and another common Cohesin component, SMC3/CAP, does not contribute to sister-chromatid cohesion in meiosis. Therefore *Drosophila* meiosis may use novel protein(s) to mediate cohesion. I also found that Rad21 contributes to the sister-chromatid cohesion in the polar body and Separase is responsible for the release of this cohesion at the arm region under the control of Securin/Pim.

ACKNOWLEDGEMENTS

First, I would like to give special thank to Dr. Andrew Swan who donated a large amount of time to help me with problem solving, experiment designing, written material proofreading and countless other things. In addition to these, Dr. Swan also helped me with the generation of the transgenic flies with the double knockdown of *sse* and *vtd* as well as the following embryo collection and *in vitro* egg activation. I would not make this far without his help. Second, I would like to give thank to the former PhD student in our lab, Osamah Batiha, who introduced me to a lot background information and taught me various techniques in conducting experiments. I would also like to thank all of the lab members, which also includes Nila Das, Mohammad Bourouh, and Biju Vasavan, for providing helpful discussions and suggestions as well as answering my questions. I appreciate the help from Mohammad Bourouh in generating centromeric FISH probes. Thanks to members in Porter Lab who introduced me to standard qRT-PCR procedures and methods in analyzing qRT-PCR results. Thanks to the Crosby Lab for lending out buffers and providing help.

TABLE OF CONTENTS

DECLARATION OF PREVIOUS PUBLICATION AND ORIGINALITY III

ABSTRACT V

ACKNOWLEDGEMENTS VI

LIST OF TABLES XI

LIST OF FIGURES XII

LIST OF ABBREVIATIONS/SYMBOLS XV

Chapter 1. Introduction 1

1.1 Regulation of DNA segregation 1

1.2 Drosophila as a model organism 11

1.3 Meiosis in female Drosophila 16

1.4 Questions to be solved 21

Chapter 2. Methods and Materials 22

2.1 Generation of RNAi fly lines 22

2.2 Fly lines used in research 25

2.3 Oocyte collection and fixation 27

2.3.1 Sonication 27

2.4 Embryo collection and fixation 29

2.5 Staining of oocytes and embryos 29

2.5.1 Fluorescent in situ hybridization (FISH) 30

2.5.2 Spindle and DNA staining 30

2.5.3 Mounting slides 31

2.6 Genomic DNA extraction 31

2.7 Construction of FISH probes 32

2.7.1 Centromeric FISH probe *32*
2.7.2 Arm FISH probe *33*
2.7.3 Terminal transferase labeling *37*
2.8 Confocal microscopy *37*
2.9 mRNA extraction and reverse transcription *37*
2.10 Quantitative reverse-transcriptase polymerase chain reaction (qRT-PCR) *39*
2.11 Western blotting *42*

Chapter 3. Results **44**
3.1 Meiotic stages of yw control fly line *44*
3.2 Knockdown of CAP and vtd in ovary *51*
3.2.1 vtd and CAP were knocked down efficiently *51*
3.2.2 CAP and Rad21 are required for proper metaphase I arrest *53*
3.2.3 CAP and Rad21 are not required for the proper completion of meiosis *59*
3.2.4 CAP and Rad21 are essential for centromeric sister-chromatid cohesion in the polar body *61*
3.2.5 Knockdown of CAP or vtd results in abnormal embryonic mitotic cycles *63*
3.3 Knockdown of sse in the ovary *65*
3.3.1 sse was knocked down efficiently *65*
3.3.2 Knockdown of sse does not cause obvious abnormality in metaphase I arrest *67*
3.3.3 Separase is required for proper separation of homologous chromosomes and sister chromatids during meiosis *69*
3.3.4 Knockdown of sse generates abnormal polar bodies with four chromosomes. *72*
3.3.5 Knockdown of sse results in early mitotic arrest in embryos *73*
3.3.6 Knockdown of sse is specific *75*
3.4 Double knockdown of sse and vtd *76*
3.4.1 Rad21 is not the target of Separase in Drosophila meiosis *76*
3.4.2 Separase regulates sister-chromatid cohesion through cleavage of Rad21 in the polar body *78*
3.4.3 Knockdown of Rad21cannot rescue the early mitotic arrest generated by sse knockdown *79*
3.5 Knockdown of pim in the ovary *81*
3.5.1 pim was knocked down efficiently *81*

3.5.2 Pim is not required for metaphase I arrest *81*

3.5.3 Pim is not required for the proper completion of meiosis *82*

3.5.4 Pim is required for sister-chromatid cohesion in the polar body *84*

3.5.5 Pim is required for the proper progression of synchronized mitosis in early embryo development *85*

3.5.6 Unhatchable pim$^{RNAi5'}$ embryos can not be rescued by the expression of GFP-pim^{wt} *85*

3.6 Non-degradable Pim *87*

3.6.1 Degradation of Pim is required for proper meiosis *88*

3.6.2 Degradation of Pim is required for the release of sister-chromatid cohesion in the polar body *91*

3.6.3 Degradation of Pim is required for syncytial mitosis *93*

3.7 Knockdown of cycB in ovary *95*

3.7.1 cycB was knocked down efficiently *95*

3.7.2 CycB is required to maitain proper metaphse I arrest *98*

3.7.3 Knockdown of cycB is specific *99*

Chapter 4. Discussion 100

4.1 Regulation of homologue separation and segregation during anaphase I *100*

4.1.1 Depletion of CAP/Rad21 or CycB generate similar defects during metaphase I arrest but the underlying molecular mechanisms are likely to be different *100*

4.1.2 CycB has additional cellular functions other than maintaining cohesion between homologues during metaphase I *105*

4.1.3 CycB is not the only candidate for the regulation of metaphase I to anaphase I transition *106*

4.2 Separase pathway may not be the only mechanism involved in releasing sister-chromatid cohesion druing meiosis *107*

4.3 The separase target that is responsible for meiotic sister-chromatid cohesion in Drosophila still remains unknown *108*

4.4 Pim may not be the only inhibitor of Separase in meiosis *109*

4.5 Polar body sister chromatid separation depends on Rad21 cleavage by Separase *110*

4.6 Separase may have additional cellular functions other than the release of sister chromatids in syncytial mitosis *111*

4.7 The loss of arm cohesion did not occur until metaphase in embryonic mitotic cycles *112*

4.8 Number of crossovers may affect the separation of sister chromatid arms after the resolution of chiasmata during meiosis *113*

4.9 Conclusion..... *117*

REFERENCES..... **118**

APPENDIX A: COPYRIGHT PERMISSION..... **126**

VITA AUCTORIS **127**

LIST OF TABLES

Table 1. Oligo DNA strands containing RNAi sequences. 24

Table 2. *Drosophila* lines used. 26

Table 3. Reagents and procedures used in the first and second round of DOP-PCR. 35

Table 4. PCR programs for the first and second round of DOP-PCR. 36

Table 5. Example plate loading pattern for qRT-PCR. 41

Table 6. qRT-PCR program. 41

Table 7. qRT-PCR primers used in this research. 41

LIST OF FIGURES

Fig 1. Mechanisms underlying Cohesin complex disassembly during mitosis and meiosis. 3

Fig 2. Separase upstream regulatory mechanisms. 6

Fig 3. *Drosophila* female oogenesis and subsequent early embryo development. 15

Fig 4. Brief introduction of various stages in female meiosis and the formation of polar body.....17

Fig 5. Confocal images of various wild type developmental stages from meiosis to mitosis. 46

Fig 6. Number of arm FISH signals in polar body and mitotic stage of different genotypes. 49

Fig 7. Quantitatively analysis of knockdown efficiency of vtd^{RNAi} and $CAP^{RNAi518}$ using Western and qRT-PCR respectively. 52

Fig 8. Quantitative analysis of premature DNA separation in stage 14 oocytes collected from *yw*, *mat-GAL4;* $CAP^{RNAi518}$, *mat-GAL4;* vtd^{RNAi} and *mat-GAL4;* $CAP^{RNAi518}$-vtd^{RNAi} flies.....54

Fig 9. Confocal images of normal and abnormal metaphase I in stage 14 oocytes collected from *yw*, *mat-GAL4;* $CAP^{RNAi518}$ and *mat-GAL4;* vtd^{RNAi} flies.....55

Fig 10. Confocal images of normal and abnormal metaphase I in stage 14 oocytes collected from *yw*, *mat-GAL4;* $CAP^{RNAi518}$-vtd^{RNAi}, *nanos-GAL4;* vtd^{RNAi} and *nanos-GAL4;* $CAP^{RNAi518}$ flies.....57

Fig 11. Confocal images of anaphase II, polar body and mitosis in embryos collected from *mat-GAL4; CAP*^{RNAi518} and *mat-GAL4; vtd*^{RNAi} flies. 60

Fig 12. Percentage distribution of the polar bodies showing various numbers of centromeric FISH signals in 0-1 hr embryos collected from *yw*, *mat-GAL4; CAP*^{RNAi518} and *mat-GAL4; vtd*^{RNAi} flies. 62

Fig 13. Confocal images of embryos collected from *yw*, *mat-GAL4; CAP*^{RNAi518} and *mat-GAL4; vtd*^{RNAi} flies. 64

Fig 14. qRT-PCR analysis of *sse* and *pim* mRNA level in stage 14 oocytes collected from *mat-GAL4; sse*^{RNAi147} and *mat-GAL4; pim*$^{RNAi5'}$ fly lines respectively. 66

Fig 15. Quantitative analysis and confocal images of phenotypes in stage 14 oocytes collected from *yw*, *mat-GAL4; sse*^{RNAi147} and *mat-GAL4; pim*$^{RNAi5'}$ flies. 68

Fig 16. Confocal images of meiosis progression and/or polar body formation in embryos collected from *mat-GAL4; sse*^{RNAi147} and *mat-GAL4; sse*^{RNAi213} flies. 70

Fig 17. Confocal images of embryos collected from *yw*, *mat-GAL4; sse*^{RNAi147} and *mat-GAL4; pim*$^{RNAi5'}$ flies. 74

Fig 18. Confocal images of meiosis progression and polar body formation in embryos collected from *mat-GAL4; sse*^{RNAi147}*-vtd*^{RNAi} flies. 77

Fig 19. Confocal images of meiosis progression and polar body formation in embryos collected from *mat-GAL4; pim*$^{RNAi5'}$ flies. 83

Fig 20. Confocal images of meiosis progression in embryos collected from *mat-GAL4; pim*$^{\Delta dk}$, *mat-GAL4; GFP-pim*$^{\Delta dk}$ and *mat-GAL4; pim*$^{RNAi5'}$*-GFP-pim*$^{\Delta dk}$ flies. 89

Fig 21. Confocal images of polar body and mitosis in embryos collected from *mat-GAL4; pim*$^{\Delta dk}$, *mat-GAL4; GFP-pim*$^{\Delta dk}$ and *mat-GAL4; pim*$^{RNAi5'}$*-GFP-pim*$^{\Delta dk}$ flies. 92

Fig 22. Western analysis and confocal images of stage 14 oocytes collected from *yw*, *mat-GAL4; cycB*^{RNAi1896} and/or *mat-GAL4; cycB*^{RNAi1015} fly lines.....97

Fig 23. Possible models for microtubule attachment after the premature separation of homologous chromosomes.....104

Fig 24. Introduction of the segregation of homologous chromosome with either one or two crossovers.....114

LIST OF ABBREVIATIONS/SYMBOLS

Ab	Antibody
Amp	Ampicillin
APC/C	Anaphase Promoting complex/Cyclosome
BDSC	Bloomington *Drosophila* Stock Center
Cdc20	Cell-division Cycle Protein 20
Cdk1	Cyclin Dependent Kinase 1
cDNA	Complementary DNA
CE	Central element
CK1	Casein Kinase 1
Cort	Cortex
CycA	Cyclin A
CycB	Cyclin B
ddH2O	Double-distilled H2O
DDK	Dbf4-dependent Cdc7 Kinase
DSB	Double strand break
FISH	Fluorescent in situ hybridization
Fzy	Fizzy
GFP	Green fluorescent protein
HRP	Horseradish peroxidase
IB	Isolation buffer

LE	Lateral element
NanoDrop	NanoDrop Spectrophotometer ND-1000
NEBD	Nuclear envelop breakdown
Pim	Pimples
Plk1	Polo-like Kinase 1
PP2A	Protein Phosphatase 2A
qRT-PCR	Quantitative reverse-transcriptase polymerase chain reaction
RNAi	Ribonucleic acid interference
RT	Room temperature
SA	Stromal Antigen
SB	Sample Buffer
SC	Synaptonemal complex
Scc	Sister-chromatid cohesion protein
SMC	Structural Maintenance of Chromosomes protein
TdT	Terminal Deoxynucleotidyl Transferase
TEV	Tobacco etch virus protease
TF	Transverse filament
Thr	Three Rows protein
TRiP	Transgenic RNAi Project
UAS	Upstream activation sequence
UTR	Un-translated region
VM	Vitelline membrane
Wapl	Wings Apart-like Protein

Chapter 1. Introduction

1.1 Regulation of DNA segregation

Unlike mitosis in which segregation of replicated DNA happens only once and generates two identical diploid daughter cells, eukaryotes generating progeny by sexual reproduction undergo a specific cell division, meiosis, during which the genomic DNA replicates once and then undergoes two successive rounds of DNA segregation to generate four haploid nuclei (Petronczki, et al. 2003). Each of the haploid nuclei contains a single set of chromosomes that are slightly different from each other because of homologous recombination (Petronczki, et al. 2003). The separation of genomic information during both mitosis and meiosis needs to be regulated precisely or otherwise it will generate various problems such as aneuploidy, cancer, birth defects or even death (Jallepalli and Lengauer, 2001). It is hoped that with a better understanding of the molecular mechanism underlying DNA separation and its regulation, we will be able to reduce the likeliness that such errors will occur.

It is known that following DNA replication sister chromatids are held together throughout G2 until anaphase by a protein complex, Cohesin (Nasmyth and Haering, 2009). This complex is composed by four subunits: Structural Maintenance of Chromosomes 1 (SMC1), SMC3, Sister-chromatid cohesion 3 (Scc3) and a kleisin subunit which is Scc1/Rad21 in mitosis but Rec8 in meiosis (Michaelis, et al. 1997; Guacci, et al. 1997; Molnar, et al. 1995). Among the four subunits, SMC1 and SMC3 are coiled coil proteins and they form a ring-like backbone structure that is locked by a kleisin subunit along with the binding of ATP (Anderson, et al. 2002; Haering, et al. 2002; Nasmyth and Haering, 2009). The fourth subunit, Scc3, does not contribute to the ring

structure of Cohesin complex but it physically attaches to the kleisin subunit (Fig 1; Haering, et al. 2002). Although the structure of Cohesin complex has been solved as described, how it associates with sister chromatids in order to bind them together is still under debate (Nasmyth and Haering, 2009). The Cohesin complex stably loads onto chromosomes during DNA replication in S phase (Gerlich, et al. 2006). This interaction between Cohesin and DNA contributes to the cohesion between sister chromatids (Haering, et al. 2004). The cohesive force, especially at the centromeric regions, is necessary to ensure the biorientation in metaphase and the proper segregation of one replicated chromatid into each daughter cell (Tessie, et al. 2009).

In yeast mitosis, the cohesion between sister chromatids is maintained until the metaphase to anaphase transition, when Cohesin complex is cleaved by a cysteine protease named Separase on both arm and the centromeric regions of chromosomes (Uhlmann, et al. 2000; Gutierrez-Caballero, et al. 2012). In the mitosis of higher eukaryotes, this process is completed through two independent pathways: the prophase pathway and the anaphase pathway (Waizenegger, et al. 2000). In the prophase pathway which occurs in prophase and prometaphase, a large amount but not all of the Cohesin complexes on chromosome arms are removed (Waizenegger, et al. 2000; Nishiyama, et al. 2013). This non-cleavage release of Cohesin is triggered by phosphorylation of either Stromal Antigen (SA) or Sororin by Polo-like Kinase 1 (Plk1) and Aurora B respectively (Fig 1A and 1B; Hauf, et al. 2005; Nishiyama, et al. 2013). SA is an ortholog of Scc3 in higher eukaryotes (Losada, A. et al. 2000). Sororin is an inhibitor for the Cohesin release factor Wings Apart-like Protein (Wapl) and gets inhibited by phosphorylation (Fig 1B; Nishivama, et al. 2010; Gandhi, et al. 2006). The remaining Cohesin complexes, mainly at the centromeric regions, are then cleaved by Separase at Scc1 subunit within 1 minute

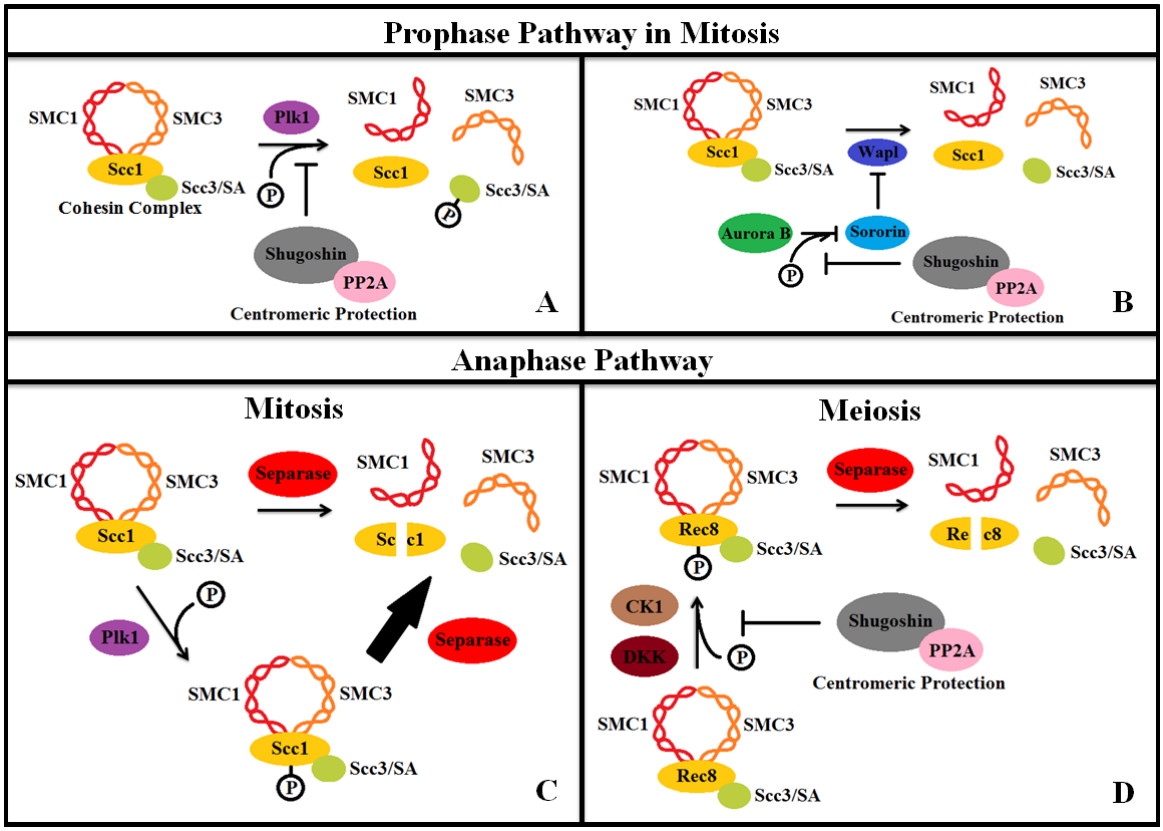

Fig 1. Mechanisms underlying Cohesin complex disassembly during mitosis and meiosis. (A and B) The two mechanisms in prophase pathway to release Cohesin complex from chromosome arms in mitosis, during which Shugoshin and PP2A prevent the phosphorylation of SA subunit (A) and Sororin (B) at centromeric region. (C and D) Separase cleaves Cohesin at the kleisin subunit which is Scc1 in mitosis (C) but Rec8 in meiosis (D): (C) Cleavage of Scc1 is facilitated by its phosphorylation in mitosis. (D) Phosphorylation of Rec8 is a requirement for Separase cleavage during meiosis and Shugoshin together with PP2A protect centromeric Cohesin from Separase cleavage by antagonizing the phosphorylation process during the first round of meiosis. (Thicker arrow means this molecular pathway is preferred).

of anaphase onset, via the anaphase pathway (Waizenegger, et al. 2000; Yaakov, et al. 2012). In both yeast and human cells, cleavage of the Scc1 subunit of Cohesin by Separase is facilitated by Plk1 dependent phosphorylation on Scc1 (Fig 1C; Hornig and Uhlmann, 2004; Hauf, et al. 2005). Only after the removal of Cohesin on both arms and the centromeric regions of chromosomes are sister chromatids able to separate from each other and segregate into two daughter cells.

Compared to mitosis, meiosis is more intricate not only because it has two successive rounds of DNA segregation but homologous chromosome recombination after DNA replication further increases the complexity of the process (Nasmyth, 2001). During early stages of prophase I, homologous chromosomes are loosely paired with each other by a mechanism that is still not fully understood (McKee, 2004; Zhang, et al. 2014). This weak connection is then strengthened by the formation of synaptonemal complexes (SC) between homologous chromosomes in zygotene and patchtene (Schmekel and Daneholt, 1995). The SC is composed of three categories of subunits: lateral elements (LEs), transverse filaments (TFs) and central elements (CEs) (Heyting, 1996). During synapsis, LEs arranged along the side of each homologous chromosome are joined together to a single line of CEs in the middle of the two homologues through TFs as bridges between LEs and CEs (Fraune, et al. 2012). Synapsis is important for DNA double strand break (DSB) initiated crossover between sister chromatids from each homologue pair and it is the crossover that leads to DNA recombination and finally the formation of chiasmata (Jang, et al. 2003; Mehrotra and McKim, 2006). After this point until metaphase I, homologous chromosomes are held together by a combination effect of both chiasmata formation and sister-chromatid cohesion (Buonomo, et al. 2000). Since SCs are dissembled at the end of prophase, they do not contribute to the connections between

homologous chromosomes in metaphase (Schmekel and Daneholt, 1995). Later during the metaphase I to anaphase I transition, the Rec8 subunit of Cohesin complexes on the chromosome arms is cleaved by Separase after being phosphorylated by Casein Kinase 1 (CK1) and Dbf4-dependent Cdc7 Kinase (DDK) during prophase (Fig 1D; Katis, et al. 2010). This cleavage leads to the disassembly of Cohesin complexes and the separation of homologous chromosomes but not sister chromatids in the first round of meiosis (Kudo, et al. 2006). Then in the next round, from metaphase II to anaphase II, centromeric Cohesin complexes are phosphorylated and cleaved to release sister chromatids that are separated into haploid nuclei at the end of meiosis (Sakuno and Watanabe, 2009).

During the time that Cohesin complexes are removed from chromosome arms through either prophase pathway in mitosis or cleavage dependent pathway in meiosis, the centromeric Cohesin complexes are protected by a protein called Shugoshin (Kitajima, et al. 2004). Shugoshin works together with Protein Phosphatase 2A (PP2A) to protect SA, Sororin or Rec8 at the centromeric region from phosphorylation, thereby preventing Cohesin release during either mitosis or meiosis (Fig 1A, 1B and 1D; Kitajima, et al. 2006; Nishiyama, et al. 2013; Gutierrez-Caballero, et al. 2012). This protection is relieved by a mechanism that is not fully understood in order to expose the remaining Cohesin complexes to Separase, so that sister chromatids are able to completely separate from each other.

As a critical element in regulating DNA separation in both mitosis and meiosis, Separase needs to be precisely regulated. It is now known that Separase is inhibited before activation by the binding of either Securin or Cyclin B (CycB) -Cyclin Dependent Kinase 1 (Cdk1) complex in higher eukaryotes (Fig 2; Ciosk, et al. 1998; Gorr, et al. 2005). Beside these two inhibitors, Separase function is also able to be effected by self-

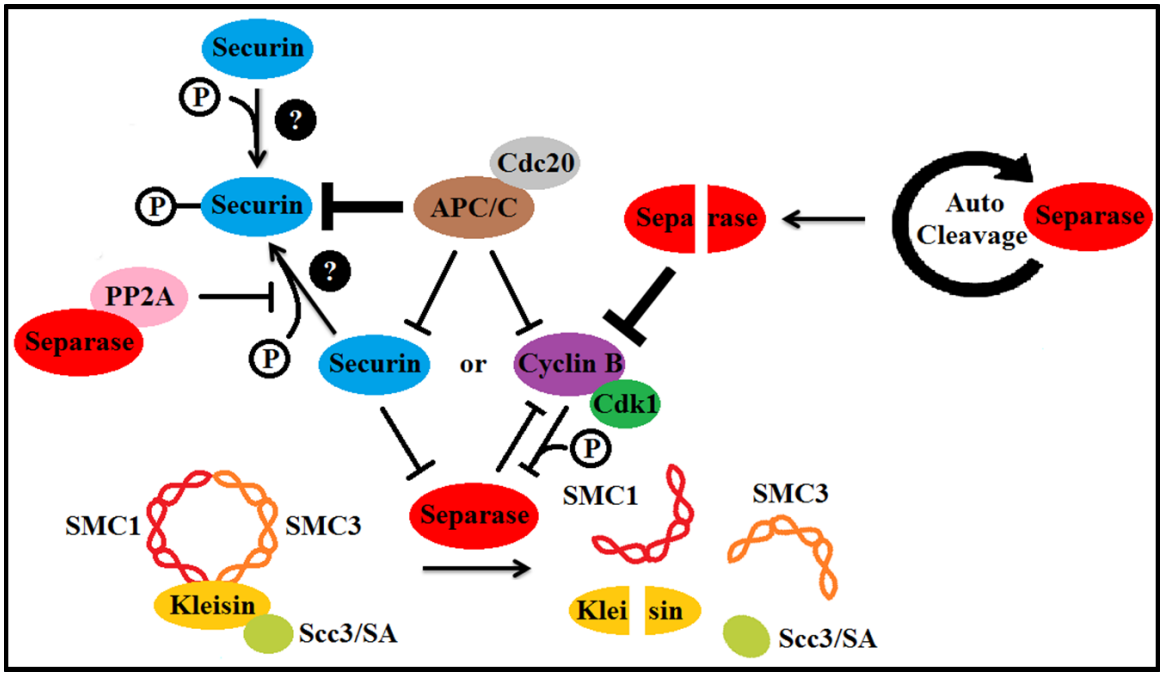

Fig 2. Separase upstream regulatory mechanisms.
Separase can be inhibited through direct binding of either Securin or CycB-Cdk1 complex, both of which are substrates of APC/C. Cytoplasmic Securin is phosphorylated by yet unknown kinase and the phosphorylated Securin is preferred by APC/C than the non-phosphorylated Separase-binding Securin because of the presence of associated PP2A. CycB-Cdk1complex inhibits Separase through a two-step phosphorylation-and-binding mechanism, during which the complex itself also gets inhibited by Separase. In addition to CycB-Cdk1, the auto cleavage of Separase also results in it being inactive on the kleisin subunit of Cohesin complex. CycB-Cdk1 is preferentially inhibited by the auto-cleaved form of Separase than the intact one. (The thicker inhibition marker indicates a preferred inhibitory pathways comparing between same inhibitors and substrates).

cleavage after being activated (Waizenegger, et al. 2002). While the molecular function of Separase auto-cleavage ability is still under investigation, evidence showed it is a mechanism not only to limit Separase activity after its activation (Herzig, et al. 2002) but also to inhibit CycB-Cdk1complex during the metaphase to anaphase transition (discussed in detail later) (Shindo, et al. 2012).

Securin regulates Separase activity through direct binding to Separase starting in G2 phase or possibly earlier (Hornig, et al. 2002). This physical interaction is commonly known to have an inhibitory effect on Separase (Zou, et al. 1999). During the metaphase to anaphase transition, an E3 ubiquitin ligase named Anaphase Promoting complex or Cyclosome (APC/C) together with its co-factor Fizzy (Fzy)/Cell-division Cycle Protein 20 (Cdc20) send Securin for degradation through ubiquitination (CohenFix, et al. 1996) and Separase will be activated after the degradation of Securin. Recently, it had been demonstrated that phosphorylation of Securin accelerates APC/C-Cdc20 mediated ubiquitinlation (Hellmuth, et al. 2014). This finding opens a door to understand the reason why PP2A binds to Separase together with Securin to form a trimeric protein complex since the G1/S phase (Holland, et al. 2007). Later research answered this question by discovering that Separase-associated PP2A dephosphorylates the Securin bound together with them to prevent early ubiquitination and hence to prevent the premature activation of Separase (Fig 2; Hellmuth, et al. 2014). In addition, under this mechanism, all the free Securin that is not associated with Separase and PP2A gets phosphorylated and ubiquitinated quicker than the PP2A protected Securins (Hellmuth, et al. 2014). This mechanism guarantees that Separase will not be re-inhibited by free Securin in the cytoplasm after activation (Hellmuth, et al. 2014).

In addition to Securin, CycB-Cdk1 complex also has the ability to inhibit Separase in a two-step mechanism, in which the complex phosphorylates Separase first and then binds to it through the CycB subunit for inhibition (Stemmann, et al. 2001; Gorr, et al. 2005). It has been demonstrated that Separase mutually exclusively interacts with either Securin or CycB-Cdk1complex for inhibition (Gorr, et al. 2005). Consistent with this finding, PP2A and CycB-Cdk1 are also found to mutually exclusively bind to Separase (Holland, et al. 2007). These discoveries demonstrated that the two inhibitors of Separase work independently. As in Securin inhibitory pathway, CycB is also ubiquitinated by APC/C for degradation at the same time with Securin during the metaphase to anaphase transition (Hagting, et al. 2002). This mechanism guarantees Separase activation on time.

Surprisingly, CycB-Cdk1 not only inhibits Separase but its own activity also gets inhibited by binding to Separase (Gorr, et al. 2005). This function of Separase serves as a mechanism to inhibit the activity of CycB-Cdk1 in addition to APC/C's ubiquitination. It was found that preventing CycB-Cdk1from binding to Separase that is still able to be inhibited by Securin causes prolonged mitosis (Holland and Taylor, 2006). This phenotype may be caused by the loss of inhibitory effect on the activity of either Separase or CycB-Cdk1 or both. Later experiments clarified the problem by showing a similar prolonged mitosis phenotype with failure in chromosome segregation after anaphase onset in the cells with hyperactive Cdk1 (Oliveira, et al. 2010). More specifically, in this research, the inhibition of APC/C's activity led to mitotic arrest at metaphase since both inhibitors of Separase were no longer degraded. In this situation, in order to trigger the onset of anaphase, the kleisin subunit of Cohesin complexes was replaced by a mutated version that can be cleaved by tobacco etch virus protease (TEV). Under such conditions, the expression of TEV induced the separation of sister chromatids but the segregation of

separated sister chromatids toward the opposite poles of spindle did not happen properly. The abnormal sister chromatid segregation phenotype was rescued by the inhibition of Cdk1 that was hyperactive as a consequence of APC/C's inhibition. These results indicate that both destruction of Cohesin complex and inactivation of Cdk1 are required for the proper completion of anaphase during mitosis (Oliveira, et al. 2010). An important question is, what Cyclin serves as the co-factor of Cdk1 during the metaphase to anaphase transition and how does the inactivation of Cdk1 lead to proper sister chromatid segregation? Earlier research demonstrated that CycB is degraded at the metaphase to anaphase transition (Peters, 2002) and consistently, hyperactive CycB-Cdk1 down regulates microtubule dynamics (Stiffler, et al. 1999). Later it was found that, during anaphase onset, the activity of a subset of CycB-Cdk1 needs to be inhibited by Separase to prevent continuous phosphorylation on chromosomes in order for sister chromatids to segregate to opposite poles (Shindo, et al. 2012). In summary, CycB-Cdk1 first inhibits Separase during metaphase and then gets inhibited by both APC/C and Separase for the proper progression of anaphase. Furthermore, instead of the intact Separase, CycB preferentially binds to the auto-cleaved form of Separase (Shindo, et al. 2012). This mechanism not only ensures the inhibition of CycB-Cdk1 even after the inactivation of Separase but also minimizes the re-inhibition of active Separase by CycB-Cdk1 (Fig 2).

Experiments showed that there may be other mechanism(s) regulating Separase activity, since after the inhibitory effects of both Securin and CycB-Cdk1 on Separase are eliminated, sister chromatids are still be able to remain together until the early stages of mitosis before premature loss of cohesion happens (Holland and Taylor, 2006). Besides their inhibitory function, both Securin and CycB-Cdk1 have positive effects on the function of Separase, though the underlying molecular mechanism is still a mystery.

Originally, defects in sister chromatids separation in mitosis were observed when Securin was mutated in *Drosophila* (Stratmann and Lehner, 1996). This could be a consequence of alteration of Separase function or location in the absence of Securin's binding. Later it was found that in yeast mitosis, Securin helps Separase to accumulate in the nucleus (Hornig, et al. 2002). Similarly, in Hela cancer cells, both Securin and CycB-Cdk1 were found to be important for directing Separase to chromosomes in mitosis (Shindo, et al. 2012).

1.2 Drosophila as a model organism

Drosophila melanogaster is used as a model organism in a wide range of research because it is easy to raise and manipulate both genetically and physically. *Drosophila* cells have only four pairs of chromosomes with a lot of functional important genes identified to be similar with those in human beings (Adams, et al. 2000). Thus, *Drosophila* is used as an important model in research to test the function of genes as well as effects generated by drugs and therapeutic procedures such as RNA interference (RNAi) treatment at the molecular level. These studies are extremely helpful in the process of investigating and understanding of human diseases together with their corresponding potential treatments.

The molecular mechanisms and related regulatory pathways underlying DNA separation have been well studied in *Drosophila* mitosis, where the kleisin subunit of Cohesin complex was found to be a homologue of Scc1 named as *Drosophila* Rad21 (Warren, et al. 2000; Vass, et al. 2003). A SMC3 homologue known as CAP was also found while the homologues of the other two components are still named as SMC1 and SA (Nasmyth and Haering, 2009). Similar to other organisms, this version of Cohesin is able to be cleaved at the Rad21 kleisin subunit by *Drosophila* Separase. *Drosophila* Separase is much smaller than its homologues in mammals including human beings (Jager, et al. 2001). Instead of auto cleavage, *Drosophila* Separase cleaves Three Rows protein (Thr) in addition to Cohesin and this inactivates Separase itself as auto cleavage does (Herzig, et al. 2002). Based on these findings and the fact that Thr always associates with Separase, it is reasonable to come up with the idea that Thr was originally a part of Separase in *Drosophila* and somehow got separated during evolution (Herzig, et al. 2002). Furthermore, Separase in *Drosophila* mitosis is regulated by a protein that is functionally

similar to Securin called Pimples (Pim) (Leismann, et al. 2000). Mutation of either Pim or Thr leads to defects in sister chromatid separation at the centromeric regions during mitosis (Stratmann and Lehner, 1996). Although the phenotypes caused by these mutations are similar, the underlying molecular mechanisms could be different, where Thr is required for the enzymatic activity of Separase (Herzig, et al. 2002) and Pim could also have positive effects on the location of Separase. Despite the uncertainty of Pim's positive roles on Separase, it was found that Pim is able to be recognized by APC/C at two specific series of amino acid sequence known as D-box and KEN-box, both of which are essential for the normal ubiquitination of Pim by APC/C (Leismann and Lehner, 2003). Mutations in either one of these sites led to the generation of stabilized Pim that blocked sister chromatids separation since Separase was no longer activated (Leismann and Lehner, 2003). In addition to Pim, CycB-Cdk1 complex may also have an inhibitory effect on Separase, since hyperactive CycB-Cdk1 activity pushes the onset of anaphase backwards in *Drosophila* embryos (Ji, et al. 2005). The delay of anaphase phenotype may not only be caused by partially inhibition of Separase but also by other potential cellular function(s) of CycB-Cdk1 complex such as down regulating microtubule dynamics (Stiffler, et al. 1999; Oliveira, et al. 2010; Shindo, et al. 2012). Another possible inhibitor of Separase instead of CycB-Cdk1 is Cyclin A (CycA)-Cdk1 complex. Since non-degradable CycA dramatically delayed the separation of sister chromatids during the metaphase to anaphase transition in *Drosophila* mitosis (Sigrist, et al. 1995; Jacobs, et al. 2001). So far, most of the investigations focusing on the regulation of DNA separation and segregation in *Drosophila* are done in embryogenesis where the expression of genes are zygotically controlled while little is known in meiosis.

To investigate DNA distribution and its regulation in meiosis, female *Drosophila* oogenesis and subsequent embryo development processes have been studied under various genetically modified backgrounds. Oogenesis begins with the asymmetric division of a germline stem cell that generates a daughter germline stem cell and a more differentiated cystoblast (Lake and Hawley, 2012). The cystoblast then undergoes four successive rounds of cell divisions giving rise to the 16-cell germline cyst, within which fifteen cells turn into nurse cells while only one becomes an oocyte. These sixteen cells including the oocyte then form an egg chamber that is considered as the first stage (S1) of oogenesis (Lake and Hawley, 2012). The oocyte becomes more mature as it gradually goes through the following stages of oogenesis, during most of which meiosis is arrested at prophase I (Hong, et al. 2003). This long prophase I arrest terminates in S13 oocytes indicated by nuclear envelope breakdown (NEBD) (Pesin and Orr-Weaver, 2007). Meiosis then progresses to metaphase I and is arrested again in stage 14. This metaphase I arrest is maintained until ovulation, during which egg activation happens (Page and Orr-Weaver, 1997a).

After egg activation, one iconic phenotype that can be observed is the hardening of the inner embryonic membrane known as vitelline membrane (VM) (Horner and Wolfner, 2008). External stimulations such as hydrostatic pressure and hypo-osmotic pressure accelerates the VM hardening but the level of VM hardening reduced significantly after stretch-activated ion channels being blocked. These phenomena indicate that egg activation can be triggered *in vitro* by external pressure through inducing the opening of stretch-activated ion channels. Further analysis revealed that embryos activated by either hydrostatic or hypo-osmotic pressure in the low Ca^{2+}containing external environment showed dramatic low level of VM hardening. This implies the

influx of Ca^{2+} through stretch-activated ion channels that open in response to external pressure is essential for egg activation (Horner and Wolfner, 2008). In the process of egg activation, meiosis resumes and then finishes quickly within twenty minutes (Heifetz, et al. 2001). Following completion of meiosis, male and female pronuclei come together to start the synchronized mitotic divisions (Mazumdar and Mazumdar, 2002). The embryo stays as a single multinucleate cell until cycle 14 of mitosis when cellulariztion occurs to form the cellular blastoderm (Fig 3). Zygotic gene products that are expressed at the beginning of cycle 11 of mitosis are involved during cellularization (Mazumdar and Mazumdar, 2002). Before that, the progression of all cellular activities in both meiosis and early mitosis depends only on the maternal proteins.

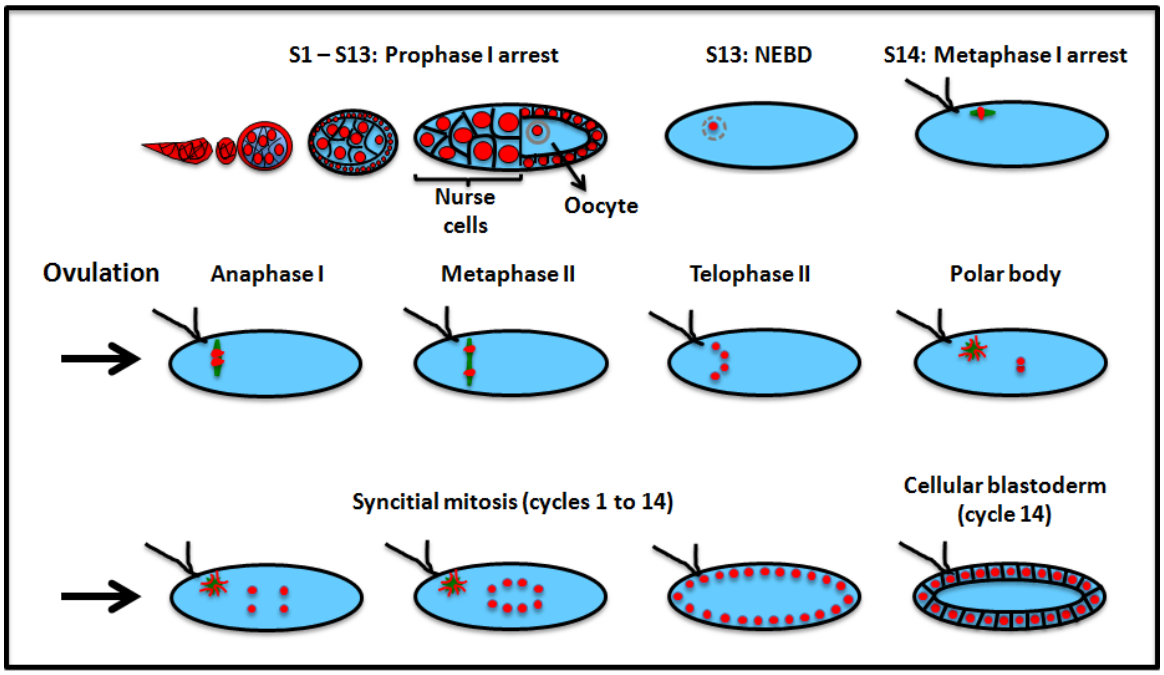

Fig 3. *Drosophila* female oogenesis and subsequent early embryo development. There are 14 oocyte developmental stages in *Drosophila* oogenesis. During the first 13 stages, meiosis is arrested at prophase I. This arrest terminates in S13 oocyte where nuclear envelope breakdown (NEBD) occurs. In stage 14 oocyte, meiosis is arrested again at metaphase I until ovulation. After that, the rest of meiosis from anaphase I to telophase II finishes quickly, within twenty minutes. After meiosis, male and female pronuclei join together to start mitosis. At the same time, the formation of polar body also takes place. Later, cellularization happens to form cellular blastoderm during the 14th cycle of mitosis.

1.3 Meiosis in female Drosophila

Female *Drosophila* meiosis starts with pre-meiotic S phase after the generation of the 16-cell germline cyst (Fig 4 G1 and S phase). During early stages of prophase, the SC assembles between non-sister-chromatid homologous chromosomes to facilitate the formation of chiasmata (Fig 4 prophase I; Lake and Hawley, 2012). During metaphase I arrest, the centromeric regions of homologous chromosomes are pulled apart by the meiotic spindle while the arm regions remain attached because of the combined effects of both sister-chromatid cohesion and chiasmata (Fig 4 metaphase I). After ovulation, meiosis progresses swiftly through anaphase I to telophase II where four haploid nuclei are formed (Fig 4). During the post-meiotic interphase, three of the four haploid cells come together and undergo DNA replication once before forming a polar body (Fig 4 interphase). At the same time the fourth haploid nucleus gets pulled away by the spindle generated by male pronucleus and joins together with it to start mitosis (Foe, et al. 1993). At the same time that male and female pronuclei go into S phase, it is expected that sister chromatids in polar bodies are held together along their length (Fig 4 polar body). As time goes, the cohesion between the arms of sister chromatids is gradually lost while the centromeric regions remains together all the time (Fig 4 polar body) (Foe, et al. 1993).

Even though a lot of studies indicate that the DNA separation mechanism in *Drosophila* mitosis is similar to that in other eukaryotes in large degree, little is known for meiosis. The first question that urgently needs to be addressed is whether the Cohesin complex is required in *Drosophila* meiosis and if so, what exactly is the kleisin subunit associated with the complex? It was shown that the gene coding for the common meiosis kleisin subunit Rec8 is not found in the *Drosophila* genome. Furthermore, the expression of another kleisin protein, C(2)M, was detected during meiosis but it does not contribute

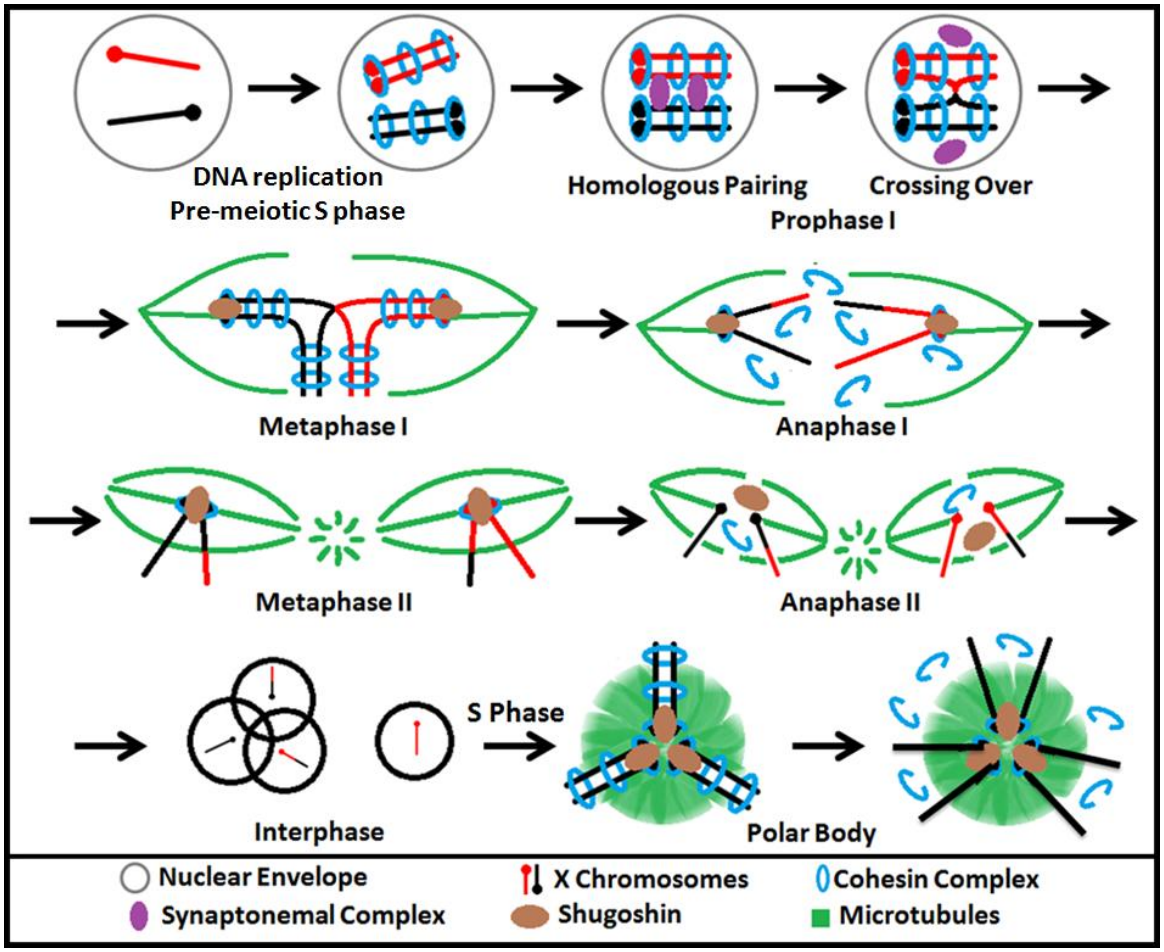

Fig 4. Brief introduction of various stages in female meiosis and the formation of polar body.
Meiosis begins from pre-meiotic S phase where DNA gets replicated and sister chromatids are bound with Cohesin complexes. After that the SC forms between homologous chromosomes assisting the formation of cross over(s), and then gets dissembled in prophase I. During metaphase I homologous chromosomes are held together by both Cohesin complexes and chiasmata. After that, in anaphase I, homologous chromosomes separate from each other because of the loss of arm Cohesin while centromeric Cohesin complexes are protected by Shugoshin. In the next round of meiosis, during the metaphase II to anaphase II transition, sister chromatids separate from each other after losing Shugoshin's protection. In interphase, three of the four haploid meiotic products come together and form a polar body. After one round of DNA replication during interphase, the polar body chromosome arms now have two sister chromatids bound together and then the sister chromatids separate from each other gradually as time increase. (For convenience, this figure only exhibits X chromosomes as an example. DNA should be diffused during interphase, for convenience the four meiotic products were drawn in condensed form in interphase).

to sister-chromatid cohesion during the process (Manheim and McKim, 2003; Heidmann, et al. 2004). In addition, the expression of mitotic Cohesin component Rad21 was detected in meiosis (Heidmann, et al. 2004). This implies the function of Rad21 could be required in both mitosis and meiosis in *Drosophila*. Recently, new evidence showed that Rad21 is only important for SC assembly during *Drosophila* meiosis but not required for the cohesion between sister chromatids during the process (Urban, et al. 2014). Furthermore, it is also not clear whether Separase and its regulatory mechanism(s) are required in *Drosophila* meiosis or not.

However, APC/C is known to be important for degradation of CycA, B and B3 as well as Pim during meiosis with the help of at least two co-factors, Fzy/Cdc20 and Cortex (Cort), in *Drosophila* (Swan and Schupbach, 2005 and 2007; Pesin and Orr-Weaver, 2007). Fzy is originally known as the common co-factor of APC/C in mitosis (Visintin, et al. 1997) and Cort is a female meiosis specific co-factor of APC/C in *Drosophila* (Swan and Schupbach, 2005 and 2007; Pesin and Orr-Weaver, 2007). Cort and Fzy have been demonstrated to share partially redundant roles in the first round of meiosis but their functions at the second round of meiosis appear to be independent (Swan and Schupbach, 2007). After knockdown of *cort*, meiosis was arrested at metaphase II with sister chromatids still remaining together. This observation implies that Cort is essential for the release of cohesion between sister chromatids during the metaphase II to anaphase II transition. Similar but not identical phenotypes were obtained after knockdown of *fzy*, where meiosis was arrested or delayed at anaphase II with separated sister chromatids. This discovery indicates that Fzy functions a little later than Cort after the metaphase to anaphase transition and Fzy is required for the proper segregation of sister chromatids

towards the opposite poles. The molecular mechanism behind these phenotypes is likely related to APC/C's inhibitory role on Pim and CycB (Swan and Schupbach, 2007).

While little is known about Pim and Separase in *Drosophila* meiosis, the distribution and degradation of the other potential Separase inhibitor, CycB, had been investigated. It was found that CycB associates with the meiotic spindle through metaphase I to anaphase II and the localization of CycB on the spindle varies among different meiosis stages, where it accumulates at the mid-zone of both metaphase I and II spindles but transiently appears throughout the entire spindle during anaphase II. Both Cort and Fzy are responsible for the degradation of spindle associated CycB, but they function at different stages of meiosis where Cort degrades the CycB located in the mid-zone of spindle (mid-zone CycB) during metaphase II and Fzy targets the CycB located throughout the entire spindle (spindle CycB) during anaphase II. These findings are consistant with previous ones where Cort functions at the metaphase II to anaphase II transition and Fzy functions later in anaphase II, implying meiotic arrest caused by knockdown of either *cort* or *fzy* is mediated by the persistence of CycB's function, likely through regulating the activity of Cdk1. Consistently with this idea, expression of non-degradable CycB in the germline led to a delay of meiosis in both rounds at either metaphase or anaphase. Considering this together with the function of Cort in the metaphase II to anaphase II transition and the degradation of the mid-zone CycB at metaphase II, it implies that cohesion between sister chromatids at metaphase II is partially disrupted by the degradation of the mid-zone CycB through Cort mediated molecular pathway. Likely the mid-zone CycB stabilizes the cohesion between sister chromatids by inhibiting the activity of Separase. Comparing to metaphase arrest, the generation of multiple small spindles during meiosis was more frequently observed after

the expression of non-degradable CycB. This could be a consequence of chromosome/chromatid mis-segregation. Taken this together with the facts that Fzy is important for the proper segregation of sister chromatids and the degradation of the spindle CycB at anaphase II, it implies that degradation of spindle CycB through Fzy is required for the proper segregation of sister chromatids in meiosis II (Swan and Schupbach, 2007). More studies are required to further understand the function of CycB in meiosis. Specifically, we need to know the loss of CycB phenotype to better understand if it has a role in the release of cohesion between sister chromatids during meiosis.

1.4 Questions to be solved

To test whether the components of Cohesin complex in *Drosophila* meiosis are the same as those in mitosis, we employed RNAi to knock down two of the important Cohesin subunits, Rad21 and CAP. If these Cohesin components are important in *Drosophila* meiosis, premature separation of sister chromatids should be observed during metaphase I arrest after knockdown of either *vtd* or *CAP* (genes encoding for Rad21 and CAP in *Drosophila*, respectively). According to the latest finding that Rad21 is only important for the formation of SC but not Cohesin complex (Urban, et al. 2014), one would expect that during metaphase I arrest homologous chromosomes but not sister chromatids are going to separate from each other after the knockdown of *vtd*.

To study whether Separase and Pim are important in *Drosophila* meiosis, RNAi fly lines expressing hairpin RNA against *sse* and *pim* (genes encoding for Separase and Pim in *Drosophila* respectively) were constructed. If Separase plays an essential role in *Dsosophila* meiosis, we expect that after knockdown of *sse*, the separation of homologous chromosomes will be blocked and meiosis will be arrested at metaphase I. It is hard to predict what is going to happen after knockdown of *pim* since Pim has both inhibitory and positive effect on Separase as described before. This is why the effects of non-degradable Pim on the process of meiosis were also investigated during the research.

To investigate whether CycB-Cdk1 complex is the inhibitor of Separase in *Drosophila* meiosis, *cycB* RNAi was employed. If the function of Separase is required in meiosis and is inhibited by CycB-Cdk1, we expect to see at least partial pre-mature separation of homologous chromosomes during metaphase I arrest after the knockdown of *cycB*. Since without CycB-Cdk1's inhibition, Separase may be pre-maturely activated and cleave the arm Cohesin that leads to the disassembly of chiasmata.

Chapter 2. Methods and Materials

2.1 Generation of RNAi fly lines

The following protocol was modified from the protocol prepared by Transgenic RNAi Project (TRiP) at Harvard Medical School named " Cloning hairpins into Valium20 and Valium22". Oligo DNA sequences containing the gene coding for the expression of RNA for RNAi fly lines were designed by Dr. Andrew Swan and manufactured by Sigma-Aldrich Canada Ltd. (Table 1). As shown in Table 1, the RNAi sequences buried in the designed oligo DNA are highlighted with grey background. $pim^{RNAi5'}$ and $pim^{RNAi3'}$ has the RNAi sequences targeting the 5' and 3' un-translated region (UTR) of *pim* mRNA respectively. $sse^{RNAi147}$ and $sse^{RNAi213}$ target different coding regions of *sse* mRNA. To anneal top and bottom strands together into double stranded DNA, 10 µl of both top and bottom oligo DNA strands (20uM) were mixed together with 80 µl of annealing buffer (10mM Tris-HCl, 0.1M NaCl and 1mM EDTA, pH7.5). Then the 100 µl mixture was heated at 90 ℃ for 5 mins and slowly cooled down to room temperature (R.T.) for annealing. The product should be a double stranded DNA with NheI recognition sequence on the 5' and EcoRI recognition sequence on the 3'. These sequences are designed to facilitate the incorporation of the oligo DNA into the target plasmid named Valium22. At the same time, Valium22 backbone was prepared by incubating the plasmid with fast digest restriction enzymes NheI and EcoRI at 37 ℃ for at least 1hr followed by gel purification using QIAquick Gel Extraction. Then the annealing product (6 µl) was ligated into Valium22 backbone (50-100ng) by incubation with 2 µl 10X ligation buffer, 1 µl of T4 DNA ligase (1U/µl, Bio Basic Inc.) and suitable amount of double-distilled H_2O (ddH_2O) to reach a total volume of 20 µl at 16 ℃ for at least 2hrs. The ligated product was then transformed into *E.coli* cells (DH5α) using standard methods. The

product was tested by restriction digest followed by sequencing using the Valium22 reverse primer (10uM, TAATCGTGTGTGATGCCTACC).

After confirmation of plasmid sequence, large amount of plasmid (at least 30ug) was prepared using QIAGEN Plasmid Midi Kit. The plasmid was then sent to Genetic Services, Inc. for site-directed injection into fly genome.

Genotype and Strand	Oligo DNA sequence
sse$^{RNAi147\text{-}top}$	CTAGCAGTCCCCGAGGCGAAGGAATATAATAGTTATATTCAAGCATATTATATTCCTTCGCCTCGGGGGCG
sse$^{RNAi147\text{-}bottom}$	AATTCGCCCCCGAGGCGAAGGAATATAATATGCTTGAATATAACTATTATATTCCTTCGCCTCGGGGACTG
sse$^{RNAi213\text{-}top}$	CTAGCAGTCTCAATTTACTACCAGGTTAATAGTTATATTCAAGCATATTAACCTGGTAGTAAATTGAGGCG
sse$^{RNAi213\text{-}bottom}$	AATTCGCCTCAATTTACTACCAGGTTAATATGCTTGAATATAACTATTAACCTGGTAGTAAATTGAGACTG
pim$^{RNAi5'\text{-}top}$	CTAGCAGTCAGCTCACTGCTAGAATTCAATAGTTATATTCAAGCATATTGAATTCTAGCAGTGAGCTGGCG
pim$^{RNAi5'\text{-}bottom}$	AATTCGCCAGCTCACTGCTAGAATTCAATATGCTTGAATATAACTATTGAATTCTAGCAGTGAGCTGACTG
pim$^{RNAi3'\text{-}top}$	CTAGCAGTTACAATATATTTAGTAGTTTATAGTTATATTCAAGCATATAAACTACTAAATATATTGTAGCG
pim$^{RNAi3'\text{-}bottom}$	AATTCGCTACAATATATTTAGTAGTTTATATGCTTGAATATAACTATAAACTACTAAATATATTGTAACTG

Table 1. Oligo DNA strands containing RNAi sequences.
The RNAi sequences are highlighted with grey background for corresponding genotypes. Colored DNA sequences indicate restriction enzyme recognition sequences: Red represents NheI recognition sequence at 5' and Purple represents EcoRI recognition sequence at 3'.

2.2 Fly lines used in research

In our research, transgene coding sequence or shRNA sequence is conjugated downstream of UAS and then injected into flies to make an UAS-transgene/RNAi fly line (McGuire, et al. 2004). Two germline driver fly lines were used, *mat*α*4-tubulin-GAL4-VP16* (*mat-GAL4*) and *nanos-GAL4-VP16* (*nanos-GAL4*) (Table 2).

As shown in Table 2, all of the five ordered RNAi fly lines express hairpin RNAs against the coding region of corresponding mRNAs. Among these, the RNAi sequences of $cycB^{RNAi1015}$ and $cycB^{RNAi1896}$ targets different coding regions of *cycB* mRNA. $CAP^{RNAi518}$ has the RNAi sequence against a specific coding region of *CAP* mRNA. $pim^{\Delta dk}$ and $GFP\text{-}pim^{\Delta dk}$ fly lines with UASp-transgenes encode non-degradable Pim protein without D-box and KEN-box ($Pim^{\Delta dk}$), which are the recognition amino acid motifs for APC/C (Batiha, 2013; Leismann, et al. 2000; Leismann and Lehner, 2003). The only difference between the $Pim^{\Delta dk}$ expressed by these two fly lines is that $GFP\text{-}pim^{\Delta dk}$ is green fluorescent protein (GFP) tagged. A transgenec fly line ($GFP\text{-}pim^{wt}$) that expresses GFP tagged wild type Pim was also included in our experiment. According to the purpose of different experiments, combined transgenic fly lines that are able to express two different transgenes at the same time with a single driver such as *mat-GAL4* were generated by crossing two single transgene bearing fly lines. The fly lines were kept at 18 ℃ and experimental crosses were always kept in 25 ℃.

Types of fly line	Full Name	Abbreviation	Landing site	Resource
Wild type control	*yellow-white*	*yw*	No transgene	Bloomington Drosophila Stock Center (BDSC)
Driver fly line	*matα4-tubulin-gal4-VP16*	*mat67-gal4*	2nd chromosome	
	nanos-gal4-VP16	*nanos-gal4*	3rd chromosome	
RNAi fly line	*UAS-cycB^{RNAi}-HMS01015-Valium20*	*cycB^{RNAi1015}*	3rd chromosome	Transgenic RNAi Project (TRiP)
	UAS-cycB^{RNAi}-HMS01896-Valium20	*cycB^{RNAi1896}*	3rd chromosome	
	UAS-cap^{RNAi}-GL00518-Valium22	*cap^{RNAi518}*	2nd chromosome	
	UAS-vtd^{RNAi}-GL00522-Valium22	*vtd^{RNAi}*	3rd chromosome	
	UAS-sse^{RNAi}-147-Valium22	*sse^{RNAi147}*	2nd chromosome	RNAi lines that we made (Chapter 2.1)
	UAS-sse^{RNAi}-213-Valium22	*sse^{RNAi213}*	3rd chromosome	
	UAS-pim^{RNAi}-5'-Valium22	*pim$^{RNAi5'}$*	2nd or 3rd chromosome (2 lines)	
	UAS-pim^{RNAi}-3'-Valium22	*pim$^{RNAi3'}$*	2nd chromosome	
Transgenic fly line	*UAS-pim$^{\Delta dk}$*	*pim$^{\Delta dk}$*	3rd chromosome	Leismann and Lehner, 2003
	UAS-GFP-pim$^{\Delta dk}$	*GFP-pim$^{\Delta dk}$*	3rd chromosome	Batiha, 2013
	UAS-GFP-pim^{wt}	*GFP-pim^{wt}*	3rd chromosome	

Table 2. *Drosophila* lines used.

2.3 Oocyte collection and fixation

Flies were first fed on yeast for at least three days to allow the generation of mature ovaries. The ovaries were then dissected and fixed with different methods according to the purpose of different experiments.

To collect stage 14 oocytes for quantitative reverse-transcriptase polymerase chain reaction (qRT-PCR) or Western analysis, ovaries were first dissected in 1ml PBS buffer mixed with 1 μl collagenase that helps separating oocytes from each other. After that, oocytes were incubated at R.T. in the collagenase containing PBS buffer for 10 mins on a nutator. After incubation, oocytes were rinsed with PBST at least three times. Before oocytes completely settled down to tube bottom during the rinsing, PBST was taken out together with the early stage oocytes that were still drifting so that the remaining are mostly stage 14 oocytes. Oocytes were then frozen in liquid nitrogen and stored in -80 ℃ for future use.

For DNA and/or fluorescent in situ hybridization (FISH) staining, ovaries were dissected into single ovarioles in isolation buffer (IB) (Page and Orr-Weaver, 1997b) which is a special buffer designed to prevent premature egg activation. Then the ovarioles were fixed with 100% methanol and stored in -20 ℃ for future use.

2.3.1 Sonication

To collect stage 14 oocytes for spindle staining together with DNA and/or FISH, specialized steps were required to remove the chorion and vitelline membranes. This was necessary for large molecules such as antibody to penetrate into oocyte. Instead of dissecting individual oocytes manually, sonication has been demonstrated as a promised method to eliminate both membranes (Tavosanis, et al. 1997). The paper did not describe the protocol for oocyte sonication in detail, so I modified and optimised sonication

protocol as follows. Ovaries were first dissected and then incubated at R.T. in 1ml IB with 1 μl collagenase before rinsing with IB for at least three times as previously described to collect non-activated stage 14 oocytes. Then the oocytes were fixed in a mixture of 540 μl PBST, 600 μl heptane, 60 μl formaldehyde and 1.2 μl EGTA at R.T. for 30 mins on a nutator. After fixation, oocytes were rinsed three times and then wash for another three times (5 mins each time) with PBST. Next, oocytes were rinsed one time with 100% methanol at R.T. and transferred into 6.5ml 100% methanol in a 15ml tube. At this time, oocytes can be stored at -20 ℃ for future use or used for sonication. The 15ml tube was then put on ice for at least 5 mins before sonication. Next, oocytes were sonicated at the third power level for fifteen times and then at the fourth power level for twenty times using 60-Fisher Scientific Sonic Dismembrator. During the process, no matter which power level was chosen, oocytes were sonicated briefly for 1s and then rested for another 1s before the next 1s sonication starts (1s sonication and 1s rest together were considered as 1 time of sonication). During sonication, the tip of the sonicator should be put into methanol but not too close to the oocytes and kept away from the side of the 15ml tube. After the sonication of each power level, oocytes were put back on ice to prevent over heating that may caused by sonication. After sonication, the oocytes were examined under optical microscope to see whether the chorion membrane was removed from most of the oocytes. In addition to removal of membranes, sonication also will destroy a small number of oocytes. It was found that antibody staining worked best if the sonication caused at least 10% of oocytes being destroyed. If most of the oocytes were found to be without chorion membrane but are intact after sonication, they would be sonicated again at the third power level 5 more times and re-examine under microscope until around 10% of them are destroyed. Afterwards, the sonicated oocytes

were suitable for either FISH and/or spindle staining depending on the purpose of experiment.

2.4 Embryo collection and fixation

Flies were put in embryo collection chambers together with daily renewed apple juice plate and yeast for at least three days before embryo collection. Depending on the purpose of experiment, embryos were collected after various periods of time after ovulation (0-20 mins, 20-40 mins or 0-1hrs). The collected embryos were first treated with 50% bleach for no more than 2 mins to get rid of the out layer chorion membrane before rinsing with tap water for around 30s. Then embryos were rinsed with embryo wash buffer for three times. Embryos were then fixed in 600 μl heptane plus 600 μl 100% methanol and the tube was inverted gently for 30 times to strip the vitelline membrane from embryos. Next, methanol and heptane together with, if any, floating embryos were discarded. The remaining embryos were rinsed with 100% methanol for three times before storing in -20 ℃ for future use.

2.5 Staining of oocytes and embryos

Depending on the purpose of experiment, oocytes/embryos are stained with different methods including FISH, DNA and spindle staining. These staining methods can be applied either individually or in combination. If used in combination, FISH is always the first staining to perform since its procedure includes high temperature treatment, which is harmful for the antibodies used in the spindle staining. For all staining, embryos stored in 100% methanol were rehydrated by rinsing them with 90%, 70% and 50% methanol in sequence before performing the following protocol(s).

2.5.1 Fluorescent in situ hybridization (FISH)

After re-hydration, oocytes/embryos were first rinsed four times and then washed three times (10 mins each time) with 1ml 2X SSCT. After that, they was washed with 1ml 20%, 40% and 50% formamide bearing 2X SSCT in sequence (10 mins each wash). Then the oocytes/embryos were incubated in 100 μl 50% formamide-2X SSCT at 37 ℃ in PCR machine for at least 5hrs. After the long incubation, 0.5 μl centromeric FISH probe and/or 1 μl arm FISH probe together with suitable amount of hybridization buffer to make the total volume of 20 μl were added and mixed well. The mixture was then heated at 91 ℃ for 3 mins before being flicked and putting back at 37 ℃ in PCR machine for overnight incubation. On the next day, oocytes/embryos were washed with 50% formamide-2X SSCT first for two times (30 mins each time) in 37 ℃ incubator and then washed one more time with 20% formamid-2X SSCT for 10 mins at R.T. on a nutator. After that, they were washed four more times with 2X SSCT (10 mins each time) at R.T. on a nutator. At this point oocytes/embryos should be successfully stained with FISH probe(s) and are ready for DNA and/or spindle staining(s) or mounting onto slide.

2.5.2 Spindle and DNA staining

Depending on the situation, oocytes/embryos were prepared differently before spindle and DNA staining: the ones stored in -20 ℃ were re-hydrated while the ones already stained with FISH were rinsed three times and washed one more time for 10 mins with PBST on a nutator. What's more, oocytes require one additional extraction step before staining comparing to embryos. In this step, 500 μl octane, 500 μl PBST and 25 μl 20% triton X100 were mixed with oocytes and incubated at R.T. for 30 mins on a nutator and then rinsed three times with PBST. Next, oocytes/embryos were blocked by 1ml PBST mixed with 67 μl 15% BSA and 5 μl 10% NaAz on a nutator (8hrs at R.T. or

overnight at 4 ℃ for oocytes; 4hrs at R.T. for embryos). After blocking, at least 0.25 µl primary antibody (1 ºAb, rat against alpha tubulin, 1mg/ml, Millipore), 1 µl RNase (10mg/ml, Invitrogen, for DNA staining, optional), 33.5 µl 15% BSA, 2 µl 10% NaAz and 500 µl PBST were added and incubated on a nutator (4 days at 4 ℃ for oocytes; overnight at 4 ℃ for embryos). Then, oocytes were washed with PBST at least three times for a total of 8hrs at R.T. while embryos were rinsed three times and then washed three times (30 mins each wash) with PBST at R.T. on a nutator. After washing, 0.5 µl 2 ºAb (647nm or 488nm anti rat, 2mg/ml, Life Technologies), 1 µl 1:20 diluted Quant-i-T OliGreen (Invitrogen, for DNA staining, optional), 33.5 µl 15% BSA, 2 µl 10% NaAz and 500 µl PBST were added and incubated on a nutator with thinfoil covers (4 days at 4 ℃ for oocytes; overnight at 4 ℃ or 3hrs at R.T. for embryos). Embryos were rinsed and washed as above for 1 ºAb staining before transferring to slides.

2.5.3 Mounting slides

The stained oocytes/embryos were first rinsed once and washed 5 mins with 100% methanol at R.T. on a nutator. Next, they were rinsed once and washed 10 mins with 100% isopropanol before mounting onto slide with 60 µl 1,2,3,4-tetrahydro-naphthalene.

2.6 Genomic DNA extraction

Genomic DNA was extracted from adult *Drosophila* flies for the preparation of centromeric FISH probe and for testing of qRT-PCR primers. Sixty *yw* female flies were flash frozen by liquid nitrogen and stored in -80 ℃ before use. During the extraction, the frozen flies were homogenized in 500 µl of solution A (0.1M Tris (pH 9), 0.1M EDTA, 1% SDS and 1% DEPC (added immediately before use)) and then incubated at 65 ℃ for 30 mins. After that, 140 µl 8M KOAc was added before incubating on ice for another 30 mins. The mixture was then centrifuged at 4 ℃ for 15 mins and the supernatant was

transferred to a new tube. The spin and transfer step was repeated 1 more time. Next, the supernatant was incubated together with 3 μl RNase (10mg/ml) at 37 ℃ for 20 mins to eliminate RNA contamination. Then genomic DNA was precipitated by adding 0.7 volume of isopropanol and centrifuged at top speed for 5 mins. After that, the pellet was washed with 80% ethanol and dried in air at R.T. for 6 mins before re-suspending in TE buffer. DNA concentration was measured by NanoDrop and the solution was stored at -20 ℃ for future use.

2.7 Construction of FISH probes

2.7.1 Centromeric FISH probe

Genomic DNA was used as template for PCR (95 ℃ for 1 min followed by 35cycles of: 95 ℃ for30s, 55 ℃ for 90s and 68 ℃ for 30s, at last 68 ℃ for 5 mins) to amplify a specific 359 bp heavily repeated DNA sequence located at the centromeric regions of *Drosophila* X chromosome using the designed primers as follows (Hsieh and Brutlag, 1979):

Forward: 5'-CGGTCATCAAATAATCATTTATTTTGC-3'

Reverse: 5'-CGAAATTTGGAAAAACAGACTCTGC-3'

The PCR product was purified using isopropanol precipitation protocol and digested by Hinf1 restriction enzyme at 37 ℃ to generate a DNA band at 359 bp on 2% agarose gel (this step can be skipped if the PCR product shows a clear 359 bp band). The digested product should be purified with isopropanol again before incubating at 37 ℃ with another restriction enzyme, AluI, which is expected to digest the 359 bp DNA fragment into 117, 96, 90 and 56 bp oligos. Then isopropanol precipitation protocol was employed for a third time to purify the oligo DNA fragments before transferring to terminal transferase labeling protocol. The centromeric FISH probe used in our research was made by me for

one time. Additional centromeric FISH probe was made by Mohammed Bourouh in our lab.

2.7.2 Arm FISH probe

To make FISH probes that target the terminal region of *Drosophila* X chromososmes, four cosmids containing insert sequences from a region near the end of *Drosophila* X chromosome (RP30-G24, RP98-29P19, RP98-805 and RP98-19J1) were transformed into *E.coli* cells (DH5α) independently. The transformed *E.coli* cells were cultured on chloramphenicol LB plate at 37 ℃ overnight. Single colonies were then incubated in 2ml 2TY at 37 ℃ overnight and cosmids were purified using QIAprep Spin Miniprep Kit. The extracted cosmid was used as template for the first round of degenerate oligonucleoride primed-PCR (DOP-PCR) (Telenius, et al. 1992) according to the procedures (Table 3, DOP-PCR-1) and PCR program (Table 4, DOP-PCR-1) listed below (Dernburg, A.F. Chapter 2 of *Drosophila* Protocols). Since the DOP-PCR primers target a wide range of DNA sequences under the annealing condition specified by the DOP-PCR-1 program, extra caution needed to be taken when preparing the PCR master mix to prevent any possible DNA contamination. ddH_2O was employed as a negative control to ensure non-specific amplification was not happening. Then the PCR product was used as template for a second round DOP-PCR that used different amount of reagents, procedures and program (Table 3 and 4, DOP-PCR-2). When testing the PCR products on an agarose gel, both PCR are expected to generate a smear of DNA bands while the molecular size range of the second PCR product should be lower and narrower. Next, the PCR product was digested by restriction enzyme AluI, MspI, Sau3AI and RsaI at 37 ℃ overnight (this step may need to be done separately if the enzymes require different buffers). The

digested DNA fragments were purified using isopropanol precipitation protocol before transferring to terminal transferase labeling protocol.

DOP-PCR-1			
DNase treated Master Mix	5 µl	10X PCR Buffer	Incubated at 37 ℃ for 1hr then transferred to 90 ℃ for 10 mins to kill the DNase
	1 µl	10mM dNTPs	
	1 µl	50mM $MgCl_2$	
	1 µl	Taq DNA Polymerase	
	1 µl	DNase	
	(31-x) µl	Ultra pure ddH_2O	
DOP-PCR-1 Reaction Mixture	(40-x) µl	DNase treated Master Mix	Put in DOP-PCR-1 program
	10 µl	DOP-PCR Primer	
	5ng (x µl)	DNA template	
DOP-PCR-2			
DOP-PCR-2 Reaction Mixture	5 µl	10X PCR Buffer	Put in DOP-PCR-2 program
	1 µl	10mM dNTPs	
	0.5 µl	50mM $MgCl_2$	
	0.5 µl	Taq DNA Polymerase	
	0.5 µl	DOP-PCR-1 Product	
	11.5 µl	DOP-PCR primer	
	31 µl	Ultra pure ddH_2O	

Table 3. Reagents and procedures used in the first and second round of DOP-PCR.

DOP-PCR-1 program		
93 ℃	4 mins	
94 ℃	30s	3 cycles
30 ℃	1 min	
72 ℃	ramp over in 3.5 mins (0.2 ℃/s)	
94 ℃	30s	3 cycles
30 ℃	1 min	
72 ℃	2 mins	
94 ℃	20s	36 cycles
56 ℃	1 min	
72 ℃	2 mins	
72 ℃	10 mins	
10 ℃	forever	
DOP-PCR-2 program		
93 ℃	4 mins	
94 ℃	30s	16 cycles
56 ℃	1 min	
72 ℃	2 mins	
72 ℃	10 mins	
10 ℃	forever	

Table 4. PCR programs for the first and second round of DOP-PCR.

2.7.3 Terminal transferase labeling

For 10 µl reaction, 1ug of oligo DNA was incubated at 95 ℃ for 3.5 mins and then put on ice for 5 mins before adding into the mixture of 1.35 µl 1mM dTTP, 0.675 µl 1mM flourescent-dUTP, 2 µl 5X TDT buffer, 0.4 µl Terminal Deoxynucleotidyl Transferase (TdT, 15U/ µl, Fermentas), and suitable amount of ddH_2O. The mixture was incubated at 37 ℃ for 5 to 6 hrs before transferring to ethanol DNA precipitation protocol.

2.8 Confocal microscopy

Olympus FluoView FV1000 laser scanning confocal microscope was employed for taking pictures of stained oocytes/embryos. All the pictures displayed in this thesis were taken using the 60X water lens with 3X zoom except the ones showing entire embryo, which are taken with 60X water lens but with 1X zoom. For the images taken as z-stacks, brightness and contrast were adjusted in Photoshop. For the images displaying green centromeric and red arm FISH siganls, the color of green and red were switched in Photoshop. Images were compiled together in Photoshop.

2.9 mRNA extraction and reverse transcription

Stage 14 oocytes were collected and stored at -80 ℃ as described in Chapter 2.4. The following procedure was modified from the corresponding protocol shown in Dhaliwal, 2011. The buffers (RLT, RW1 and RPE) and RNeasy mini spin column used in this experiment were provided in RNeasy Plus Mini Kit. Before starting to extract mRNA, the working bench, gloves, equipments and tools involved in this experiment were wiped by RNase WiPER to prevent any contamination of RNase. After retrieving frozen oocytes from liquid nitrogen, a tight pestle and pre-made homogenization buffer (600 µl RLT + 6 µl 2-Mercaptoethanol) were placed immediately into the tube and oocytes were homogenized by physical force. The pestle was rinsed with 300 µl RLT which was then

added into the lysate. The lysate was incubated at R.T. for 5 mins before centrifuging at maximum speed for 3 mins at R.T.. The supernatant was carefully transferred into another 1.5ml micro-centrifuge tube together with 600 μl 70% ethanol and mixed immediately by pipetting. Up to 700 μl mixture together with any precipitate that may have formed was transferred into a RNeasy column placed in a 2ml collection tube. The column was then centrifuged at 10,000 rpm (8000g) for 15s at R.T. and the flow through was discarded. The last two steps were repeated to use up the remaining mixture. After that, 700 μl RW1 was added to wash the column and the column was centrifuged at 10,000 rpm for 15s. Then 500 μl RPE was added onto the column and centrifuged again at 10,000 rpm for 15s and this step was repeated one more time. However instead of 15s of centrifugation, the column was centrifuged for 2 mins. After each of these centrifugation steps, the flow through was discarded. The column was then centrifuged at full speed for 1 min to dry the RNeasy silica-gel membrane at the bottom of the column. Finally, 32 μl RNase-free water was add in the center of the RNeasy membrane and the column was incubated at 37 ℃ for 5 mins before centrifuging at 10,000 rpm for 1 min to elute mRNA. The elution step was repeated one more time with 30 μl RNase-free water. The concentration of mRNA was detected by NanoDrop. The two eluted mRNA solution were kept separate and stored in -80 ℃ for future use.

Complementary DNA (cDNA) was constructed using the RevertAid First Strand cDNA Synthesis Kit. A total of 2.5ug of mRNA was usually used to start the reverse transcription. The cDNA product was store at -20 ℃ for short term storage (one week).

2.10 Quantitative reverse-transcriptase polymerase chain reaction (qRT-PCR)

Before starting qRT-PCR the cDNA solution generated using mRNA extraction and the mixture containing Fast SYBR Green Master Mix together with forward and reverse primers were prepared and loaded separately onto the MicroAmp Optical 384-well Reaction plate. As shown in Table 5, 4 µl cDNA with a concentration around 170ng/µl was loaded into corresponding wells of the plate in triplicates. ddH2O served as a negative control, *yw* cDNA was used as positive control and cDNA prepared from mRNA of an RNAi fly line was the experimental group. Two sets of master mix containing mixture was prepared with different primers. One was mixed with the primers targeting the control RNA, *rp49* (Dhaliwal, 2011). The other set of master mix was combined with the primers targeting the gene knocked down by RNAi. The primers used in all of the qRT-PCR performed in our research are shown in Table 7. To prepare the master mix for all nine wells with the same primers (Table 5), 35 µl fast SYBR green was mixed with 17.5 µl of each forward and reverse primers (8uM). Out of the 70 µl master mix made in the last step, 6 µl was loaded into each of the wells with same primers as shown in Table 5. After the loading, the plate was covered by an optically clear sealing tape and sealed carefully using a plastic scraper to scratch the edge of wells especially the wells loaded with qRT-PCR samples. All 384 wells on the plate were covered by the sealing tape. The plate was vortexed and centrifuged at 1000 rpm for 5 mins at 4 ℃ before putting into ViiA 7 (Life Technologies).

ViiA 7 software v1.1 was employed to run the qRT-PCR. To set up the qRT-PCR program, under "Experiment Properties" category, 384-well block, comparative C_T, SYBR Green Reagents and Fast in sequence were chosen. Then the primer targets and cDNA samples used in the experiment were defined. After that, each of the wells with

corresponding primers and cDNA used as shown in Table 5 were assigned into the programe. At last, the qRT-PCR was run according to the program shown in Table 6.

For data analysis, the target wells were selected and analyzed automatically to generate the results displayed in the forms of both excel file and bar graph. In the excel file, RQ values were used to calculate the amount of mRNA levels.

For all tested RNAi lines, each qRT-PCR experiment (each consisting of 3 replicates as described above) was performed three times using mRNA extracted independently from three groups of stage 14 oocytes with the same genotype. The only exception is *pim* RNAi line, for which qRT-PCR was performed twice.

Primers	*rp49*			*target gene*		
Triple-replicates	X	X	X	X	X	X
	X	X	X	X	X	X
	X	X	X	X	X	X
cDNA	ddH_2O	*yw*	*RNAi*	ddH_2O	*yw*	*RNAi*

Table 5. Example plate loading pattern for qRT-PCR.

qRT-PCR program		
95 ℃ (1.9 ℃/s)	20s	
95 ℃ (1.9 ℃/s)	1s	PCR stage (40 cycles)
60 ℃ (1.6 ℃/s)	20s	
95 ℃ (1.9 ℃/s)	15s	Melting Curve stage
60 ℃ (1.6 ℃/s)	60s	
95 ℃ (0.05 ℃/s)	15s	

Table 6. qRT-PCR program.

Genotypes	Primer Name	Oligo DNA sequence	Resource
$CAP^{RNAi518}$	Forward	ACTCCGATGCTTTCACAGGGAT	Primers that we designed
	Reverse	TTGCATCCAGCGCCTGATCTAT	
$sse^{RNAi147}$	Forward	CGACTGGAAATCGCAGA	
	Reverse	GGTCTAGACGCTCATCGACTA	
$pim^{RNAi5'}$	Forward	AATGTGGTCAGCAGGGAT	
	Reverse	TCTCTGTGACCGGCTT	
rp49	Forward a	CGTGAAGAAGCGCACCAAGCAC	Dhaliwal, 2011
	Reverse a	GCGCCATTTGTGCGACAGCTTAG	

Table 7. qRT-PCR primers used in this research.

2.11 Western blotting

Frozen stage 14 oocytes were homogenized in 2X Sample Buffer (SB) and stored in -20 ℃ for future use. Before loading onto a polyacrylamide electrophoresis gel, the protein sample was heated at 95 ℃ for 5 mins and centrifuged at full speed for another 5 mins at R.T. All Western blot results shown in this thesis were done with 8% polyacrylamide gel. The gel was running in TGS buffer under 150V voltage. Then the protein was transferred from gel to Nitrocellulose Membranes (0.45um) in transfer buffer with 350mA electric current for at least 1hr in a low temperature environment.

The membrane was blocked with 5% milk made by TBST for 2hrs at R.T. on a shaker. After that, 1 ºAb (one or multiple from the follows: 1/40 mouse anti-CycB from Developmental Studies Hybridoma Bank; 1/2500 diluted rabbit anti Rad21 from Margarette Heck lab; 1/5000 for mouse anti actin from Millipore; 1/500 for mouse anti-tubulin from Millipore) were used to stain the membrane for at least 4hrs at R.T. or overnight at 4 ℃. Then TBST was used to rinse the membrane three times and wash it for another three times (20 mins each time). 2 ºAb (1/7000 horseradish peroxidase (HRP) labeled goat anti mouse; 1/7000 HRP labeled goat anti rabbit; both from Invitrogen) were incubated with the membrane for at least 2hrs at R.T. or overnight at 4 ℃. The membrane was treated with SuperSignal West Pico or Femto Chemiluminescent Substrate (Thermo Scientific). Immediately after the chemiluminescence treatment, the pictures were taken by Alpha Innotech and analyzed by FluorChem HD2-AlphaEase FC software.

The intensity of unsaturated protein bands from control and experimental group were compared to determine the amount of protein decreasing after RNAi treatment. The intensity value of the protein bands were normalized with the intensity value of random protein bands picked from Ponceau staining to estimate loading. Since the Ponceau

staining, but not actin or tubulin, always positively related to the total amount of protein loaded at the beginning of Western.

Chapter 3. Results

3.1 Meiotic stages of yw control fly line

Before investigating the defects of *Drosophila* meiosis generated by various mutants, it was necessary to study meiosis in wild type flies. For this purpose, stage 14 oocytes and embryos were collected from *yw* flies and stained for microtubule by tubulin targeting antibody, centromeric regions of X chromosome by FISH and either DNA by Oligreen (Fig 5A-5I) or arm regions at the end of X chromosomes by FISH (Fig 5J-5V). Although different stages of *Dosophila* meiosis and polar body formation had been well studied before (Buonomo, et al. 2000; Riparbelli and Callaini, 2005; Foe, et al. 1993), our research has compared the arm and centromere cohesion in each of the stages during these processes.

During metaphase I arrest, homologous chromosomes stay together indicated by a single mass of DNA. At this time, the centromeric regions of homologous X chromosomes either stay together as a single mass or more frequently are separated into two masses by the stretching force of spindle towards the two opposite poles (Fig 5A). We also stained metaphase I arrested meiosis with arm FISH probe. Instead of staining a specific region, the probe stained the whole area between the two centromeric FISH signals as a smear that looked like DNA staining but just a little smaller (data not shown). However, the arm FISH probe is able to identify discrete but closely located arm regions of X chromosomes after *in vivo* or *in vitro* egg activation. Following egg activation, meiosis quickly goes through the remaining stages starting from anaphase I. As shown in Fig 5J, a single arm FISH signal was observed between the two centromeric signals, indicating homologous chromosome arms were more visible but not separated yet during

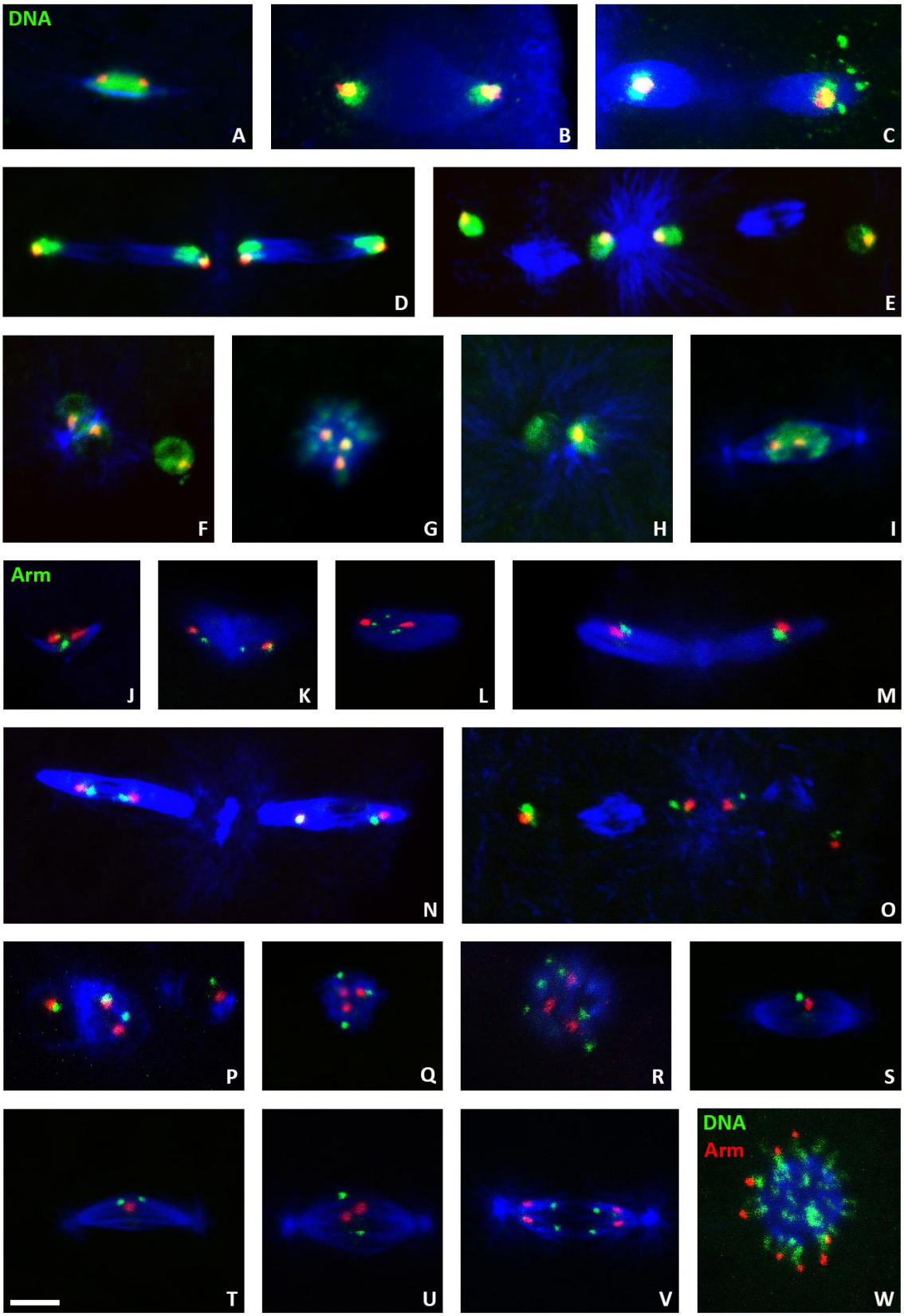
DNA
A
B
C
D
E
F
G
H
I
Arm
J
K
L
M
N
O
P
Q
R
S
T
U
V
DNA
Arm
W

Fig 5. Confocal images of various wild type developmental stages from meiosis to mitosis. In (A-V), blue represents spindle, red represents centromeric FISH signal; In (A-I), green represents DNA; In (J-V), green represents arm FISH signal. In (J-N), meiosis process at metaphase I arrest was activated *in vitro*, the rest were obtained from stage 14 oocyte or embryo collections. In (W), blue represents spindle, red represents arm FISH signal and green represents DNA. (A) Metaphase I arrest. (B, K and L) Anaphase I. (C and M) Metaphase II. (D and N) Anaphase II. (E and O) Telophase II. (F) Polar body formation during interphase. (G) Polar body. (H) Fusion of male and female gametes during interphase. (I) Mitosis. (J) Early anaphase I after egg activation. (P) Four haploid meiotic products. (Q) Polar body at early stage where chromosome arms are together. (R) Mature polar body where chromosome arms are separated. (S) Early stage metaphase mitosis in a male embryo with the arm regions of chromosome arms unseparated. (T) Later stage metaphase mitosis in a male embryo with the arm regions of chromosome arms separated. (U) Early stage metaphase mitosis in a female embryo with the arm regions of chromosome arms unseparated. (V) Anaphase of mitosis in a female embryo with both centromeric and arm regions of chromosomes separated. (W) Mature polar body with separated chromosome arms from un-fertilized embryo. The scale bar indicates 5um.

early anaphase I. These observations imply that DNA may go through a structural transformation during the metaphase to anaphase transition after egg activation, with the newly formed DNA being more accessible for the arm FISH probe. During anaphase I, homologous chromosomes separated from each other as indicated by the equally split DNA masses, each with a centromeric FISH signal (Fig 5B). At this time, either one or two of the arm FISH signals were observed together with each of the two centromeric signals, indicating the attached and separated arm regions of sister chromatids, respectively (Fig 5K and 5L). As meiosis progress into the second round, the shape of the meiotic spindle changes severely, where two twin spindles are formed on the opposite sides of a central aster (Fig 5C-D and 5M-O). From anaphase I to metaphase II, no obvious change was observed in the separated homologous chromosomes indicated by two DNA masses each with a single centromeric FISH (Fig 5B and 5C). Even at the stage of metaphase II, the un-separated arm regions of sister chromatids can still be observed (Fig 5M). Together with anaphase I observations, it indicates that the arm regions of sister chromatids do not always appear to be separated after the separation of homologous chromosomes. Sister chromatids are finally separated from each other at anaphase II, where the two DNA masses split again into four masses (Fig 5D). Each of these four DNA masses contains one centromeric and one arm FISH signal (Fig 5N). DNA and both FISH signals remain the same when meiosis progresses from anaphase II to telophase II (Fig 5E and 5O). However, meiotic spindle in telophase II is different than that in anaphase II, where the twin spindles on each side of the aster no longer connect to DNA masses but stay in the middle of the two newly split DNA masses (Fig 5E and 5O).

After meiosis, four haploid meiotic products are formed. Each of the four haploid nuclei showed one centromeric and one arm FISH signal (Fig 5P). During interphase,

before the formation of polar body, the four haploid nuclei undergo one round of DNA replication. Afterwards, three out of the four nuclei come together (Fig 5F) to form a polar body (Fig 5G). The formed polar body initially contains three centromeric FISH signals on the inside and three arm signals on the outside (Fig 5Q). As time pregresses (as indicated by the increase of embryonic mitotic cycles), the number of arm signals gradually increases to a maximum of six while the number of centromeric FISH signals remains the same (Fig 5R and Fig 6). This implies the separation of arm regions but not the centromeric regions of polar body sister chromatids.

To test whether this arm region separation in the polar body depends on mitosis progression or not, polar bodies of un-fertilized *yw* embryos that do not progress through mitotic divisions and embryo development were examined. Since there is no male pronucleus that pulls one of the haploid nuclei away, all four meiotic products will combine together to form a polar body that contains four copies of each chromosome, each with two sister chromatids. In this case, if the arm region separation of sister chromatids in the polar body happens independently from the progression of mitosis, we expect to see a maximum of eight arm FISH signals in the polar bodies of un-fertilized embryos. Indeed, our preliminary experimental results support this expectation (Fig 5W). Hence, the progression of mitosis and the sister chromatid separation at the arm regions in the polar body are two independent processes.

At the same time as the formation of polar body, the fourth haploid nucleus is pulled away and combined with the male pronucleus (Fig 5H) to start mitosis (Fig 5I). Then the embryo undergoes 14 rounds of synchronized nuclear divisions before cellulariztion happens (Mazumdar and Mazumdar, 2002). Looking specifically at

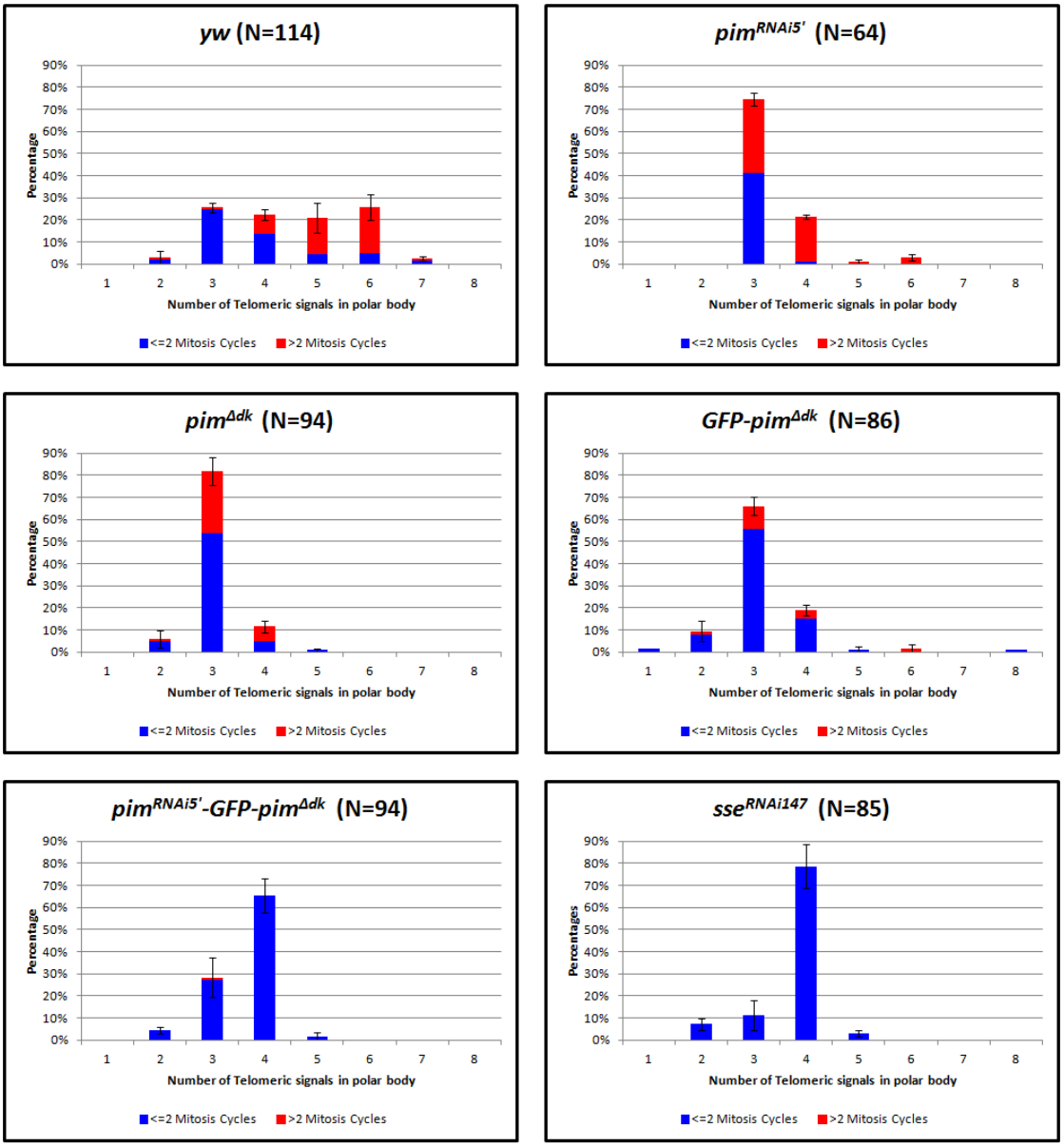

Fig 6. Number of arm FISH signals in polar body and mitotic stage of different genotypes. Blue represents polar bodies with less than or equal to two mitosis cycles and red represents polar bodies with more than two mitosis cycles.

embryos in which all nuclei were in metaphase, we saw either sister chromatids attached together at both centromeric and arm regions (Fig 5S) or the sister-chromatid cohesion at arm regions was lost while centromeres remained unseparated (Fig 5T). These phenomena indicate that the arm regions of sister chromatids lose cohesion before centromeric regions but do not separate until early anaphase. In both Fig 5S and 5T, images of mitosis in male embryos have been displayed, where only one X chromosome centromeric FISH signal can be observed in the middle of the mitotic spindle. In female embryos, two centromeric FISH signals together with two arm signals were observed during metaphase (Fig 5U). In anaphase, two centromeric signals with two arm signals on each side of a anaphase spindle was also observed (Fig 5V), indicating sister chromatids were completely separated from each other during anaphase. Overall, our observations on wild type meiosis, polar body and mitosis match with the current knowledge and also provide new information about these processes.

3.2 Knockdown of CAP and vtd in ovary

To investigate whether the components of mitotic Cohesin complex are essential for the cohesion between sister chromatids in *Drosophila* meiosis, vtd^{RNAi} and $CAP^{RNAi518}$ fly lines were ordered from the Transgenic RNAi Project. *CAP* and *vtd* are the genes encoding the *Drosophila* Cohesin components, SMC3 and Rad21, respectively. The GAL4/UAS-RNAi method was employed to knock down these genes specifically in the ovary. GAL4 is a yeast transcriptional activator that activates an enhancer known as upstream activation sequence (UAS) to drive gene expression (Brand and Perrimon, 1993). For the purpose of our research, two driver fly lines that express GAL4 in the early stages of ovary development were used (*mat-GAL4* and *nanos-GAL4*, Table 2). After crossing the RNAi fly lines to these germline specific driver fly lines, the expression of *vtd* and *CAP* will be knocked down in the ovaries of progeny flies. Such knockdown of *vtd* or *CAP* resulted in females laying eggs that did not hatch, indicating that either meiosis or the early stages of mitosis, both of which depend on maternal proteins, is blocked by the knockdown.

3.2.1 vtd and CAP were knocked down efficiently

To test the knockdown efficiency of *vtd* in *mat-GAL4;* vtd^{RNAi} flies, stage 14 oocytes were collected and Rad21 expression levels were analyzed by Western blots. After three repeated Westerns using stage 14 oocytes collected from three independently established crosses, the results from these Westerns showed that the expression level of Rad21 in vtd^{RNAi} is 18% of that in *yw* (Fig 7A), indicating *vtd* was knocked down efficiently.

Since we do not have an antibody that is able to target CAP, qRT-PCR was employed to evaluate the *CAP* mRNA level in the stage 14 oocytes of *mat- GAL4;*

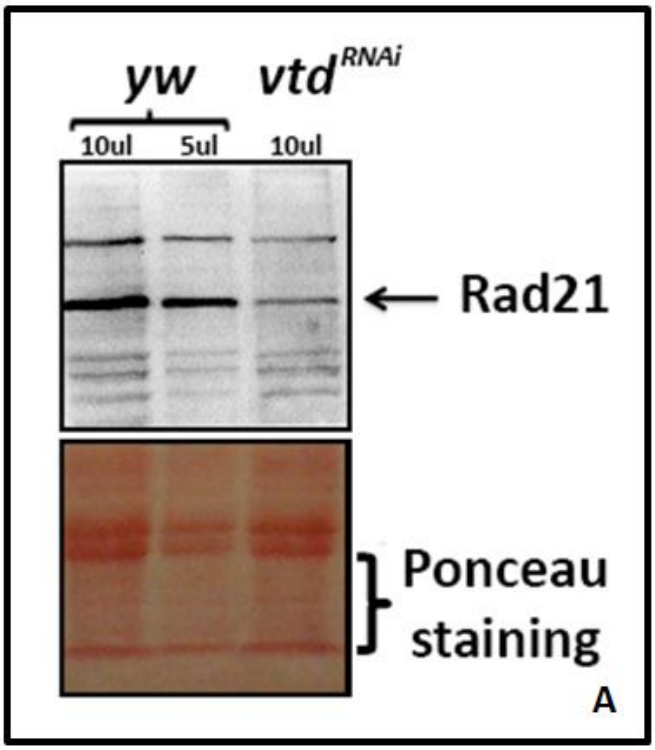

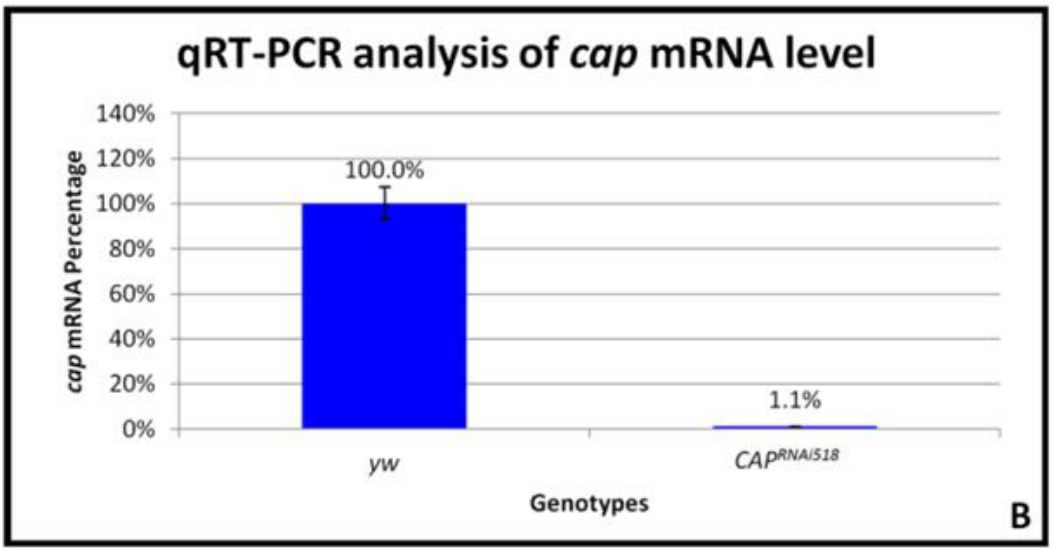

Fig 7. Quantitatively analysis of knockdown efficiency of *vtd*^{RNAi} and *CAP*^{RNAi518} using Western and qRT-PCR respectively.

(A) A representative figure that is chosen from one of the three Westerns showing that Rad21 expression level is dramatically reduced in *vtd*^{RNAi} comparing to that in *yw*. A specific area from Ponceau staining was used to estimate loading. According to the results collected from three repeated experiments, the expression level of Rad21 in *vtd*^{RNAi} is 18±3.5% of that in *yw*. (B) A representative figure that is chosen from one of the three qRT-PCRs showing that *CAP* mRNA level reduced dramatically in *CAP*^{RNAi518} comparing to that in *yw*. According to the results of the three repeated qRT-PCRs, the *CAP* mRNA level in *CAP*^{RNAi518} is 1.3±0.4% of that in *yw*.

CAP^{RNAi518} flies. After three qRT-PCR repeats using mRNA extracts prepared from three groups of stage 14 oocytes that were collected independently, it was found that the *CAP* mRNA level in *CAP*^{RNAi518} is only 1.3% of that in *yw* (Fig 7B). This demonstrated that *CAP* was efficiently knocked down by RNAi.

3.2.2 CAP and Rad21 are required for proper metaphase I arrest

To see whether metaphase I arrest is affected by knockdown of *CAP* and/or *vtd*, stage 14 oocytes were examined with staining for DNA, tubulin and centromere of X chromosomes (Fig 9A-9G). For *yw* flies, meiosis is normally arrested at metaphase I in stage 14 oocytes (Fig 5A and 9A) and rarely shows premature DNA separation. The data collected from our experiments indicates approximately 6% of these wild type oocytes exhibiting premature DNA separation (Fig 8). After knockdown of either *CAP* or *vtd* using the germline specific driver *mat-GAL4*, it was found that the majority of stage 14 oocytes maintained normal metaphase I arrest (Fig 9B and 9E). However there are some oocytes showing premature DNA separation. Approximately 17% of stage 14 oocytes of both *CAP*^{RNAi518} and *vtd*^{RNAi} exhibited premature DNA separation (Fig 8). The most common abnormal phenotype in both *CAP*^{RNAi518} and *vtd*^{RNAi} stage 14 oocytes is represented by two equally sized DNA masses each with a single centromeric signal inside (Fig 9C and 9F). Rarely, the separation of DNA into more than two un-equally sized masses can be observed (Fig 9D). These phenotypes presumably imply the complete (2 DNA masses) or partial (more than 2 DNA masses) premature separation of homologous chromosomes. Furthermore, in some cases, only one of the DNA masses exhibited two centromeric FISH signals (Fig 9D), implying the mis-segregation of homologous chromosomes. All of these abnormal phenotypes described above could be caused by the loss of homologous chromosome pairing. This may be caused by either a

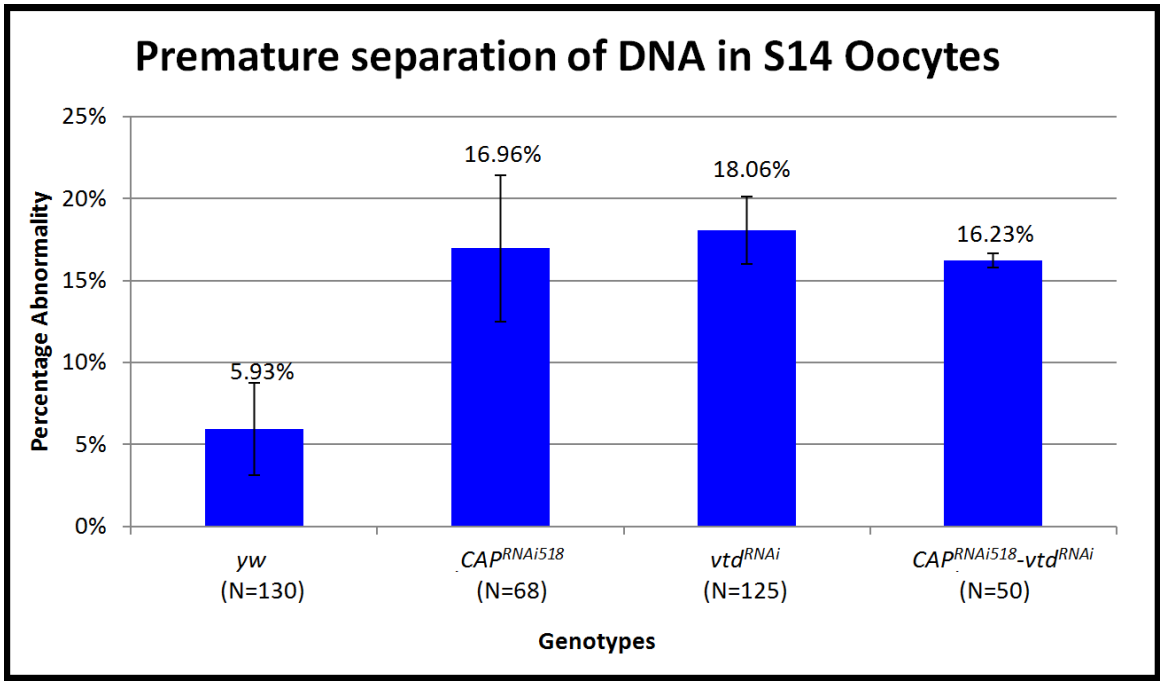

Fig 8. Quantitative analysis of premature DNA separation in stage 14 oocytes collected from *yw*, *mat-GAL4; CAP*^{RNAi518}, *mat-GAL4; vtd*^{RNAi} and *mat-GAL4; CAP*^{RNAi518}*-vtd*^{RNAi} flies.

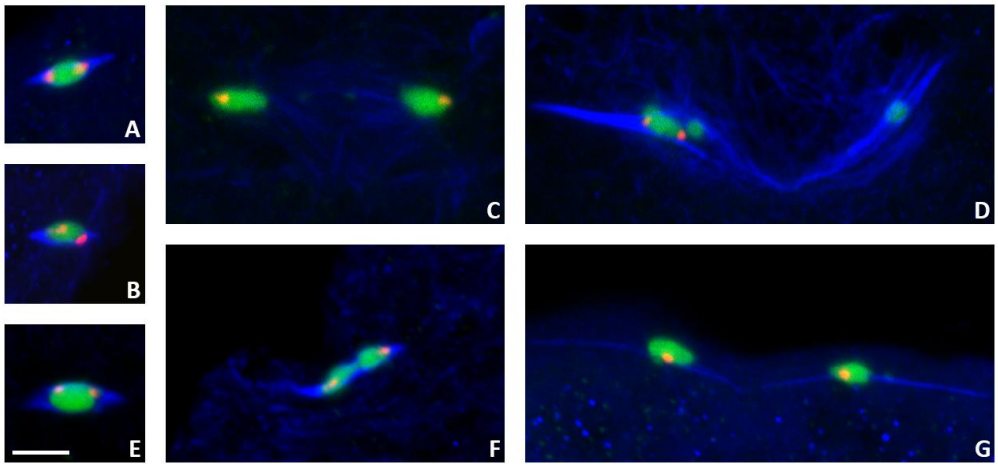

Fig 9. Confocal images of normal and abnormal metaphase I in stage 14 oocytes collected from *yw*, *mat-GAL4; CAP*^{RNAi518} and *mat-GAL4; vtd*^{RNAi} flies.
Blue represents spindle, red represents centromeric FISH signal, green represents DNA. (A) Normal metaphase I arrest in *yw* stage 14 oocyte. (B-D) Phenotypes from *mat-GAL4; CAP*^{RNAi518} stage 14 oocytes: (B) Normal metaphase I arrest. (C) Equally separated DNA masses with centromeric FISH signals in each of them. (D) More than two DNA masses with FISH signals in one of them and (D) also shows abnormal spindle phenotype. (E-G) Phenotypes from *mat-GAL4; vtd*^{RNAi} stage 14 oocytes: (E) Normal metaphase I arrest. (F and G) Equally separated DNA masses with centromeric FISH signals in each of them; (G) Abnormal spindle phenotype. The scale bar indicates 5um.

loss of cohesion between sister chromatids or the absence of chiasmata formation (Buonomo, et al. 2000). If CAP and Rad21 are really required for sister-chromatid cohesion during meiosis, we expect to see premature sister chromatid separation at centromeric regions of chromosomes. However, for all of the stage 14 oocytes collected from both RNAi fly lines, no more than two centromeric FISH signals was detected, indicating sister chromatids did not separate. Sometimes, instead of a single spindle normally observed in the first round of meiosis (Fig 5A-B, 5J-L, 9A-B and 9E), abnormal spindle phenotypes were observed in the stage 14 oocytes collected from both RNAi fly lines (Fig 9D and 9G). These spindle abnormalities could be a consequence of premature DNA separation.

To see whether it is possible to improve the knockdown effects of *CAP* and *vtd* on meiosis, several approaches were tried. Instead of single knockdown, double knockdown of both *CAP* and *vtd* driven by a single *mat-GAL4* driver was introduced in fly ovaries. Most of the stage 14 oocytes with the double knockdown exhibited normal metaphase I phenotypes (Fig 10B). In addition, they exhibited similar premature DNA separation phenotypes (Fig 10C-10F) and frequency (Fig 8) compared to those of the stage 14 oocytes with *CAP* or *vtd* single knockdown. However, none of the stage 14 oocytes with double knockdown displayed more than two centromeric FISH signals. This indicates that sister chromatids did not separate even after the double knockdown of both *CAP* and *vtd*.

As described before, only the Cohesin complexes loaded onto chromosomes during S phase are expected to contribute to the cohesion between sister chromatids (Gerlich, et al. 2006; Haering, et al. 2004). However the earliest expression of *mat-GAL4* was detected in stage 1 oocytes in which meiosis is already arrested at prophase I (Urban, et al. 2014). Considering these facts, it is reasonable to think that the *mat-GAL4* driven

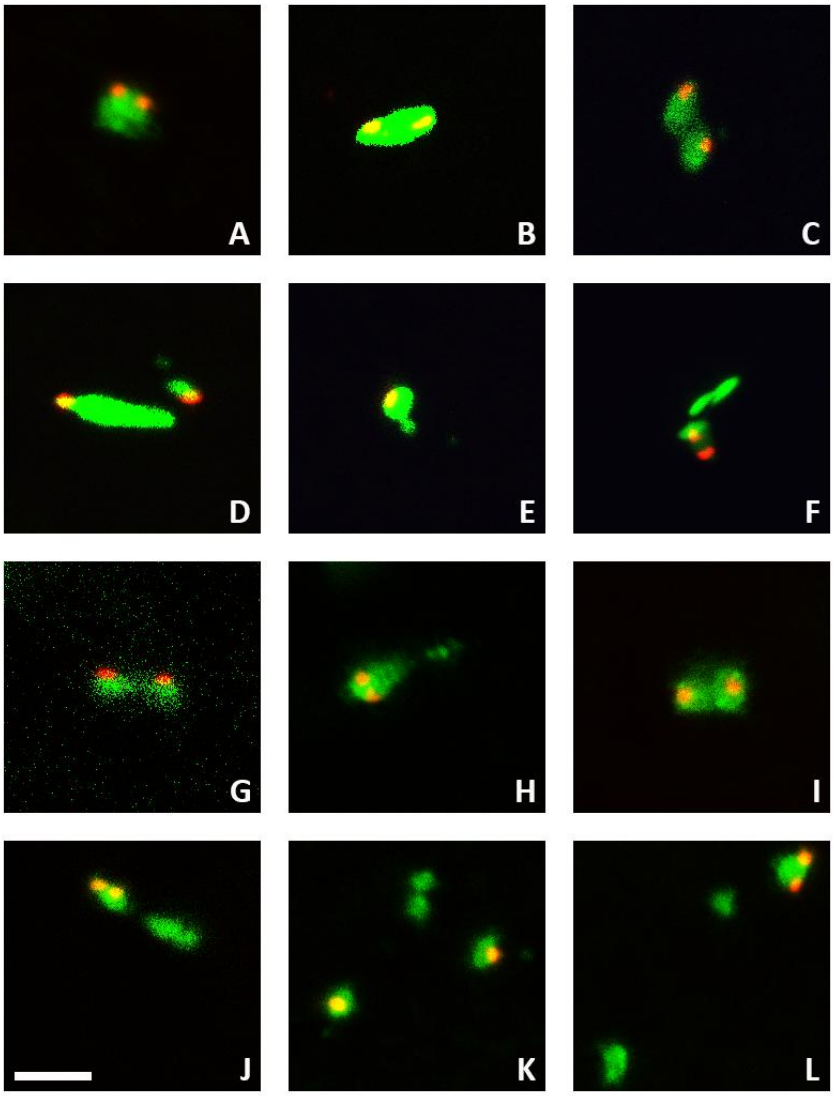

Fig 10. Confocal images of normal and abnormal metaphase I in stage 14 oocytes collected from *yw*, *mat-GAL4; CAP*^{RNAi518}*-vtd*^{RNAi}, *nanos-GAL4; vtd*^{RNAi} and *nanos-GAL4; CAP*^{RNAi518} flies.

Red represents centromeric FISH signal, green represents DNA. (A) Normal metaphase I arrest in *yw* stage 14 oocyte. (B-F) Phenotypes displayed in stage 14 oocytes collected from *mat-GAL4; CAP*^{RNAi518}*-vtd*^{RNAi} flies: (B) Normal metaphase I arrest. (C) Equally separated DNA masses each with a centromeric FISH signal. (D and E) Un-equally separated DNA masses with separated (D) and unseparated (E) FISH signals. (F) More than two DNA masses with separated FISH signals. (G-H) Abnormal phenotypes of DNA premature separation displayed in *nanos-GAL4; vtd*^{RNAi} stage 14 oocytes: (G) Equally separated DNA masses each with a FISH signal. (H) Un-equally separated DNA masses with FISH signals in one of them. (I-L) Various abnormal phenotypes of premature DNA separation displayed in *nanos-GAL4; CAP*^{RNAi518} stage 14 oocytes: (I and J) Equally separated DNA masses with FISH signals in each of them (I) and in one of them (J). (K and L) More than two DNA masses with FISH signals in two of them (K) and in one of them (L). The scale bar indicates 5um.

CAP and *vtd* RNAi did not knock down the expression of CAP and Rad21 early enough to affect the formation of Cohesin complexes during S phase. Hence, another GAL4 driver that is expressed much earlier, *nanos-GAL4* (Wang, et al. 1994), was employed to knock down the expression of CAP and Rad21. Though only a small number of oocytes were examined, the percentages of stage 14 oocytes exhibiting premature DNA separation in all of the examined oocytes of *nanos-GAL4; CAP*^{RNAi518} (65%, N=20) and *nanos-GAL4; vtd*^{RNAi} (35%, N=20) were much higher than those of the stage 14 oocytes collected from the *mat-GAL4* driven RNAi fly lines. As before, premature separation (Fig 10G-10L) and mis-segregation (Fig 10H, 10J and 10L) of homologous chromosomes were observed in stage 14 oocytes of the two *nanos-GAL4* driven RNAi fly lines. Nonetheless, sister chromatids separation indicated by more than two centromeric FISH signals was still not observed in the stage 14 oocytes collected from both of the *nanos-GAL4* driven RNAi fly lines.

Attempts had also been made to knockdown CAP and Rad21 with both *mat-GAL4* and *nanos-GAL4* drivers in the ovaries of *CAP*^{RNAi518}*-vtd*^{RNAi} flies. However with such strong double knockdowns, the ovaries of these flies were completely lacking later stage oocytes. This phenotype may be generated because of the early and strong knockdown of both *CAP* and *vtd* inhibits the mitosis that is important for the development of the 16-cell germline cyst.

The experimental results from this section imply that CAP and Rad21 play a role in maintaining proper orientation of homologous chromosomes during metaphase I arrest. However, no evidence could be found to support their role in sister-chromatid cohesion during meiosis.

3.2.3 CAP and Rad21 are not required for the proper completion of meiosis

Although a small amount of premature DNA separation had been detected in metaphase I arrest of *mat-GAL4* driven $CAP^{RNAi518}$ and vtd^{RNAi} flies, it remains unknown whether the following stages of meiosis are affected by the knockdown of *CAP* and *vtd*. Thus, embryos that were laid within 1hr (0-1hr embryos) were collected from the *mat-GAL4*; $CAP^{RNAi518}$ (Fig 11A-11F) and *mat-GAL4*; vtd^{RNAi} (Fig 11G-11L) flies and stained for tubulin, centromere of X chromosome and either DNA or arm regions of X chromosome. It was found that both RNAi lines successfully progress into anaphase II where four DNA masses each with a centromeric FISH signal were observed (Fig 11A and 11G). This indicates that both homologous chromsomes and sister chromatids are separated from each other and they look very similar to the anaphase II seen in *yw* flies (Fig 5D). After meiosis, normal looking interphase that exhibits three combined haploid nuclei each with one centromeric and one arm FISH signal were observed in both RNAi fly lines (Fig 11D and 11J). These images look similar to Fig 5P showing *yw* interphase except that in Fig 5P all four haploid meiotic products are still close together while in Fig 11D and 11J one of the haploid nuclei has already been pulled away by the male pronucleus. Given that we observed chromosome mis-segregation in some oocytes, we expected to see some abnormalities in later meiosis. The fact that we did not is likely due to the relative infrequency of these aberrant meiosis. Overall, the results suggest that most of the meiosis is finished normally in both *mat-GAL4;* $CAP^{RNAi518}$ and *mat-GAL4;* vtd^{RNAi} flies, implying that both CAP and Rad21 are not required for meiosis.

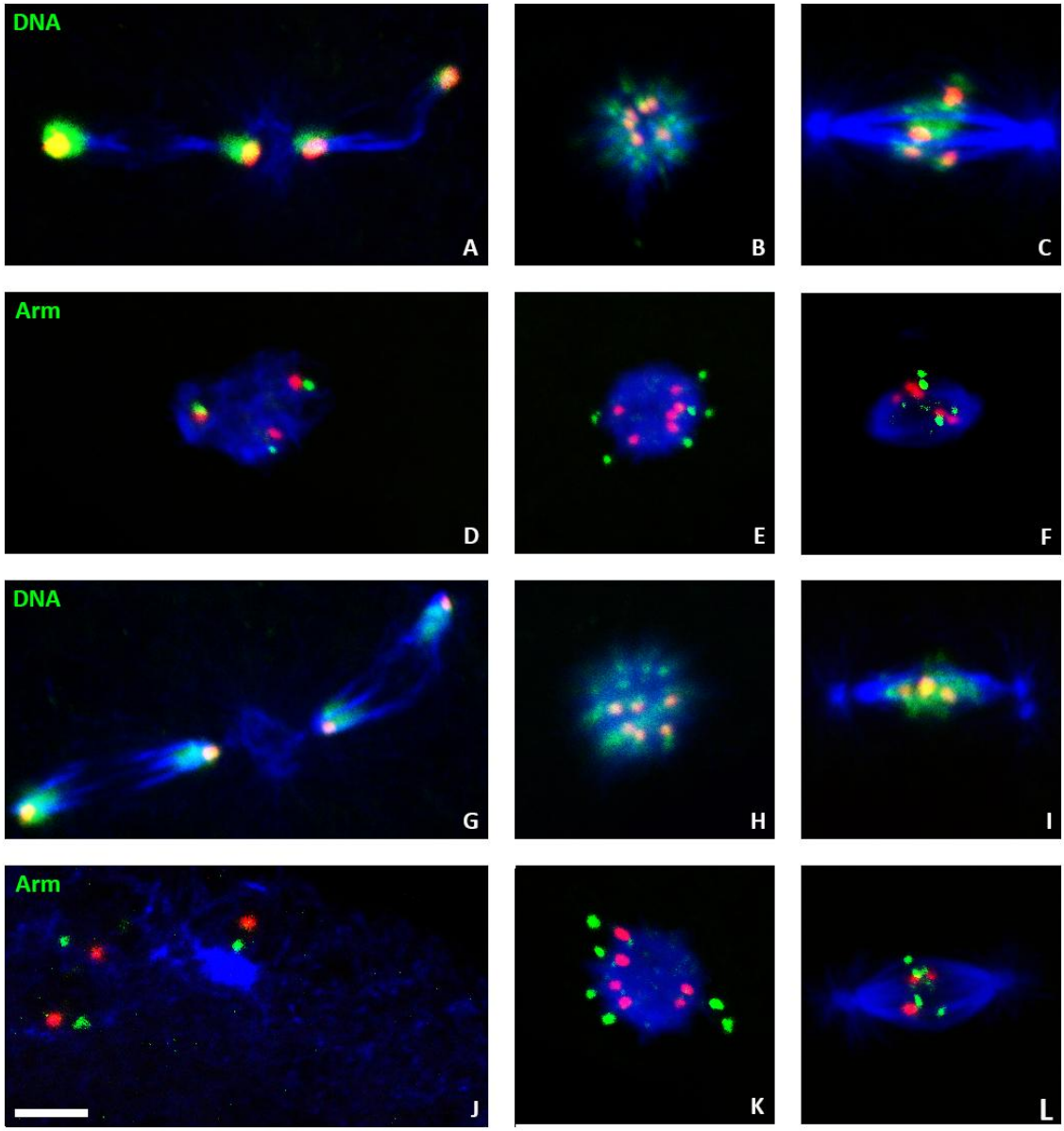

Fig 11. Confocal images of anaphase II, polar body and mitosis in embryos collected from *mat-GAL4; CAP*^{RNAi518} and *mat-GAL4; vtd*^{RNAi} flies.
In (A-L), blue represents spindle, red represents centromeric FISH signal; In (A-C and G-I), green represents DNA; In (D-F and J-L), green represents arm FISH signal. (A-F) Phenotypes displayed in *mat-GAL4; CAP*^{RNAi518} flies: (A) Anaphase II. (B) Abnormal polar body with six centromeric FISH signals. (C) Abnormal mitosis with four centromeric FISH signals. (D) Interphase; (E) Abnormal polar body with six centromeric and six arm FISH signals. (F) Abnormal mitosis with four centromeric and four arm FISH signals. (G-L) Phenotypes displayed in *mat-GAL4; vtd*^{RNAi} flies: (G) Anaphase II. (H) Abnormal polar body with six centromeric FISH signals. (I) Abnormal mitosis with three centromeric FISH signals. (J) Interphase. (K) Abnormal polar body with six centromeric and six arm FISH signals. (L) Abnormal mitosis with three centromeric and four arm FISH signals. The scale bar indicates 5um.

3.2.4 CAP and Rad21 are essential for centromeric sister-chromatid cohesion in the polar body

Although meiosis is able to finish properly after knockdown of *CAP* and *vtd*, it is still interesting to examine whether polar body formation and the embryonic mitotic divisions are affected by the knockdowns. It was found that DNA and microtubules appear normal in polar bodies after the knockdown of either *CAP* or *vtd* (Fig 11B and 11H). However further investigation with centromeric FISH staining revealed that the centromeric regions of X chromosomes no longer remain together (Fig 11B, 11E, 11H and 11K) as they do in the *yw* flies (Fig 5G and 5Q). It was found that instead of seeing three centromeric FISH signals in polar bodies, around 40% of polar bodies in $CAP^{RNAi518}$ and 60% of polar bodies in vtd^{RNAi} exhibited more than three centromeric signals (Fig 12). These percentages of abnormal polar bodies are higher than that seen in *yw* flies (8%). For the two RNAi fly lines, the maximum number of centromeric FISH signals observed in the polar body is six (Fig 11B, 11E, 11H and 11K) (except 1 showed seven FISH signals out of the 77 polar bodies examined). There are two possible models that can explain this abnormal phenotype seen in the polar bodies. One is that the centromeric cohesion between sister chromatids in polar bodies is lost after knockdown of either *CAP* or *vtd*, which leads to the complete separation of the sister chromatids. The other possibility is that *CAP* or *vtd* knockdown results in re-replication in the meiotic products to result in a complete or partial doubing of chromosome number in the polar bodies. If this is the case we may expect to see a further doubling of the arm FISH signals from 6 to up to 12 in the polar body. Further investigation with both centromeric and arm FISH staining revealed that commonly a maximum of six arm signals can be observed in the abnormal polar bodies (except 1 out of 40 polar bodies showed seven arm signals),

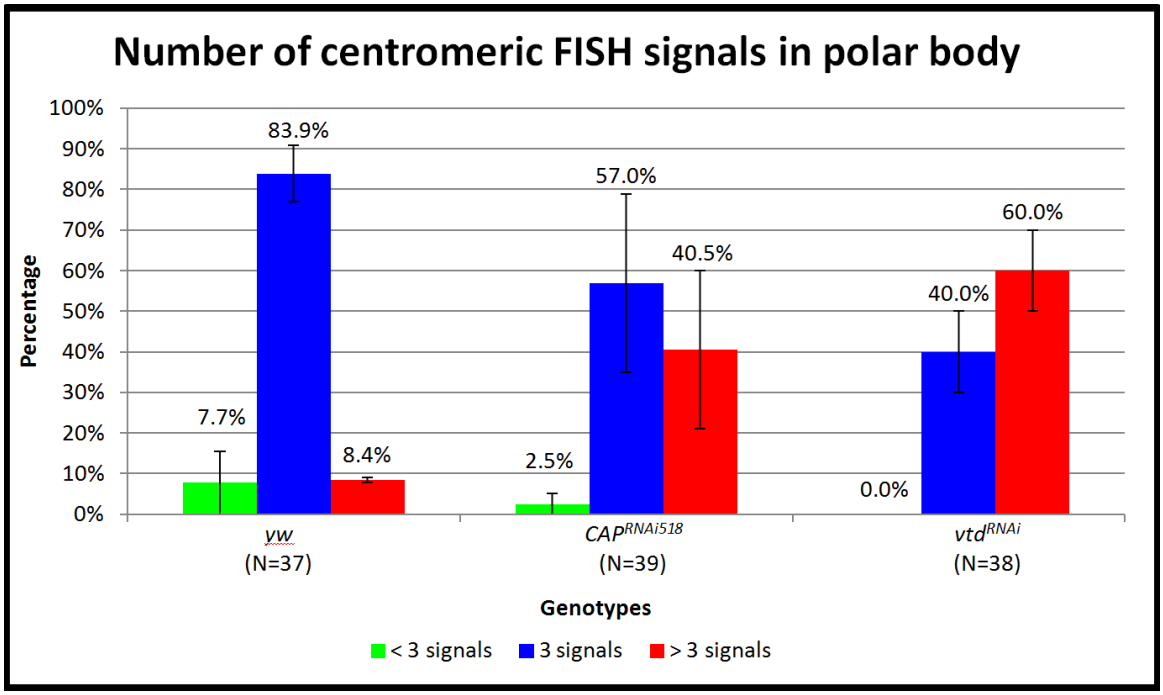

Fig 12. Percentage distribution of the polar bodies showing various numbers of centromeric FISH signals in 0-1 hr embryos collected from *yw*, *mat-GAL4; CAP*^{RNAi518} and *mat-GAL4; vtd*^{RNAi} flies.

usually together with six centromeric signals (Fig 11E and 11K). This observation eliminated the second possibility mentioned earlier. Therefore, all these experiments demonstrated that both CAP and Rad21 are essential for the centromeric cohesion between sister chromatids in polar bodies.

3.2.5 Knockdown of CAP or vtd results in abnormal embryonic mitotic cycles

In addition to the abnormalities observed in polar bodies, abnormal phenotypes were also detected in mitosis after knockdown of either *CAP* or *vtd*. In embryos, instead of two centromeric FISH signals per mitotic spindle (Fig 5U), three or four centromeric signals were observed in *CAP* and *vtd* knockdowns (Fig 11C, 11F, 11I and 11L). This implies knockdown of either *CAP* or *vtd* leads to the loss of cohesion between sister chromatids in mitosis, as has been seen in other cell types in *Drosophila* (Eichinger, et al. 2013; Vass, et al. 2003). In addition to the loss of sister-chromatid cohesion, the evenly distributed and synchronized mitotic divisions that are normally seen in *yw* embryos (Fig 13A) is no longer observed after knockdown of *CAP* and *vtd*. Instead, randomly distributed mitotic cycles with different spindle sizes and at various division stages were observed in $CAP^{RNAi518}$ and vtd^{RNAi} embryos (Fig 13B and 13C). It was revealed that 97.6±2.4% (N=37) of $CAP^{RNAi518}$ embryos and 91.7±8.3% (N=30) of vtd^{RNAi} embryos exhibited abnormal mitotic divisions, which are significantly higher than that of *yw* embryos (4.2±4.2%, N=37). These phenotypes are presumably the consequences of the abnormal progression of mitosis resulting from premature sister chromatid segregation as described before.

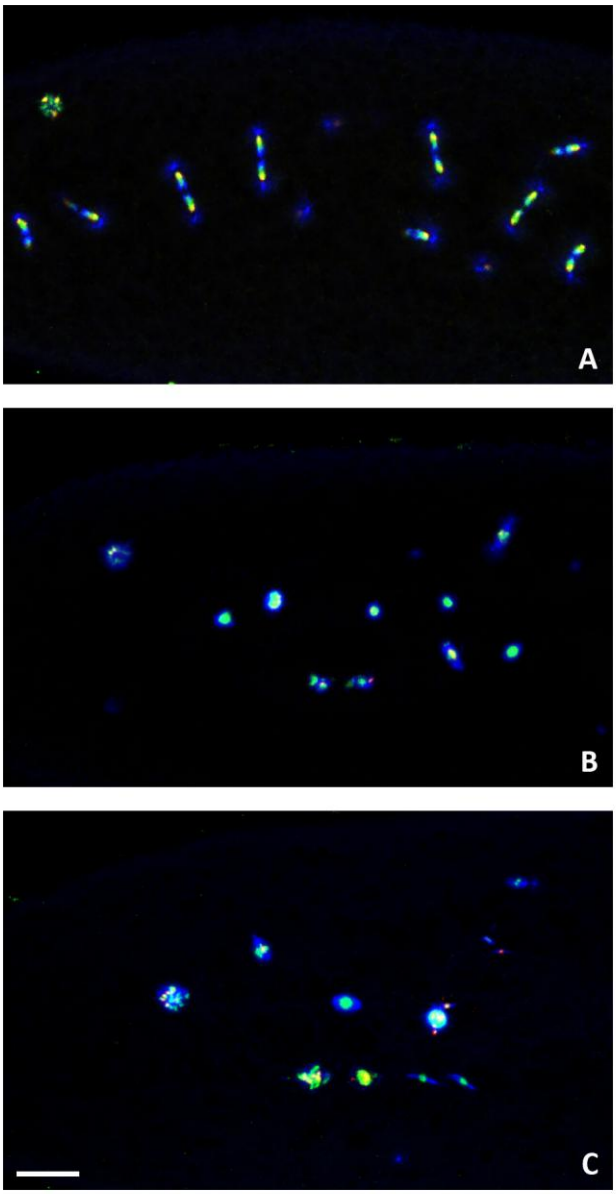

Fig 13. Confocal images of embryos collected from *yw*, *mat-GAL4; CAP*^{RNAi518} and *mat-GAL4; vtd*^{RNAi} flies.
Blue represents spindle, red represents centromeric FISH signal, green represents DNA. (A) *yw* embryo with synchronized mitotic divisions evenly distributed in the embryo. (B) *CAP*^{RNAi518} embryo. (C) *vtd*^{RNAi} embryo. (B and C) Abnormal distribution of non-synchronized mitosis with different spindle sizes. The scale bar indicates 20um..

3.3 Knockdown of sse in the ovary

According to previous findings, the kleisin protein Rad21 and the Rec8-like protein C(2)M are not required to maintain sister-chromatid cohesion in *Drosophila* meiosis (Urban, et al. 2014; Heidmann, et al. 2004). This leads us to ask whether Separase, the enzyme that cleaves the kleisin is also not required for this process. To answer this question, we generated two RNAi lines, $sse^{RNAi147}$ and $sse^{RNAi213}$, targeting different parts of the coding region of *sse* mRNA. After knockdown of *sse* in the ovaries by *mat-GAL4* driven RNAi, both of the fly lines produced un-hatchable eggs. To study the reason, stage 14 oocytes and embryos collected from *mat-GAL4*; $sse^{RNAi147}$ flies were examined.

3.3.1 sse was knocked down efficiently

qRT-PCR was employed to test the knockdown efficiency of *sse* in $sse^{RNAi147}$ flies. After three repeated qRT-PCR experiments (each employing 3 replicates) using mRNA extracted independently from three groups of $sse^{RNAi147}$ stage 14 oocytes, it was found that the mRNA level of *sse* in $sse^{RNAi147}$ is only 1.2% of that in *yw* (Fig 14A). These qRT-PCR experiments demonstrated that *sse* was knocked down efficiently by the RNAi.

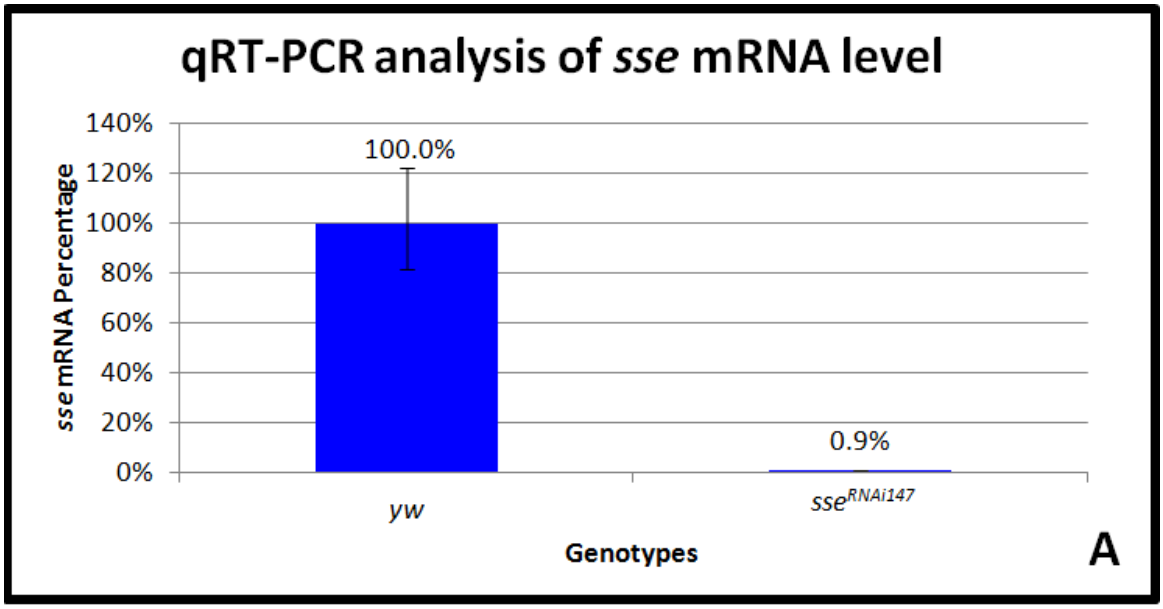

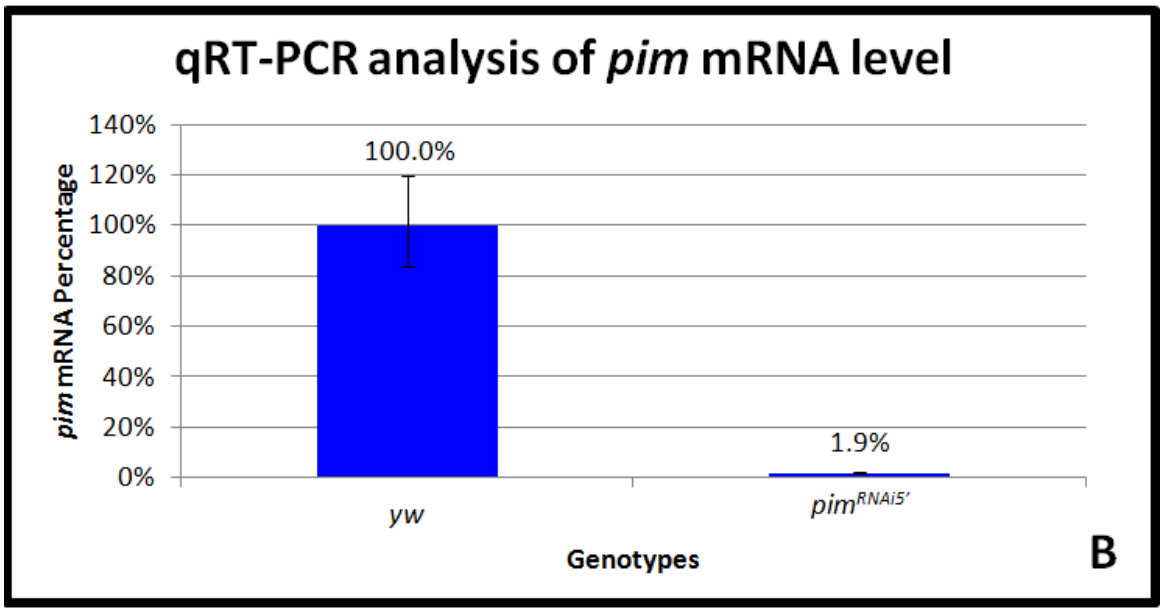

Fig 14. qRT-PCR analysis of *sse* and *pim* mRNA level in stage 14 oocytes collected from *mat-GAL4; sse*^{RNAi147} and *mat-GAL4; pim*$^{RNAi5'}$ fly lines respectively.
(A) A representative figure that is chosen from one of the three qRT-PCRs showing that *sse* mRNA level reduced dramatically in *sse*^{RNAi147} comparing to that in *yw*. According to the results of the three repeated qRT-PCRs, the *sse* mRNA level in *sse*^{RNAi147} is 1.2±0.3% of that in *yw*. (B) A representative figure that is chosen from one of the two qRT-PCRs showing that *pim* mRNA level reduced dramatically in *pim*$^{RNAi5'}$ comparing to that in *yw*. According to the results of the two repeated qRT-PCRs, the *pim* mRNA level in *pim*$^{RNAi5'}$ is 1.7±0.2% of that in *yw*.

3.3.2 Knockdown of sse does not cause obvious abnormality in metaphase I arrest

To study whether knockdown of *sse* generates any defect in metaphase I arrest, phenotypes of stage 14 oocytes collected from *mat-GAL4; sse*^{RNAi147} fly line were analyzed and compared to those collected from *yw* flies (Fig 15A-15D). It was found that the majority of oocytes collected from *sse*^{RNAi147} flies exhibited normal metaphase I arrest as seen in *yw* flies (Fig 15B and 15C). It was demonstrated that 15% *sse*^{RNAi147} oocytes showed premature DNA separation (Fig 15A). This percentage of abnormality is not significantly different from that in *yw* flies (Fig 15A). Noticeably, *sse*^{RNAi147} oocytes showed higher percentage abnormality with larger range of standard error (Fig 15A). This was caused by the inconsistent results generated by four repeated experiments. Among the four repeats, two of them indicated that 100% of the *sse*^{RNAi147} stage 14 oocytes showed normal metaphase I arrest but in the other two experiments, a small group (25% and 35% specifically) of *sse*^{RNAi147} stage 14 oocytes exhibited prematurely separated DNA masses (Fig 15D). In all of these four repeats, at least 20 stage 14 oocytes were examined. It appears from these results that Separase is not required for metaphase I arrest. However, due to the inconsistancy among the repeats, more experiments are required to confirm this point.

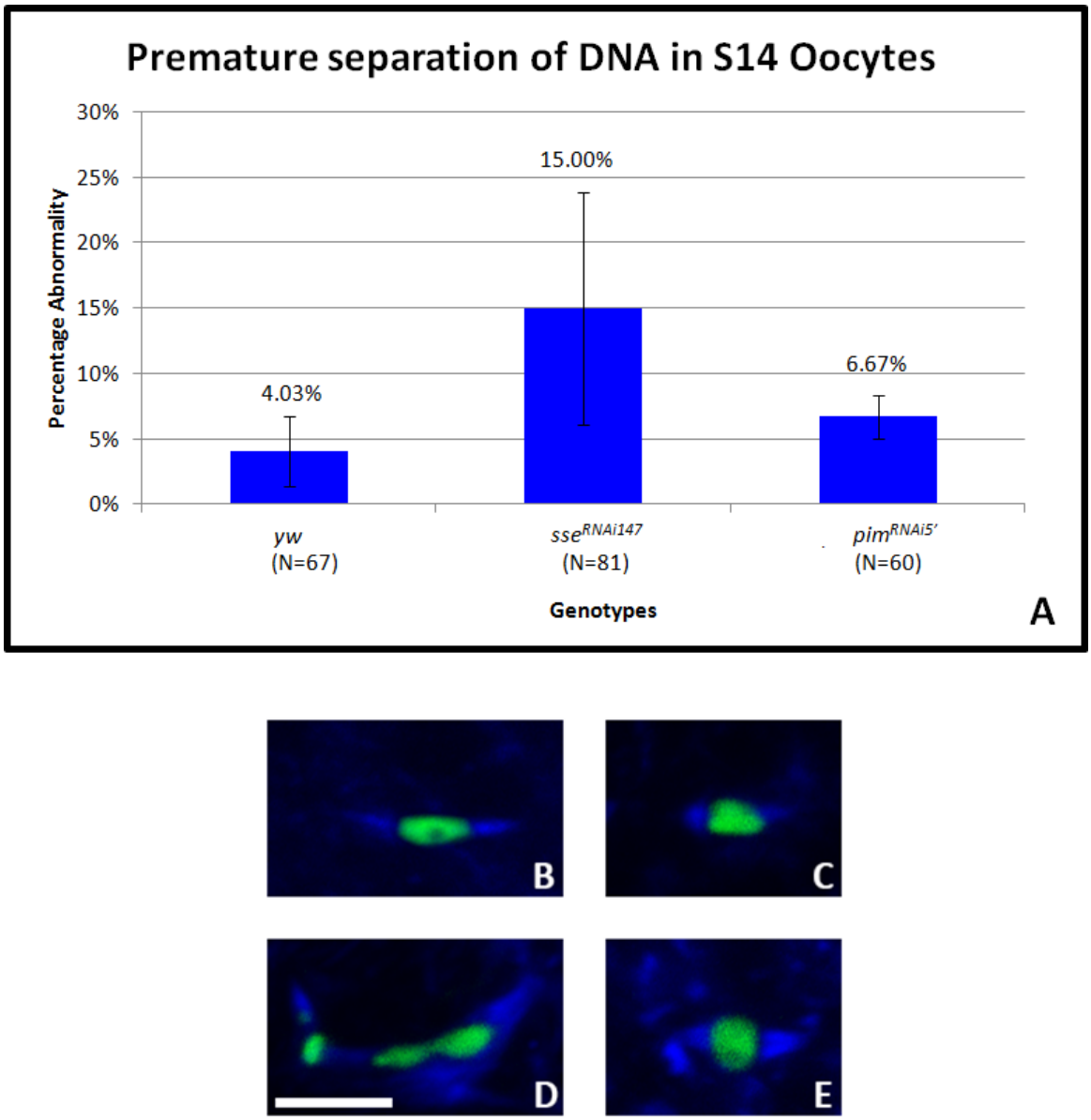

Fig 15. Quantitative analysis and confocal images of phenotypes in stage 14 oocytes collected from *yw*, *mat-GAL4; sse*^{RNAi147} and *mat-GAL4; pim*$^{RNAi5'}$ flies.
(A) Quantitative analysis of premature DNA separation in stage 14 oocytes. (B-E) Blue represents spindle, green represents DNA. (B) Normal metaphase I arrest in *yw*. (C-D) Phenotypes displayed in *sse*^{RNAi147}: (C) Normal metaphase I arrest. (D) Un-equally separated DNA. (E) Normal metaphase I arrest in *pim*$^{RNAi5'}$. The scale bar indicates 5um.

3.3.3 Separase is required for proper separation of homologous chromosomes and sister chromatids during meiosis

To study whether the activity of Separase is required for meiosis after egg activation, 0-20 mins and 0-1hr embryos collected from *mat-GAL4; sse*^{RNAi147} flies were stained for tubulin, centromere of X chromosome and either DNA (Fig 16A-16F) or arm regions of X chromosome (Fig 16G-16M). Most of the metaphase II phenotypes appeared to be normal where two equally separated DNA each with a single centromeric FISH signal were observed within a typical metaphase II spindle (Fig 16A). Separated centromeric signals each with one or two arm signals were also observed (Fig 16G). These phenotypes look similar to normal metaphase II seen in *yw* flies (Fig 5C and 5M), which indicates homologous chromosomes separated normally in most of the meiosis in *sse*^{RNAi147} embryos. However defect was found in few embryos displaying the metaphase II spindle, where the arm signal was located in central aster and separated centromeric signals were placed in the twin spindles (Fig 16H). Furthermore, the centromeric FISH signals on the right side of the spindle had already split into two, implying the onset of anaphase II. However, the centromeric signal on the left side was not separate yet but stretched, implying the release of centromeric sister-chromatid cohesion was negatively affected by the knockdown of *sse*. More interestingly, as both the spindle phenotype and centromeric FISH signals suggested that meiosis had gone into the second round, the sister chromatid arms still remained together indicated by a single arm FISH signal (Fig 16H). This further implies that not only the centromeric but the arm sister-chromatid cohesion was also negatively affected by the knockdown of *sse*. In addition to this abnormality, some of them displayed abnormal spindle together with separated but stretched DNA each with a centromeric FISH signal (Fig 16B). This phenotype indicates

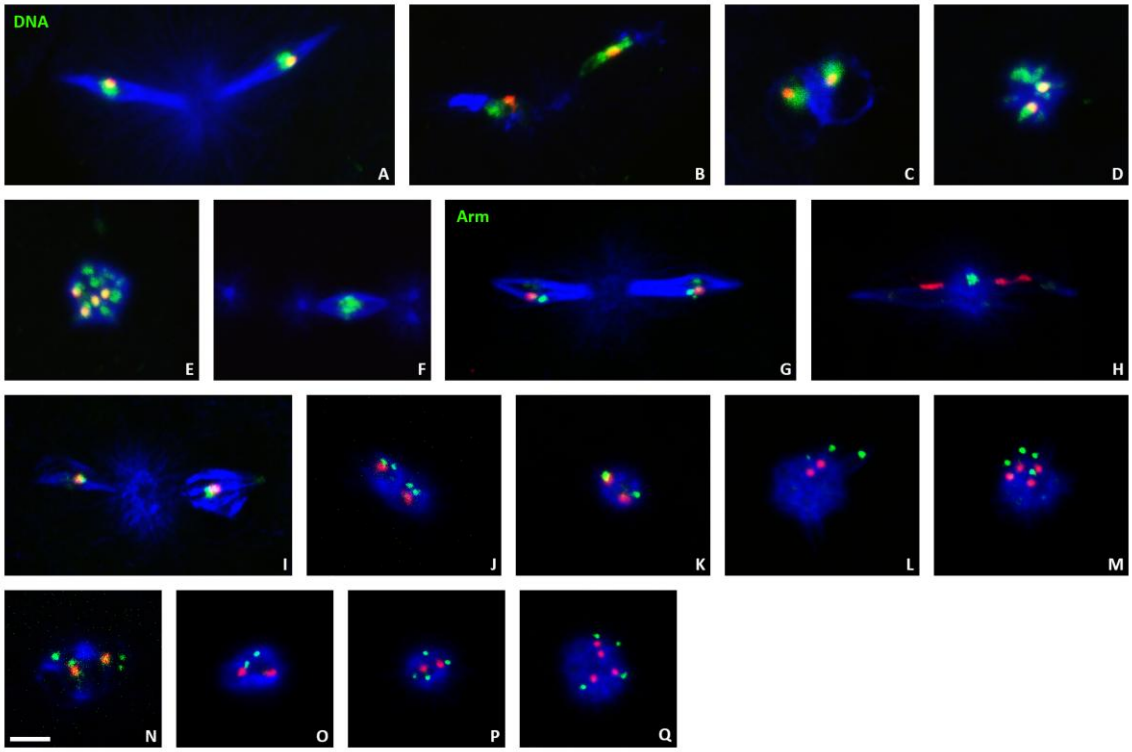

Fig 16. Confocal images of meiosis progression and/or polar body formation in embryos collected from *mat-GAL4; sse*^{RNAi147} and *mat-GAL4; sse*^{RNAi213} flies.
In (A-Q), blue represents spindle, red represents centromeric FISH signal; In (A-F), green represents DNA; In (G-Q), green represents arm FISH signal. (A-M) Phenotypes seen in embryos collected from *mat-GAL4; sse*^{RNAi147} flies: (A) Normal metaphase II with equally separated DNA and centromeric FISH signals. (B) Abnormal metaphase II with twisted spindle and stretched centromeric DNA. (C) Interphase showing only two DNA masses each with a centromeric signals. (D) Polar body with two centromeric signals. (E) Polar body with four centromeric signals. (F) Mitosis generated by male pronuclei with no centromeric signal. (G) Normal metaphase II displaying two separated centromeric signals each with either one (on the left) or two (on the right) arm signals. (H) Abnormal metaphase II spindle with three separated centromeric signals and one arm signal in the center. (I) Telophase II spindle containing two separated centromeric signals each with one arm signal. (J) Two meiotic products come together to form a polar body, each with a single centromeric signal associated with two arm signals. (K) Polar body with two centromeric and two arm signals. (L) Polar body with two centromeric and arm signals. (M) Polar body with four centromeric and four arm signals. (N-Q) Phenotypes seen in embryos collected from *mat-GAL4; sse*^{RNAi213} flies: (N) Interphase with two centromeric FISH signals each associated with two arm signals. (O) Polar body with two centromeric signals and two arm signals. (P) Polar body with two centromeric signals and four arm signals. (Q) Polar body with four centromeric signals and four arm signals. The scale bar indicates 5um.

that although homologous chromosomes somehow were separated in these cases, the attempt to separate sister chromatids had failed. Furthermore, among all of the *sse*^{RNAi147} embryos in meiosis, 81% (N=16) were in metaphase II. However, among all of the *yw* embryos in meiosis, only 5% of them were in metaphase II while 86% (N=21) were in latter meiotic stages of either anaphase II or telophase II. These data further demonstrated that meiosis is delayed at metaphase II in *sse*^{RNAi147}embryos. Importantly none of the *sse*^{RNAi147} embryos were found to exhibit four centromeric FISH signals even if it displayed a spindle that was similar to the one seen in *yw* telophase II (Fig 5E and 5O). In all of the telophase II spindles seen in *sse*^{RNAi147} embryos, only two separated centromeric signals each with one or two arm signals could be detected (Fig 16I). These findings demonstrate that the separation of sister chromatids in meiosis is largely inhibited by the knockdown of *sse*.

If there is no separation of sister chromatids, how is meiosis going to finish? Further analysis demonstrated that instead of forming four haploid nuclei (Fig 5F and 5P), only two meiotic products were generated. This was proved by the observation that among all of the *sse*^{RNAi147} embryos in post-meiotic interphase, 83% (N=12) of them displayed only two separated DNA masses (Fig 16C). Although most of these DNA masses were associated with only one centromeric FISH signal (Fig 16C), some of them were associated with two, indicating originally unseparated meiotic sister chromatids start to separate at this stage. More rarely, all of the centromeric signals were observed in only one of the two separated DNA masses, which implies the segregation of homologous chromosomes had completely failed. None of the interphase *yw* embryos (N=15) showed similar phenotypes. All the experimental results shown in this section demonstrated that

Separase is essential for the proper separation of homologous chromosomes and sister chromatids during meiosis.

3.3.4 Knockdown of sse generates abnormal polar bodies with four chromosomes

If there are only two meiotic products formed in *sse*^{RNAi147} embryos, will the formation of polar body still occur? If yes, what is the orientation of chromosomes in the polar body? Further studies revealed that after interphase, the two meiosis products came together. This was represented by two separated centromeric FISH signals with either separated (Fig 16J) or unseparated (Fig 16K) arm signals apparently coming together to form a polar body. The newly formed polar bodies commonly had only two centromeric signals (Fig 16D and 16L).

The phenotypes from meiosis to early polar body formation mentioned above were mainly collected from 0-20min *sse* knockdown embryos. Polar body phenotypes displayed in 0-1hr embryos indicated that the number of centromeric signals in the polar body gradually increased to the maximum of four (Fig 16E, 16M and Fig 6) (only 1 out of 113 polar bodies showed five centromeric signals). These observations imply that the centromeric regions of sister chromatids that did not separate during the second round of meiosis were finally separated from each other in the polar body. The arm FISH signals that represent the arm regions of sister chromatids were detected to be able to separate from each other as early as in metaphase II (Fig 16G) and as late as within the polar body (Fig 16L). Regardless of when they separate, the maximum number of arm signals commonly observed in a polar body of *sse* knockdown embryo is four (Fig 16M) (except 3 out of 85 polar bodies exhibited five arm signals). This matches with the maximum number of centromeric signals seen in the polar body. The phenotypes showed by both FISH signals (Fig 16M) indicating the four chromosomes are completely separated from

each other in the polar body. In *yw* flies, the polar body chromosomes are composed of two sister chromatids generated through DNA replication during interphase (Chapter 3.1). For $sse^{RNAi147}$ flies, most likely, the sister chromatids in the polar body failed to separate from each other because of the *sse* knockdown. Nonetheless, it is also possible that DNA replication during interphase is inhibited by *sse* knockdown. This will result in the lack of sister chromatids in the polar body chromosomes. However, the latter possibility is eliminated by the polar body phenotypes exhibited in the double knockdown of both *sse* and *vtd* as described below (Chapter 3.4).

3.3.5 Knockdown of sse results in early mitotic arrest in embryos

Compared to *yw* embryos (Fig 17A), only one or, less frequently, two mitotic spindles was observed together with polar body in all of the 85 examined $sse^{RNAi147}$ embryos that finished meiosis (Fig 6 and Fig 17B). This indicates that the progression of mitotic divisions had been blocked because of the knockdown of *sse*, presumably by preventing the cleavage of Rad21 that is crucial for the separation of sister chromatids (Oliveira, et al. 2010). Moreover, these mitotic spindles were found to contain either one (48%, N=58) or no (52%) centromeric FISH signal (Fig 16F), indicating a single or no X chromosome was present respectively. The absence of spindles with more than one centromeric signal suggets specifically a mitotic arrest prior to sister chromatid segregation. This is consistent with the expectation that the separation of sister chromatids is not going to occur without Separase. Furthermore, the observation of one or no centromeric FISH signal implies that these mitotic spindles were generated by male pronuclei only. This result is consistent with our finding that polar bodies contain all four female meiotic products after knockdown of *sse*.

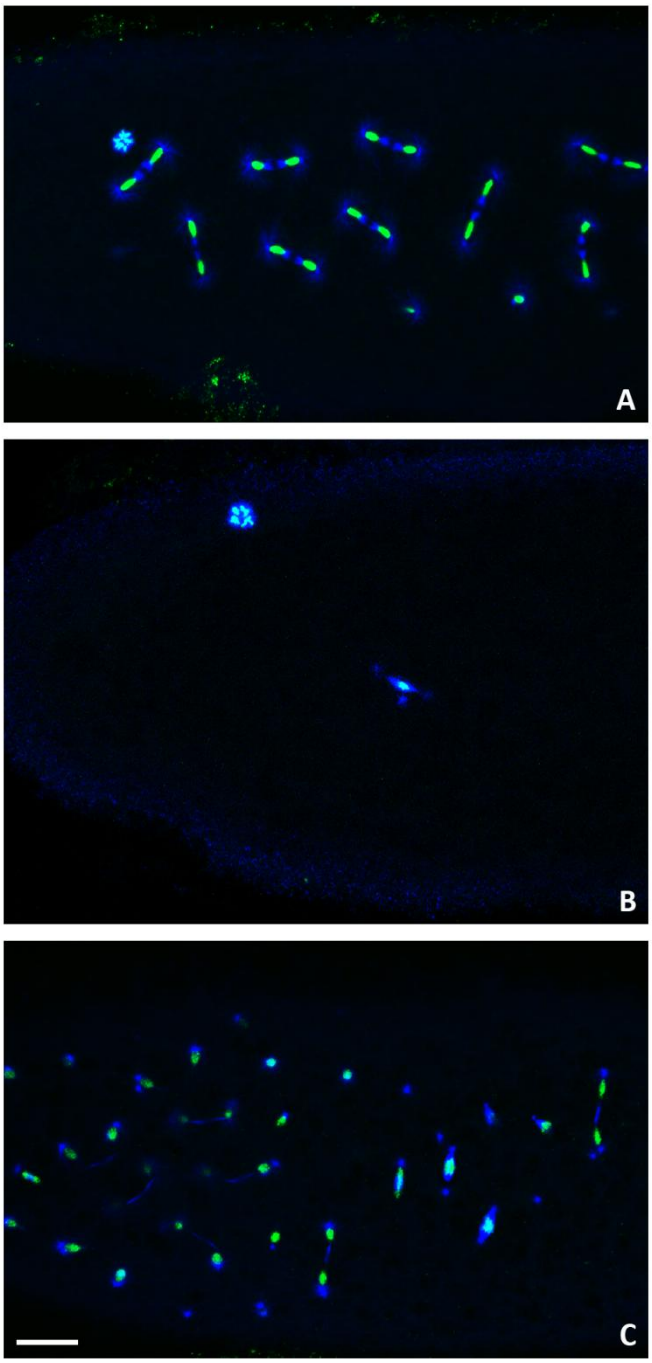

Fig 17. Confocal images of embryos collected from *yw*, *mat-GAL4; sse*^{RNAi147} and *mat-GAL4; pim*$^{RNAi5'}$ flies.
Blue represents spindle, green represents DNA. (A) *yw* embryo with synchronized mitotic divisions evenly distributed in the embryo. (B) *sse*^{RNAi147} embryo with one polar body and one male pronucleus. (C) *pim*$^{RNAi5'}$ embryo displaying abnormal distribution of non-synchronized mitosis with different spindle sizes. The scale bar indicates 20um..

3.3.6 Knockdown of sse is specific

To test for the specificity of *sse* knockdown, another fly line, $sse^{RNAi213}$, was generated with RNAi sequence that targets a different region of *sse* mRNA compared to $sse^{RNAi147}$. Phenotypes observed in 0-1hr $sse^{RNAi213}$ embryos show no difference from what was found in $sse^{RNAi147}$ embryos. As shown in Fig 16N-16Q, in $sse^{RNAi213}$ embryos, during interphase only two meiotic products were observed (Fig 16N). These two meiotic products formed a polar body that contains two centromeric FISH signals (Fig 16O and 16P). Similar with the polar body phenotypes displayed in $sse^{RNAi147}$ embryos, a maximum of four centromeric signals were also observed in $sse^{RNAi213}$ polar bodies (Fig 16Q). The separation time of arm signals is uncertain but the maximum number of arm signals detected is four (Fig 16N-16Q). Most commonly, only one mitotic spindle was found in these embryos. Given that two different RNAi lines give the same phenotypes, it is fair to say that the knockdown of *sse* by $sse^{RNAi147}$ is specific.

3.4 Double knockdown of sse and vtd

3.4.1 Rad21 is not the target of Separase in Drosophila meiosis

As mentioned before, Rad21 is not likely required for *Drosophila* meiosis (Chapter 3.2.3). However, the experimental results in *vtd* single knockdown do not completely eliminate the possibility that Rad21 serves as the kleisin subunit of Cohesin complex in meiosis since another mechanism may be involved in sister-chromatid cohesion in addition to the Separase-dependent anaphase pathway (see below in discussion, Chapter 4.2). Since Rad21 is a substrate of Separase (Warren, et al. 2000; Nasmyth, 2002), knockdown of *vtd* mimics the situation in which all of the Rad21 had been cleaved by Separase even in the situation where *sse* is knocked down. If Rad21 participates in the cohesion between sister chromatids during *Drosophila* meiosis, then knockdown of *vtd* together with *sse* should override the phenotypes generated by *sse* single knockdown during meiosis. To test if this is true, a combined RNAi fly line including both $sse^{RNAi147}$ and vtd^{RNAi} was generated. Preliminary experimental results showed that, after driving the expression of both RNAi using *mat67-GAL4* driver, the abnormal meiosis progression seen in $sse^{RNAi147}$ flies was not changed. For each of the meiotic phenotypes detected in $sse^{RNAi147}$-vtd^{RNAi} embryos, a corresponding similar phenotype can be found in $sse^{RNAi147}$ embryos (Fig 18A, 18B and 18C comparing to Fig 16G, 16I and 16K respectively). These results strongly demonstrated that Rad21 is not involved in the cohesion between sister chromatids as the target of Separase during meiosis.

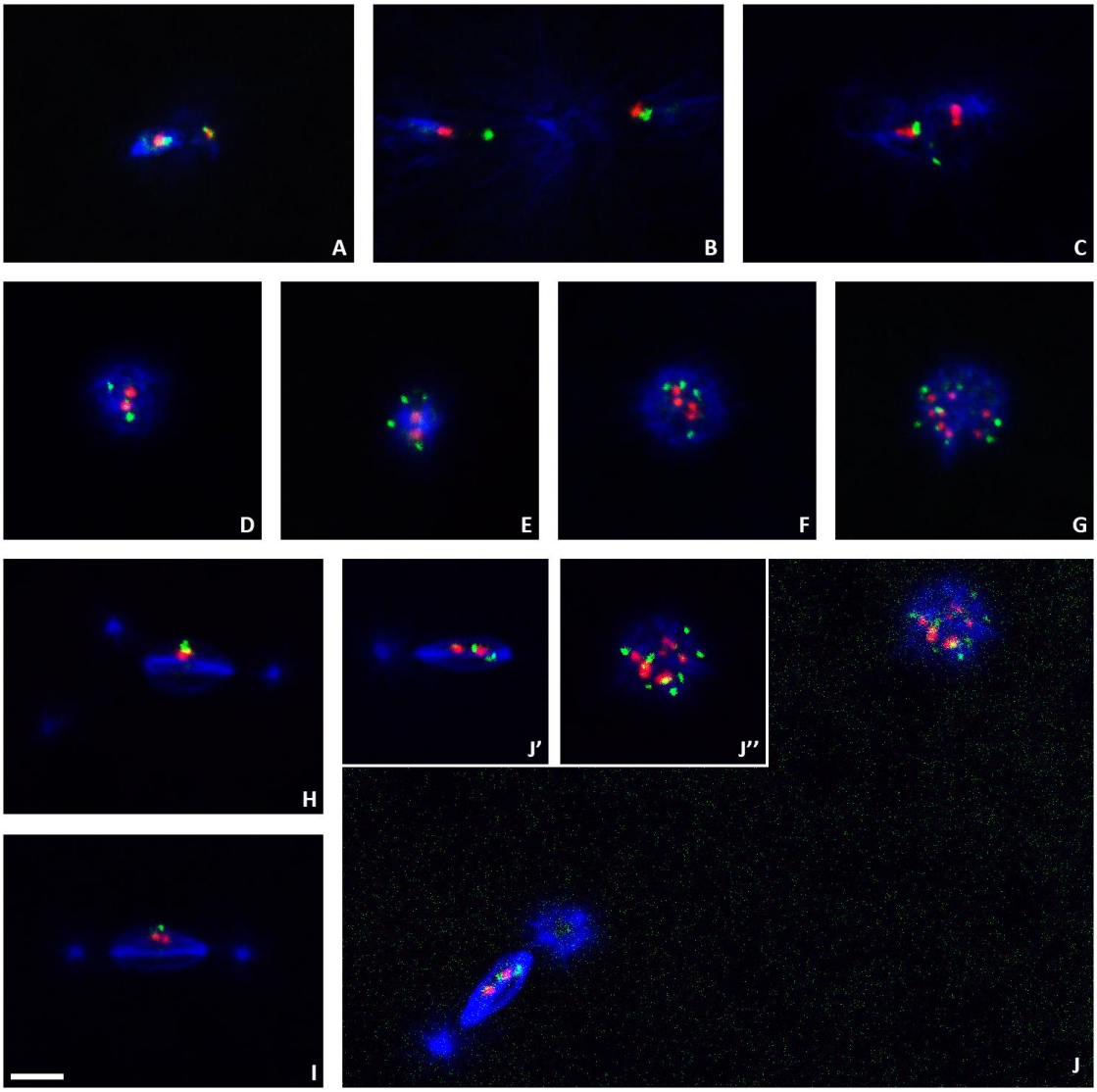

Fig 18. Confocal images of meiosis progression and polar body formation in embryos collected from *mat-GAL4; sse*^{RNAi147}*-vtd*^{RNAi} flies.
Blue represents spindle, red represents centromeric FISH signal, green represents arm FISH signal. (A) Normal metaphase II with two separated centromeric FISH signals, each with either one (on the left) or two (on the right) arm signals. (B) Abnormal meiosis II spindle containing two separated centromeric signals each with one arm signal. (C) Interphase spindle with two centromeric and two arm signals. (D) Polar body with two centromeric and two arm signals. (E) Polar body with two centromeric and four arm signals. (F) Polar body with four centromeric and four arm signals. (G) Polar body with eight centromeric and eight arm signals. (H) Mitosis generated by male pronuclei with one centromeric and one arm signal. (I) Mitosis generated by male pronuclei with two centromeric and one arm signal. (J) Embryo containing one mitotic spindle (J') and one polar body (J''); (J') A mitosis with two centromeric and two arm signals; (J'') A polar body with seven centromeric and eight arm signals. The scale bar indicates 5um.

3.4.2 Separase regulates sister-chromatid cohesion through cleavage of Rad21 in the polar body

As mentioned before, after knockdown of *sse*, an abnormal polar body with four separated chromosomes was generated (Fig 16M). This polar body phenotype is most likely a result of the failure to release the sister-chromatid cohesion at the arm region, though we can not be certain since it is not known whether these chromosomes are composed of two sister chromatids or not. To answer this question, polar bodies generated in $sse^{RNAi147}$-vtd^{RNAi} embryos were examined. The polar body phenotypes exhibited by $sse^{RNAi147}$-vtd^{RNAi} embryos (Fig 18D-18F) is similar to that seen in $sse^{RNAi147}$ embryos (Fig 16J-16M) and $sse^{RNAi213}$ embryos (Fig 16N-16Q). However, comparing to embryos with single knockdown of *sse*, in $sse^{RNAi147}$-vtd^{RNAi} embryos the maximum number of centromeric signals that can be observed has increased to eight (Fig 18G). This observation indicates that there are two sister chromatids in each of the chromosomes in the polar bodies of $sse^{RNAi147}$-vtd^{RNAi} embryos. This confirms the previous finding that knockdown of *sse* leads to defects in the separation of sister chromatid arms (Chapter 3.3.4) and Rad21 is required for the centromeric sister-chromatid cohesion in the polar body (Chapter 3.2.4). Furthermore, the maximum number of arm signals in polar bodies of $sse^{RNAi147}$-vtd^{RNAi} embryos has also increased to eight (Fig 18G). This phenotype indicates that the originally bound arm regions of sister chromatids are now separated because of the loss of Rad21. This demonstrates that Rad21 is also essential for the cohesion at the arm regions of sister chromatids in the polar body, presumably by serving as the kleisin subunit of Cohesin complex. This further implies that the defect generated in the polar body sister chromatid separation after knockdown of *sse* is caused by the

persistance of Rad21. Therefore, the separation of sister chromatid arms in the polar body is regulated by Separase through Rad21 cleavage.

3.4.3 Knockdown of Rad21cannot rescue the early mitotic arrest generated by sse knockdown

As mentioned before, knockdown of *vtd* leads to the loss of cohesion between sister chromatids in embryonic mitotic cycles and, in turn, results in non-synchronized mitotic divisions (Chapter 3.2.5). Meanwhile, knockdown of *sse* results in mitotic arrest in embryos that is presumably caused by persistence of Rad21 between sister chromatids (Chapter 3.3.5). Since Separase cleaves Rad21 during the metaphase to anaphase transition to release sister chromatids in mitosis (Nasmyth and Haering, 2009), the depletion of Separase should not generate any effect on the embryonic mitotic cycles where Rad21 is absent. Hence mitosis in the double knockdown embryos is expected to be similar to mitosis seen in *vtd* single knockdown (Chapter 3.2.5). However, contrary to our expectation, the mitosis phenotypes displayed in $sse^{RNAi147}$-vtd^{RNAi} embryos were not the same as those seen in *vtd* single knockdown but more similar to those observed in the single knockdown of *sse* (Chapter 3.3.5 and Fig 17B). According to the preliminary experimental results, in $sse^{RNAi147}$-vtd^{RNAi} embryos, 92% (N=25) of the mitotic divisions were arrested at very early stages (no more than two mitotic spindles), indicating knockdown of both *vtd* and *sse* did not push the embryonic mitotic cycles progress any further than solely knockdown of *sse*. This demonstrated that the persistence of Rad21caused by knockdown of *sse* is not the only reason for the early mitotic arrest in $sse^{RNAi147}$ embryos, which further implies a function of Separase other than Rad21 cleavage is important for the progression of mitosis in embryos.

While the mitotic divisions in *sse*^{RNAi147}-*vtd*^{RNAi} embryos were arrested with metaphase-like spindles, these mitosis exhibited three different FISH signal patterns. In some of the metaphase mitosis, one centromeric together with one arm FISH signal were observed (Fig 18H), indicating only one X chromosome was present. This is consistent with the failed meiosis and pronuclear migration discribed in *sse* knockdown embryos (Chapter 3.3.5). In another group of mitosis at metaphase, two centromeric signals with only one arm signal were detected (Fig 18I), indicating the centromeric region of sister chromatids were separated while the arm region still remains together. This abnormal metaphase phenotype was never seen in *yw* embryos and it implies that the abnormal separation of sister chromatids at centromeric regions was a consequence of *vtd* knockdown. This interpretation was further confirmed by the observation in which one abnormal mitotic metaphase spindle containing two centromeric and two arm signals was presented together with a polar body displaying eight arm signals in the same embryo (Fig 18J, 18J' and 18J"). Since there were eight arm signals seen in the polar body (Fig 18J"), no female pronucleus was produced to join with the male pronucleus. The presence of two FISH signals in this metaphase spindle (Fig 18J') indicates the complete separation of sister chromatids of the X chromosome coming from the male pronucleus, resulting from *vtd* knockdown. Overall, the pattern of FISH signals seen in mitosis of *sse*^{RNAi147}-*vtd*^{RNAi} embryos demonstrate that knockdown of *vtd* does lead to the separation of mitotic sister chromatids. However, mitotic divisions are still arrested with metaphase-like spindles, which further confirms our previous hypothesis that during the progression of embryonic mitotic cycles, Separase may have additional cellular function(s) other than the release of sister-chromatid cohesion.

3.5 Knockdown of pim in the ovary

Knowing Separase is required for the proper separation of homologous chromosomes and sister chromatids during meiosis, it is interesting to investigate whether Pim still serves as a regulator for Separase during this process. For this purpose, $pim^{RNAi5'}$ and $pim^{RNAi3'}$ transgenic flies were generated. After driving the expression of the RNAi in the ovary by *mat-GAL4*, it was found $pim^{RNAi5'}$ flies laid un-hatchable eggs but $pim^{RNAi3'}$ flies layed eggs that hatch at a frequency similar to wild type (data not shown). Since Pim is known to be required for mitosis during later stages of development (Stratmann and Lehner, 1996), we focused our study on $pim^{RNAi5'}$ assuming that its sterility was a consequence of efficient knockdown.

3.5.1 pim was knocked down efficiently

qRT-PCR was employed to test the knockdown efficiency of *pim* in stage 14 oocytes collected from $pim^{RNAi5'}$ flies. The experiment was repeated two times using mRNA extracts prepared independently from two groups of $pim^{RNAi5'}$ stage 14 oocytes. The results revealed that the *pim* mRNA level in $pim^{RNAi5'}$ is only 1.7% of that in *yw* (Fig 14B). This result demonstrated that *pim* was knocked down efficiently.

3.5.2 Pim is not required for metaphase I arrest

Evidence showed that Pim inhibits Separase in mitosis (Leismann, et al. 2000). Pim was also demonstrated to have positive role on the function of Separase (Stratmann and Lehner, 1996). Furthermore, it was demonstrated earlier that Separase is required for the proper separation of homologous chromosomes (Chapter 3.3.3). If Pim is only required for the inhibition of Separase in meiosis, then after knockdown of *pim*, we expect to observe the premature separation of homologous chromosomes caused by prematurely activated Separase. Alternatively, if Pim also has positive function on the

activity of Separase during meiosis, then we expect to observe normal metaphase I arrest since Separase would not be functional. To test which one of these two hypothesis is true, stage 14 oocytes, collected from *mat-GAL4; pim*$^{RNAi5'}$ fly lines, were examined. It was found that the majority of the stage 14 oocytes collected from *pim*$^{RNAi5'}$ flies exhibited a normal metaphase I arrested (Fig 15B and 15E). It was demonstrated that only 6.67% of *pim*$^{RNAi5'}$ oocytes showed premature DNA separation (Fig 15A). This percent of abnormality is very similar to that seen in *yw* oocytes. These observations match with our latter expectation, where Pim is required for the proper function of Separase. However, it could also be interpreted by another two possibilities: one is that Separase is not inhibited by Pim in meiosis and the other one is that Separase is inhibited by redundant mechanisms including Pim during the process.

3.5.3 Pim is not required for the proper completion of meiosis

If during meiosis, Pim has a positive effect on the function of Separase as in mitosis (Stratmann and Lehner, 1996), we expect that knockdown of *pim* will have the same effect on meiosis pregression that was seen with *sse* knockdown. To test if this is true, 0-20 mins and 0-1hr embryos collected from *mat-GAL4; pim*$^{RNAi5'}$ flies were stained for tubulin, centromere of X chromosomes and either DNA (Fig 19A-19F) or the arm of X chromosomes (Fig 19G-19I). It was found that all of the meiosis stages observed in *pim*$^{RNAi5'}$ embryos looked similar to that seen in *yw* embryos (Fig 19G and 19B comparing to Fig 5M and 5E respectively). A regular metaphase II spindle containing two separated centromeric FISH signals each with one or two arm signals were observed (Fig 19G), indicating homologous chromosomes separated properly. After that, during the metaphase II to anaphase II transition, two dividing DNA masses each with two centromeric signals were observed (Fig 19A). Normal anaphase II spindles with four DNA masses each

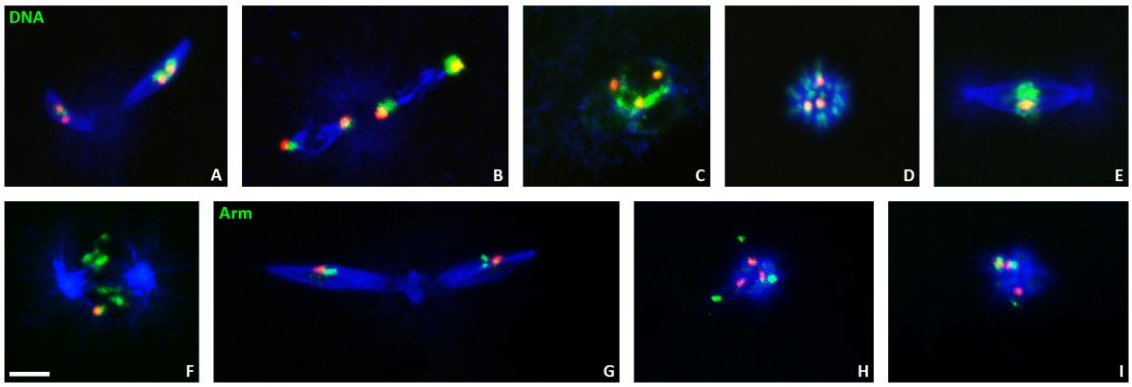

Fig 19. Confocal images of meiosis progression and polar body formation in embryos collected from *mat-GAL4; pim*$^{RNAi5'}$ flies.

In (A-I), blue represents spindle, red represents centromeric FISH signal; In (A-F), green represents DNA; In (G-I), green represents arm FISH signal. (A) The metaphase II to anaphase II transition, where two dividing DNA masses each with two centromeric FISH signals were observed in a metaphase II spindle. (B) Normal anaphase II with four separated DNA masses each with one centromeric signal. (C) Normal interphase with three diffused DNA each with one centromeric signal combining to form a polar body. (D) Polar body with three centromeric signals. (E) Normal mitosis at metaphase with one centromeric signal. (F) Abnormal mitosis with one centromeric signal. (G) Normal metaphase II with two centromeric signals each with either one (on the left) or two (on the right) arm signals. (H) Polar body with three centromeric and three arm signals. (I) Polar body with three centromeric and four arm signals. The scale bar indicates 5um.

accompanied by a single centromeric signal were also detected (Fig 19B). These phenotypes indicate that sister chromatids also separated normally. After meiosis, three meiotic products each with one centromeric FISH signal come together during interphase (Fig 19C) as in wild type (Fig 5F). These results presented so far indicate that depletion of Pim has no effect on meiosis progression.

3.5.4 Pim is required for sister-chromatid cohesion in the polar body

To determine if Pim is required for sister-chromatid cohesion in the polar body, the phenotypes displayed by polar bodies in $pim^{RNAi5'}$ embryos were examined. Normal polar bodies with three centromeric FISH signals (Fig 19D) were observed in almost all of the embryos (93%, N=57) that finished meiosis. The phenotypes displayed by these polar bodies exhibited no difference from that seen in *yw* embryos (Fig 5G). Further analysis with arm FISH probes revealed that among all of the $pim^{RNAi5'}$ embryos with polar bodies, around 75% of them had 3 arm signals in their polar body (Fig 19H and Fig 6). Most other polar bodies (21%) exhibited four arm signals (Fig 19I and Fig 6) while the ones with more than four arm signals were extremely rare (Fig 6). These polar body phenotypes are very different than what was seen in *yw* flies (Fig 5R). Given that most of the polar bodies in $pim^{RNAi5'}$ embryos displayed three centromeric and three arm FISH signals (Fig 19H), it is reasonable to conclude that the arm cohesion between sister chromatids persists in these polar bodies. This implies that Pim is required for proper separation of polar body sister chromatid arms. Since this arm separation is regulated by Separase (Chapter 3.4.2) and the polar body phenotype seen in $pim^{RNAi5'}$ embryos is similar to that seen in *sse* knockdown, where in both cases sister chromatid arms in most of the polar bodies did not separate. This further implies that Pim is required for proper function of Separase for the release of sister-chromatid cohesion in the polar body. This

matches with the hypothesis that Pim has positive effects on Separase (Stratmann and Lehner, 1996). However, a small group of *pim*$^{RNAi5'}$ polar bodies exhibited four arm FISH signals (Fig 19I). This is likely not a result of failed pronuclear migration since almost all of the polar bodies in *pim*$^{RNAi5'}$embryos exhibited three centromeric signals. These polar bodies with four arm signals are more likely generated by the loss of arm cohesion on only one of the polar body chromosomes, implying either Separase does not completely lose its function in the absence of Pim or that *pim* knockdown is incomplete.

3.5.5 Pim is required for the proper progression of synchronized mitosis in early embryo development

The early mitotic divisions in *pim*$^{RNAi5'}$ embryos appear to be normal. Fig 19E displays an example of normal metaphase mitosis found in a male embryo (containing only one centromeric FISH signal). As the number of mitotic divisions increased, more and more abnormal mitotic cycles appear. Fig 19F displays an example of abnormal mitosis. Unlike *yw* embryos, in which synchronized mitotic divisions were evenly distributed throughout the whole embryo (Fig 17A), randomly distributed non-synchronized mitotic cycles were observed in *pim*$^{RNAi5'}$ embryos (Fig 17C). All these phenotypes could be a consequence of elevated Separase activity without the inhibition of Pim or a loss of the positive function of Pim on Separase (Stratmann and Lehner, 1996).

3.5.6 Unhatchable pim$^{RNAi5'}$ *embryos can not be rescued by the expression of GFP-pim*^{wt}

To test whether wild type Pim is able to rescue the unhatchable *pim*$^{RNAi5'}$ embryos, both *pim*$^{RNAi5'}$ and *GFP-pim*^{wt} driven by a single copy of *mat-GAL4* was expressed in fly ovaries. Since *GFP-pim*^{wt} does not have the 5' UTR region that *pim*$^{RNAi5'}$ targets, its expression should not be affected by the RNAi. However, the embryos generated by these flies did not hatch either. This is not surprising, because not only knockdown of *pim* but

also over expression of even moderate amounts of *pim* causes defects in mitosis (Leismann, et al. 2000).

3.6 Non-degradable Pim

To study whether Pim has an inhibitory function on Separase during meiosis, non-degradable Pim with mutations on both D-box and Ken-box (*pim*$^{\Delta dk}$) (Batiha, 2013; Leismann, et al. 2000; Leismann and Lehner, 2003) were employed in our research. If Pim inhibits Separase during meiosis, then we expect that without the degradation of Pim, Separase activity will be blocked constantly. This will lead to embryonic phenotypes that are similar to those of *sse* embryos. According to the previous experimental results from our lab, it was found that embryos collected from *GFP-pim*$^{\Delta dk}$ flies (Table 2) appear to be able to get through meiosis though some aberrant meiosis were observed (Batiha, 2013). Furthermore, based on cytological appearance, it was also demonstrated that the non-degradable Pim caused failure of arm cohesion release in the polar body (Batiha, 2013). However, from this work, it is not known whether the GFP tag affects the function of Pim or not. In addition, these previous experiments were performed in the presence of endogenous Pim. It is possible that endogenous Pim compete with non-degradable Pim for binding to Separase. This could reduce the effect generated by non-degradable Pim since part of Separase will be active after the degradation of endogenous Pim. For this reason, in our research, *pim*$^{RNAi5'}$ flies were crossed to *GFP-pim*$^{\Delta dk}$ flies to generate recombinant transgenic flies that express both *pim* RNAi and non-degradable Pim. Since *pim*$^{RNAi5'}$ was designed to target the 5' UTR region of *pim* mRNA while *GFP-pim*$^{\Delta dk}$ mRNA does not have this region, *pim*$^{RNAi5'}$ is only going to knockdown the expression of endogenous *pim* but not *GFP-pim*$^{\Delta dk}$. In addition, to test whether the GFP tag affects the function of Pim or not, embryos that express *pim*$^{\Delta dk}$ (Table 2) without a GFP tag (generated by O. Batiha) were also examined. *mat-gal4* expression of *pim*$^{\Delta dk}$, *GFP-pim*$^{\Delta dk}$

and *pim*$^{RNAi5'}$-*GFP-pim*$^{\Delta dk}$ produced eggs that do not hatch, indicating defects in either meiosis or mitosis.

3.6.1 Degradation of Pim is required for proper meiosis

To study whether meiosis is affected by the failure to degrade Pim, 0-1hr embryos were collected from three fly lines that express non-degradable Pim driven by *mat-GAL4*: *pim*$^{\Delta dk}$ (Fig 20A-20C), *GFP-pim*$^{\Delta dk}$ (Fig 20D-20F) and *pim*$^{RNAi5'}$-*GFP-pim*$^{\Delta dk}$ (Fig 20G-20L). In both *pim*$^{\Delta dk}$ and *GFP-pim*$^{\Delta dk}$ embryos, meiosis appeared to progress normally. Metaphase II shaped spindles were observed with two separated DNA masses each with either one or two arm FISH signals (Fig 20A and 20D). Meiosis is also able to progress into anaphase II, where four separated DNA masses each with one arm signal were detected (Fig 20B and 20E). In Fig 20E, one of the DNA masses is not detected, but both spindle phenotype and the other three DNA and FISH signals suggested that anaphase II occurred and sister chromatids separated correctly. Furthermore, in *pim*$^{\Delta dk}$ and *GFP-pim*$^{\Delta dk}$ embryos, most of the interphases (73%, N=15) looked normal, where three diffused DNA masses each with one arm signal were detected (Fig 20C). However the rest of interphases (27%) showed abnormal phenotype where either two or, less frequently, three meiotic products were associated with arm signals in each of the two or two out of the three DNA masses (Fig 20F). These phenotypes are similar to the interphase seen in *sse* knockdown embryos (Chapter 3.3.3). This implies that failed or, at least, abnormal separation of sister chromatids that is caused by inactivation of Separase happened in a low frequency in the presence of both endogenous and non-degradable Pim. These results are consistent with the meiotic phenotypes observed in *GFP-pim*$^{\Delta dk}$ embryos as described in Batiha, 2013.

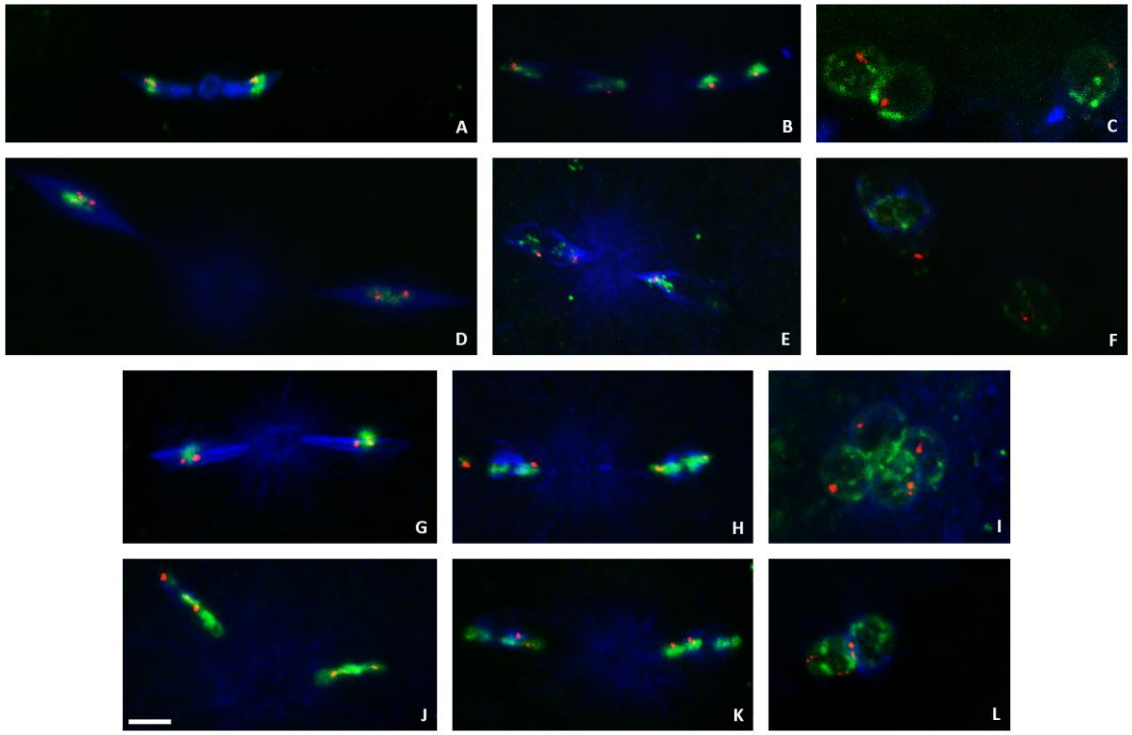

Fig 20. Confocal images of meiosis progression in embryos collected from *mat-GAL4; pim*$^{\Delta dk}$, *mat-GAL4; GFP-pim*$^{\Delta dk}$ and *mat-GAL4; pim*$^{RNAi5'}$*-GFP-pim*$^{\Delta dk}$ flies.
Blue represents spindle, red represents arm FISH signal, green represents DNA. (A-C) Phenotypes from *pim*$^{\Delta dk}$ flies: (A) Normal metaphase II. (B) Normal anaphase II. (C) Normal interphase. (D-F) Phenotypes from *GFP-pim*$^{\Delta dk}$ flies: (D) Normal metaphase II. (E) Anaphase II with only three DNA masses each containing one arm FISH signal. (F) Abnormal interphase with three DNA masses but only two of them contain arm signal. (G-L) Phenotypes from *pim*$^{RNAi5'}$*-GFP-pim*$^{\Delta dk}$ flies: (G) Normal metaphase II. (H) Abnormal anaphase II where on the left side three instead of two DNA masses were observed. (I) Interphase with four combining meiotic products each containing one arm signal. (J) Abnormal metaphase II with stretched DNA masses. (K) Abnormal anaphase II where only one of the DNA masses in each twin spindle contains arm signals. (L) Abnormal interphase with only two meiotic products one on the left containing two arm signals and one on the right containing one arm signal. The scale bar indicates 5um.

While non-degradable Pim has little effect in the presence of endogenous Pim, when expressed together with *pim* RNAi (*pim*$^{RNAi5'}$), defects started to be detected during meiosis progression. Although normal metaphase II oocytes (Fig 20G) were observed, indicating the separation of homologous chromosomes, anaphase II did not occur properly in *pim*$^{RNAi5'}$*-GFP-pim*$^{\Delta dk}$ embryos. Abnormally stretched DNA masses each with two arm signals were observed (Fig 20J), indicating resistance against the separation of sister chromatids was generated. In other cases, more than two DNA masses with separated centromeric FISH signals were observed in one of the twin spindles (Fig 20H). This indicates that although X chromosome sister chromatids are separated, defects were generated during the separation of other sister chromatids. Furthermore, anaphase II spindle with two separated DNA masses on each side had also been detected while only one of the DNA masses contained two arm FISH signals (Fig 20K). This phenotype indicates that separation of X chromosome sister chromatids is inhibited during anaphase II. These phenomena seen in *pim*$^{RNAi5'}$*-GFP-pim*$^{\Delta dk}$ embryos are similar but not as severe as those seen in the *sse* knockdown embryos, implying that sister chromatids did not separate properly with the persistence of non-degradable Pim. Among the interphase displaying *pim*$^{RNAi5'}$*-GFP-pim*$^{\Delta dk}$ embryos, 41% (N=17) of them exhibited abnormal interphase showing only two DNA masses each with one or two arm FISH signals (Fig 20L). This interphase phenotype is similar to those seen in *sse* knockdown embryos, indicating defects in sister chromatid separation occurred with the presence of non-degradable Pim. The increase in the interphase abnormality percentage in *pim*$^{RNAi5'}$*-GFP-pim*$^{\Delta dk}$ embryos (41%) comparing to *pim*$^{\Delta dk}$ and *GFP-pim*$^{\Delta dk}$ embryos (27%) matches with the predication that the inhibitory effect on Separase generated by non-degradable Pim will be increased by the knockdown of endogenous *pim*. In addition to these 41%

embryos, 29.5% embryos exhibited normal interphase with four DNA masses each containing one arm FISH signal (Fig 20I). While in these normal interphase phenotypes, four meiotic products were generated, none appeared to migrate to the male pronucleus. This may indicate a delay in the completion of meiosis, presumably resulting from the delayed sister chromatid segregation. Another 29.5% of interphases in *pim*$^{RNAi5'}$*-GFP-pim*$^{\Delta dk}$ embryos were without any defect and delay.

Overall, the results shown in this section demonstrated that non-degradable Pim generates defects in the release of sister-chromatid cohesion during meiosis, presumably through inhibiting the activity of Separase. However, the defects generated by non-degradable Pim are not as strong as those seen in *sse* knockdown, implying either Pim may not be the only regulatory mechanism for Separase during meiosis or the incomplete knockdown of endogenous *pim*.

3.6.2 Degradation of Pim is required for the release of sister-chromatid cohesion in the polar body

After meiosis, polar body formation was also examined in *pim*$^{\Delta dk}$ (Fig 21A-21D), *GFP-pim*$^{\Delta dk}$ (Fig 21E-21H) and *pim*$^{RNAi5'}$*-GFP-pim*$^{\Delta dk}$ (Fig 21I-21L) fly lines. In the embryos collected from the three non-degradable Pim expressing fly lines, most of the polar bodies were observed with either three (Fig 21A, 21E and 21I) or four (Fig 21B, 21F and 21J) arm FISH signals (Fig 6). The polar bodies with three arm signals are likely generated by normally progressed meiosis after which three female pronuclei come together during interphase. In addition, the separation of sister chromatid arms are blocked in these polar bodies. Since Separase is responsable for releasing arm sister-chromatid cohesion in the polar body (Chapter 3.4.2), non-degradable Pim blocks this release of coheison process presumably by inhibiting Separase activity. However, there

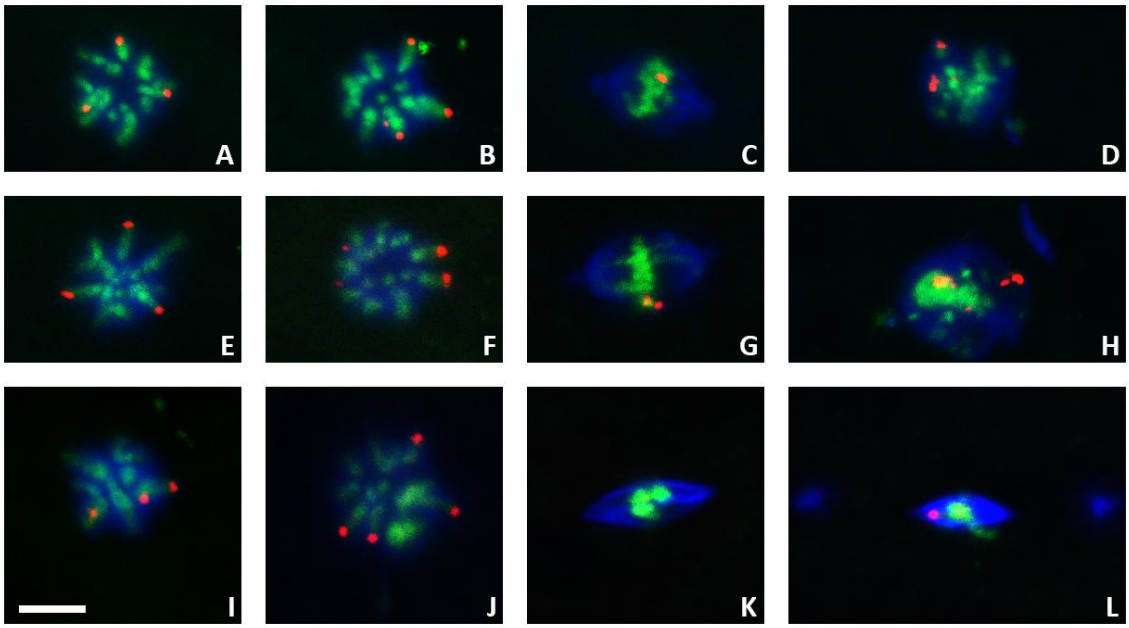

Fig 21. Confocal images of polar body and mitosis in embryos collected from *mat-GAL4; pim*$^{\Delta dk}$, *mat-GAL4; GFP-pim*$^{\Delta dk}$ and *mat-GAL4; pim*$^{RNAi5'}$*-GFP-pim*$^{\Delta dk}$ flies.
Blue represents spindle, red represents arm FISH signal, green represents DNA. (A-D) Phenotypes from *pim*$^{\Delta dk}$ flies: (A) Polar body with three arm FISH signals. (B) Polar body with four arm signals. (C) Normal mitosis. (D) Abnormal mitosis. (E-H) Phenotypes from *GFP-pim*$^{\Delta dk}$ flies: (E) Polar body with three arm signals. (F) Polar body with four arm signals. (G) Normal mitosis. (H) Abnormal mitosis. (I-L) Phenotypes from *pim*$^{RNAi5'}$*-GFP-pim*$^{\Delta dk}$ flies: (I) Polar body with three arm signals. (J) Polar body with four arm signals. (K) Mitosis generated by male pronuclei without arm signal. (L) Mitosis generated by male pronuclei with one arm signal. The scale bar indicates 5um.

are also cases where four polar body arm signals were detected. This may be caused by either the separation of one of the polar body chromosomes due to the incomplete inhibition of Separase or the combination of all of the four meiotic products due to the delayed meiosis process. However, it was revealed that in the three non-degradable Pim expressing fly lines, almost all of the polar bodies exhibited either three or four arm FISH signals. This distribution pattern of polar body arm signals is very different than that seen in *yw* flies and implies that the sister chromatid separation in the polar body is blocked by non-degradable Pim.

3.6.3 Degradation of Pim is required for syncytial mitosis

After meiosis, a small group of embryos collected from both $pim^{\Delta dk}$ and *GFP-*$pim^{\Delta dk}$ flies exhibited more than two cycles of mitotic divisions (Fig 6). Both normal (Fig 21C and 21G) and abnormal (Fig 21D and 21H) phenotypes were observed among these mitosis. However, in $pim^{RNAi5'}$*-GFP-*$pim^{\Delta dk}$ embryos, mitotic divisions were arrested at very early stages (Fig 6). These phenotypes are consistent with the previous finding that the degradation of Pim is required for mitosis progression (Batiha, 2013).

Further analysis revealed that the mitosis in $pim^{RNAi5'}$*-GFP-*$pim^{\Delta dk}$ embryos are likely to be generated from male nucleus only, since 45% (N=20) of them showed no arm FISH signal (Fig 21K) while the rest of them showed only one arm signal (Fig 21L). These mitosis phenotypes seen in $pim^{RNAi5'}$*-GFP-*$pim^{\Delta dk}$ embryos are very similar to that observed in *sse* knockdown embryos. Furthermore, the distribution of polar body arm FISH signals were also very similar comparing between $pim^{RNAi5'}$*-GFP-*$pim^{\Delta dk}$ and $sse^{RNAi147}$ fly lines (Fig 6). This further confirms our previous findings that throughout the progression from meiosis to polar body formation: the expression of non-degradable Pim

always results in similar phenotypes seen after knockdown of *sse*, presumably by inhibiting Separase.

3.7 Knockdown of cycB in ovary

In addition to Pim, CycB-Cdk1 could be another inhibitor of Separase during meiosis, since it was found to be required for the proper progression of meiosis (Dhaliwal, 2011). To study whether this is true and to identify other potential functions that CycB may have during meiosis, two RNAi lines were obtained: *cycB*^{RNAi1015} and *cycB*^{RNAi1896}. After expressing *cycB* RNAi with *mat-GAL4* in fly ovaries, it was found that both fly lines laid un-hatchable eggs, indicating defects in embryo development. To study whether the defect(s) are generated in meiosis, stage 14 oocytes collected from these fly lines were first examined.

3.7.1 cycB was knocked down efficiently

To test the knockdown efficiency of *cycB* in *mat-GAL4;cycB*^{RNAi1896} flies, CycB expression level in stage 14 oocytes was analyzed by Western blot. After three repeated Westerns using independently collected stage 14 oocytes, it was shown that the expression level of CycB in *cycB*^{RNAi1896} is 19.6% of that in *yw* (Fig 22A), indicating the knockdown for *cycB* was efficient in *cycB*^{RNAi1896} flies. In addition, similar knockdown efficiency was also observed in stage 14 oocytes collected form *cycB*^{RNAi1015} fly line (M. Bourouh, unpublished).

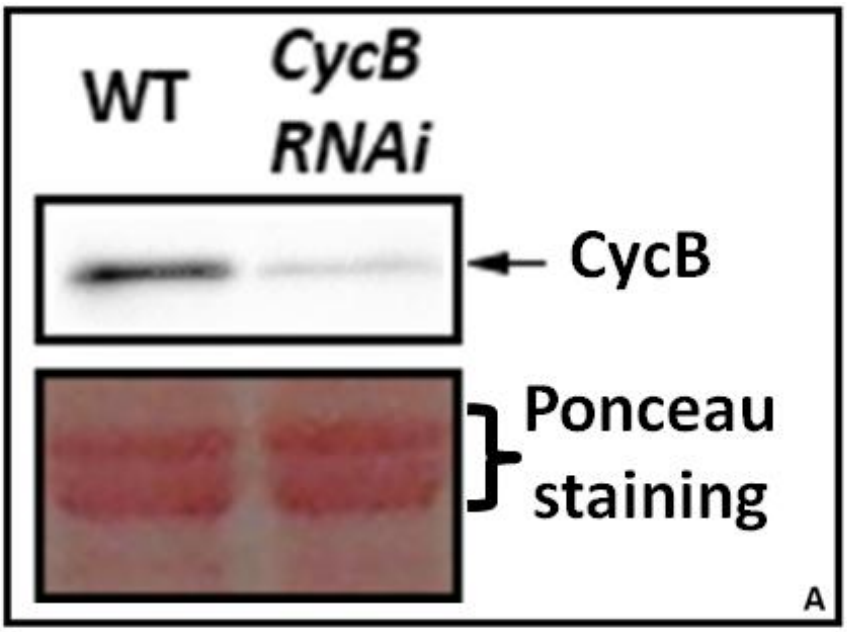
WT
CycB
RNAi
CycB
Ponceau
staining
A

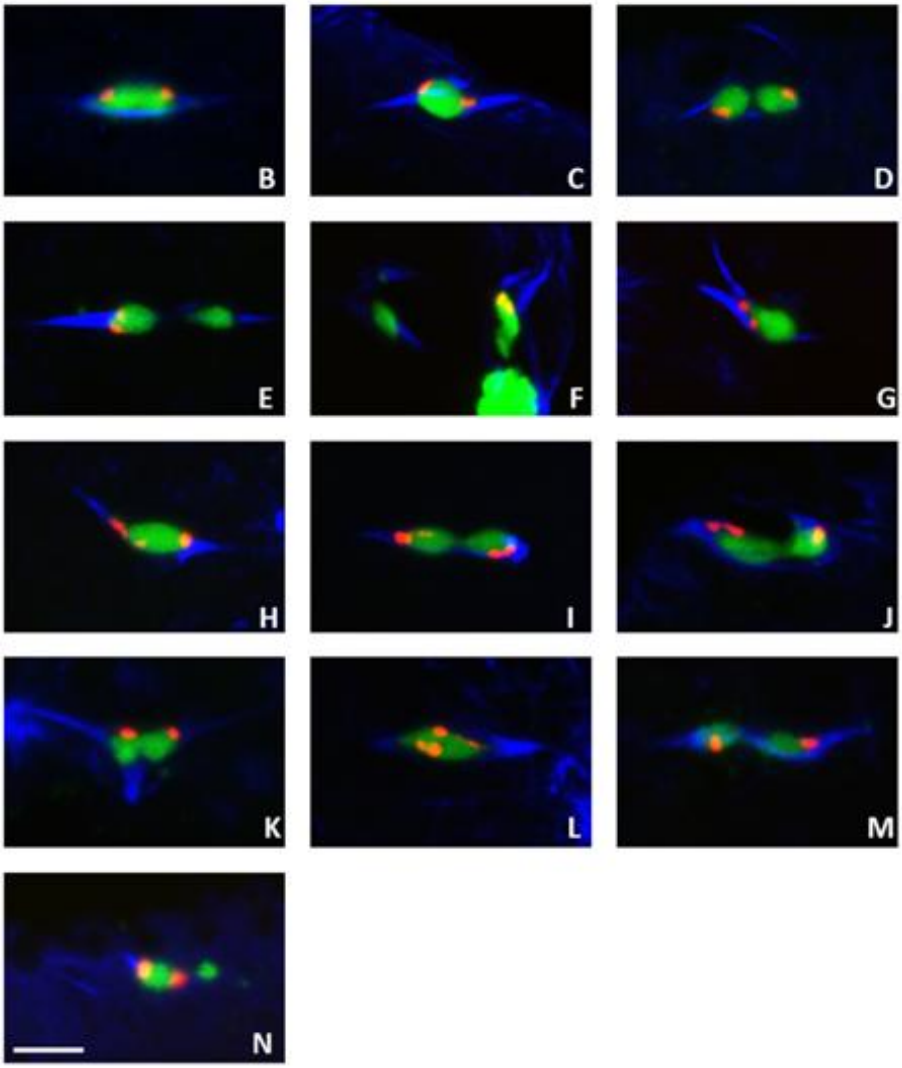
B
C
D
E
F
G
H
I
J
K
L
M
N

Fig 22. Western analysis and confocal images of stage 14 oocytes collected from *yw*, *mat-GAL4; cycB*^{RNAi1896} and/or *mat-GAL4; cycB*^{RNAi1015} fly lines.
(A) A representative figure selected from one of the three Westerns showing that CycB expression level is dramatically reduced in *cycB*^{RNAi1896} comparing to that in *yw*. Loading was determined by measuring the intensity of Ponceau staining of a region of the blot. According to the results collected from the three repeated experiments, the expression level of CycB in *cycB*^{RNAi1896} is 19.64±2.49% of that in *yw*. (B-N) Blue represents spindle, red represents centromeric FISH signal, green represents DNA: (B) Normal metaphase I arrest in *yw* stage 14 oocyte. (C-K) Metaphase I arrest phenotypes from *cycB*^{RNAi1896} stage 14 oocyte: (C) Normal metaphase I arrest. (D) Two equally separated DNA masses each with a single centromeric FISH signal in a abnormal spindle. (E) Two unequally separated DNA masses with only one of them containing two centromeric signals. (F) More than two unequally separated DNA masses with only one of them containing two centromeric signals in an abnormal spindle. (G) One DNA mass with two centromeric signals in a tri-polar spindle. (H) A single DNA mass with broken centromeric signals. (I) Two equally separated DNA masses with broken centromeric signals. (J) Two un-equally separated DNA masses with broken centromeric signals. (K) Two equally separated DNA masses each with one centromeric signal in a tri-polar spindle. (L-N) Metaphase I arrest phenotypes from *cycB*^{RNAi1015} stage 14 oocyte: (L) A single DNA mass with broken centromeric signals. (M) Two equally separated DNA masses each with a centromeric signal. (N) Two unequally separated DNA masses with only one of them containing centromeric signals in abnormal spindle. The scale bar indicates 5um.

3.7.2 CycB is required to maitain proper metaphse I arrest

To study whether CycB is required for metaphase I arrest, stage 14 oocytes collected from *cycB*^{RNAi1896} embryos were compared to those seen in *yw* embryos (Fig 22B-22N). As mentioned before, during metaphase I in *yw* flies, homologous chromosomes are held together while the centromeric regions are stretched towards the opposite spindle poles (Fig 22B). This normal DNA configuration during metaphase I arrest is detected in the majority of the *cycB*^{RNAi1896} stage 14 oocytes (Fig 22C). However, among all of the *cycB*^{RNAi1896} stage 14 oocytes examined, 26.4±7.3% (N=145) of them exhibited defects in maintaining normal metaphase I. This percentage of abnormality is much higher than that found in *yw* flies (4.2±1.5%, N=94). The abnormal DNA phenotypes can be basically characterized into three groups. In the first group, premature DNA separation indicated by equal or more than two DNA masses was observed (Fig 22D-22F and 22I -22K). This implies the complete (2 DNA masses) or partial (more than 2 DNA masses) premature separation of homologous chromosomes during metaphase I arrest. The second group of DNA abnormalities are represented by the observation of two centromeric FISH signals located in a single DNA mass after premature DNA separation (Fig 22E and 22F). This, as mentioned before, indicates the mis-segregation of homologous chromosomes. The third group of DNA abnormality is represented by the observation of a single DNA mass in a properly formed spindle but the centromeric FISH signal appears broken apart (Fig 22H-22J) instead of the intact single dot that is normally seen (Fig 22C). This phenotype may result from increased stretching force from the spindle. For some embryos, DNA and FISH was combined with tubulin staining. This revealed that 30% (N=27) of them showed abnormal spindle phenotypes (Fig 22D, 22F, 22G and 22K) such as tri-polar spindle (Fig 22G and 22K). Interestingly, these spindle

abnormalities do not always correlate with aberrant chromosome configurations (Fig 22D, 22F and 22I-22K comparing to Fig 22G).

3.7.3 Knockdown of cycB is specific

Most of these abnormal metaphase I phenotypes generated after depletion of CycB level in stage 14 oocytes had already been discovered by a former master student (Dhaliwal, 2011). However, in that research, a different method of reducing the level of CycB had been employed other than *cycB* RNAi. The only abnormal phenotype that was not described is the broken centromeric FISH signal (Fig 22H-22J). This abnormal phenotype was observed again in the stage 14 oocytes collected from another *cycB* RNAi fly line, $cycB^{RNAi1015}$ (Fig 22L). This fly line expresses RNAi against a different part of *cycB* mRNA than that of $cycB^{RNAi1896}$ fly line. All of the other abnormal metaphase I phenotypes found in $cycB^{RNAi1896}$ stage 14 oocytes were observed in $cycB^{RNAi1015}$ oocytes (Fig 22M and 22N). These observations together with previous findings discovered by Dhaliwal demonstrate that the knockdown of *cycB* in $cycB^{RNAi1896}$ flies is specific.

Chapter 4. Discussion

4.1 Regulation of homologue separation and segregation during anaphase I

4.1.1 Depletion of CAP/Rad21 or CycB generate similar defects during metaphase I arrest but the underlying molecular mechanisms are likely to be different

After knockdown of *CAP* or *vtd* (*CAP*/*vtd*), premature DNA separation and mis-segregation of homologous chromosomes was observed in metaphase I arrest in stage 14 oocytes (Chapter 3.2.2). These abnormalities were also detected after knockdown of *cycB* (Chapter 3.7.2). However, the molecular mechanisms behind the knockdowns of *CAP*/*vtd* or *cycB* could be very different.

It was known that homologous chromosomes are held together by both chiasmata and sister-chromatid cohesion (Buonomo, et al. 2000). From our experiments, no evidence was found to support the idea that CAP and Rad21 contribute to the cohesion between sister chromatids during meiosis since no more than two centromeric FISH signals had ever been observed during metaphase I (Chapter 3.2.2-3.2.3 and 3.4.1). The experimental data from another study also demonstrated that premature cleavage of Rad21 does not affect sister-chromatid cohesion (Urban, et al. 2014). However, there are uncertainties in both of these studies. In our experiments, a small amount of Rad21 could still persist after the knockdown of *vtd* (Fig 7) and this may be enough to sustain centromeric sister-chromatid cohesion during meiosis. In the Urban 2014 paper, they could not exclude the possibility that the premature cleavage of Rad21 could be blocked by the binding of Shugoshin-PP2A complex at centromeric region (Gutierrez-Caballero, et al. 2012). Furthermore, it is possible that CAP and Rad21 are only responsible for the arm but not the centromeric cohesion during meiosis. However, other research does not support this hypothesis, since stabilized Rad21 did not generate any defects in meiosis but

successfully blocked mitosis (Urban, et al. 2014). Taking all these facts into consideration, it may be concluded that CAP and Rad21 are not likely to contribute to sister-chromatid cohesion during meiosis. Since CAP serves as one of the backbone proteins for the ring structure of Cohesin complex, unless there is a substitution for it that has not been discovered yet, the importance of Cohesin complex in *Drosophila* meiosis is also brought into question.

Because sister-chromatid cohesion is unlikely to be affected by the knockdowns of *CAP* and *vtd*, the premature separation of homologous chromosomes observed in these knockdowns is presumably caused by the failed formation of chiasmata. Then, how are the Cohesin complex components involved in this process? It was demonstrated that Rad21 is required for the maintenance of synaptonemal complexes (SC) during prophase, presumably through interacting with one of the important SC components, C(2)M (Urban, et al. 2014; Manheim and McKim, 2003). Although there is no direct evidence yet, CAP may also play a role in maintaining SC since it was found to be associated with C(2)M too (Heidmann, et al. 2004). Inactivation of Rad21 led to the premature dissociation of SC (Urban, et al. 2014). We expected that the same situation also stays true after loss the function of CAP. Therefore, the premature homologous chromosome separation generated by knockdown of either *CAP* or *vtd* is presumably caused by difficulties in maintaining SC that is important for the formation of chiasmata (Jang, et al. 2003; Mehrotra and McKim, 2006). In this model, since both CAP and Rad21 are involved in maintaining SC, presumably through interacting with one of the SC components, C(2)M (Urban, et al. 2014; Heidmann, et al. 2004), they are likely to function in the same molecular pathway. Hence, single knockdown of either CAP or Rad21 should affect the pathway in a similar degree and it is also expected that double knockdown of both of

them does not produce more severe abnormalities. Indeed, there was no obvious difference produced among the premature DNA separation percentages generated by either the single knockdowns or the double knockdown (Fig 8). Furthermore, it was found that the *mat-GAL4* driver is expressed during prophase in S1 oocytes (Urban, et al. 2014) but the SC assembly starts earlier during the generation of the 16-cell cyst (Lake and Hawley, 2012). This could be the reason that only low percentages (around 17%, Fig 8) of premature DNA separation were detected in the knockdowns driven by *mat-GAL4*. However, similar abnormal metaphase I phenotypes with increased premature DNA separation percentages were detected after substituting *mat-GAL4* driver with *nanos-GAL4* that expresses much earlier (Chapter 3.2.2; Wang, et al. 1994). This matches with the expectation that the earlier SC is affected the more severe consequences will be generated.

CycB was not reported to be involved in the formation and maintenance of SC during meiosis. However, in mitosis, at least in vertebrate cells, CycB-Cdk1 inhibits Separase (Gorr, et al. 2005). Separase was demonstrated to be essential for the separation of both homologous chromosomes and sister chromatids during meiosis (Chapter 3.3.3). Hence, the premature homologous chromosome separation observed after knockdown of *cycB* could be the result of premature activation of Separase. This early activation of Separase only releases the cohesion between homologous chromosomes but not sister chromatids, since Shugoshin should be still protecting the centromeric region during metaphase I (Gutierrez-Caballero, et al. 2012). If this model is true, we expect that after knockdown of both *cycB* and *sse*, the premature homologous chromosome separation caused by *cycB* knockdown will be suppressed. By the same principle, if both CycB and Shugoshin are eliminated, we expect to see early separation of sister chromatids, because

the prematurely activated Separase will release the cohesion at centromeric regions that are no longer protected by Shugoshin.

Although the molecular mechanisms that leads to homologous chromosome separation are different after knockdown of either *CAP*/*vtd* or *cycB*, the consequences of this premature separation could be similar. In the situation where all of the homologous chromosomes within the oocyte are separated, anaphase I will happen prematurely (Fig 23A). During this process, the microtubules coming from the same spindle pole could attach to the kinetochores of both homologous chromosomes and this will result in the mis-segregation of the homologues to the same spindle pole instead of opposite poles (Fig 23B). Furthermore, if only some of the homologous chromosomes are detached within a oocyte, these homologues will be pulled apart while the rest will still be attached together. The pulled away homologous chromosomes could drift away from other ones and result in the appearance of multi DNA masses. Afterwards, microtubules may assemble around the randomly separated chromosomes and hence lead to abnormal spindle phenotypes. Indeed, all of these phenomena were observed after knockdown of either *CAP*/*vtd* or *cycB*.

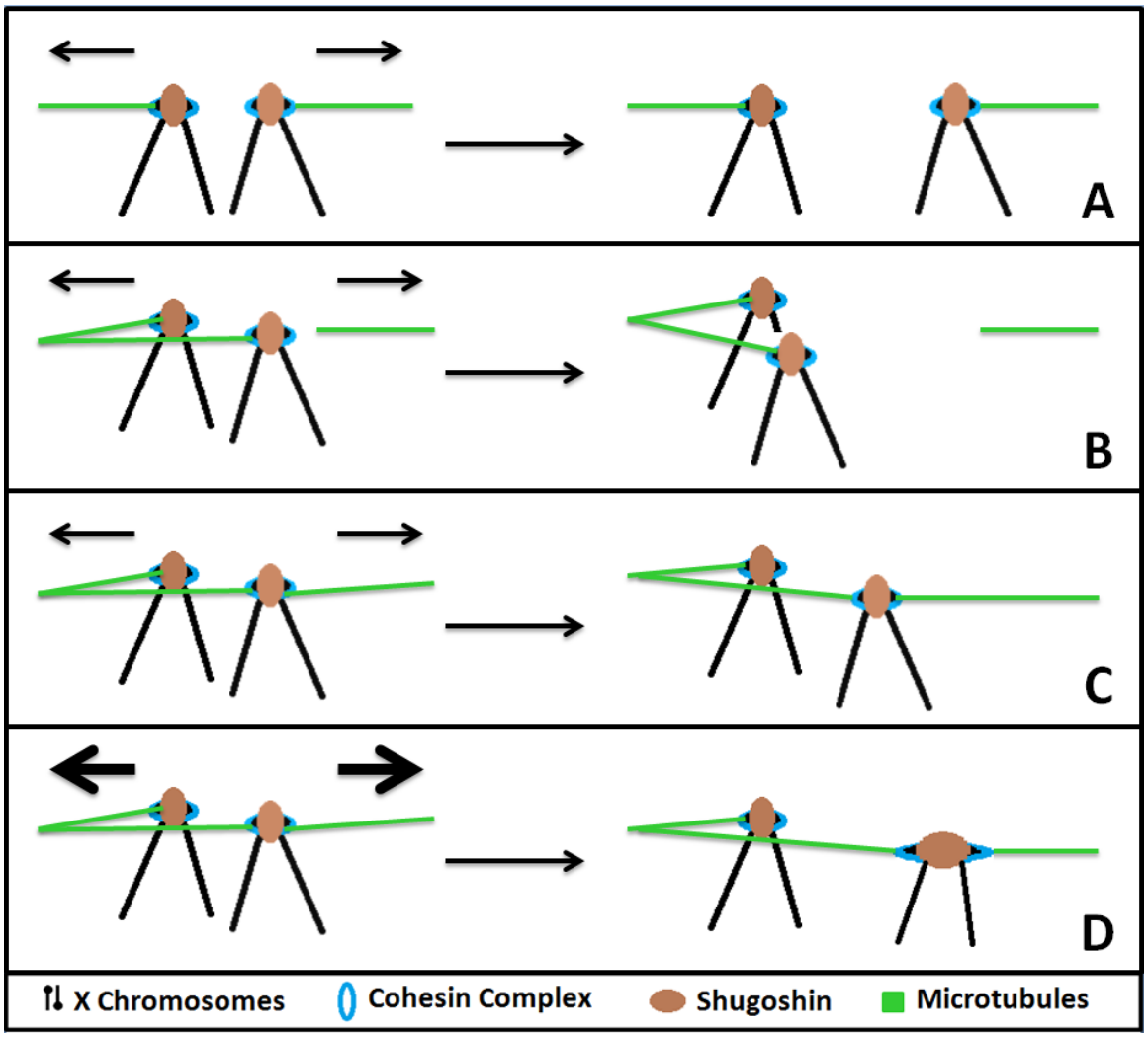

Fig 23. Possible models for microtubule attachment after the premature separation of homologous chromosomes.
(A) Normal attachment of microtubules to the kinetochores of homologous chromosomes. (B) Kinetochores of both homologous chromosomes are attached to the microtubules coming from the same pole of spindle, leading to the mis-segregation of homologues. (C-D) Kinetochore of one of the homologous chromosomes is attached to the microtubules coming from the two opposite poles of spindle. This may lead to the stretched or even broken centromeric region of a chromosome if the stretching force of microtubules increases to a certain level (D). **(**For convenience, only X chromosomes are exhibited in this figure. Thicker arrow indicates greater stretching force generated by microtubules).

4.1.2 CycB has additional cellular functions other than maintaining cohesion between homologues during metaphase I

Besides the abnormal chromosome separation phenotypes mentioned above, other phenotypes of broken centromere and spindle abnormality that were not seen in *CAP/vtd* knockdown were also observed after the knockdown of *cycB*. This difference implies that CycB may have extra functions during metaphase I arrest other than maintaining the cohesion between homologous chromosomes. It was previously shown that CycB associates with the meiotic spindle from metaphase I to anaphase II (Swan and Schupbach, 2007). Therefore, it is possible that CycB is also required for spindle organization during meiosis. Knockdown of *cycB* may result in defects in meiotic spindle organization such as tri-polar spindles (Fig 22). Moreover, the degradation of CycB was proven to be essential for proper sister chromatid segregation during mitosis, presumably through increasing the stretching force of microtubules by inactivating the Cdk1 located near the chromosomes (Shindo, et al. 2012). Hence, knockdown of *cycB* during metaphase I mimics the situation of premature CycB degradation and should also increase microtubule stretching force. This increase of stretching force does not generate obvious defects when the microtubule attachment on homologous chromosomes are like those shown in Fig 23A and 23B. However, after the premature separation of homologues, there should be circumstances in which microtubules from both spindle poles attach on the kinetochores of sister chromatids within a single chromosome (Fig 23C and 23D). Under such a condition, if the stretching force of microtubules increases because of the knockdown of *cycB*, the centromeric region of the chromosome could be broken by the force (Fig 23D). This phenotype was not observed after either single or double knockdown of *CAP* and/or *vtd*.

4.1.3 CycB is not the only candidate for the regulation of metaphase I to anaphase I transition

Considering that the degradation of CycB is important for both homologous chromosome separation and microtubule tension suppression during metaphase I, we expect to observe a high frequency of abnormality in the stage 14 oocytes after knockdown of *cycB*. However, according to the experiments, only around 30% abnormality was detected (Chapter 3.7.2). One possible explanation could be that although CycB levels in stage 14 oocytes had decreased to around 18% (Chapter 3.7.1), the remaining CycB was able to sustain its normal function in most of the oocytes. Another possibility is that CycB may not be the only regulator that is responsible for those cellular events during metaphase I. CycA could be a candidate that shares redundant functions with CycB during this process. Since preliminary experimental results from our lab suggest that non-degradable CycA may block the segregation of sister chromatids (Dhaliwal, 2011), indicating that CycA could be responsible for the suppression of microtubule tension during the second round of meiosis while its role in earlier meiosis stages remains unknown. Furthermore, in *Drosophila* mitosis, non-degradable CycA delayed the separation of sister chromatids (Sigrist, et al. 1995; Jacobs, et al. 2001) and enhanced the effect of stabilized Pim (Leismann and Lehner, 2003). These observations suggest that CycA may have the ability to inhibit Separase during mitosis, presumably through the molecular mechanism similar to that of CycB-Cdk1 (Gorr, et al. 2005). Therefore, CycA could serve a redundant role with CycB during metaphase I. If this hypothesis is correct, then double knockdown of both *cycA* and *cycB* is expected to generate more severe defects and higher abnormality percentage than the single knockdowns.

4.2 Separase pathway may not be the only mechanism involved in releasing sister-chromatid cohesion druing meiosis

Although the proper separation of both homologous chromosomes and sister chromatids during meiosis requires Separase participation, neither of these two processes were completely inhibited after knockdown of *sse* (Chapter 3.3.3-3.3.4). This is not likely a consequence of inefficient *sse* knockdown because of the following reasons. First of all, qRT-PCR demonstrated that the *sse* mRNA level were decreased dramatically to only 1.2% of that in the wild type flies (Chapter 3.3.1). Second, if the residual amount of mRNA is able to produce a small amount of Separase, this Separase should be able to cause arm separation of sister chromatids in polar bodies though it did not (see below, Chapter 4.5). Then, why are the homologous chromosome and sister chromatid separations finally occuring during meiosis? One possible hypothesis is that another mechanism sharing redundant molecular function with Separase is involved in the stepwise release of sister-chromatid cohesion during meiosis. The prophase pathway that happens during mitosis is a strong candidate (Hauf, et al. 2005; Nishiyama, et al. 2013; Fig 1). Notably, the Shugoshin-PP2A complex is known to protect centromeric regions against cohesin removal by both known prophase pathways (Nishiyama, et al. 2013; Gutierrez-Caballero, et al. 2012; Fig 1). This protection is necessary for the two-round separation of chromosomes during meiosis. To test this hypothesis, knockdown of *sse* together with one of or both of the key components (*plk1* and *wapl*) in the prophase pathways is required.

4.3 The separase target that is responsible for meiotic sister-chromatid cohesion in Drosophila still remains unknown

As mentioned before, Separase is required for the proper separation of both homologous chromosomes and sister chromatids (Chapter 3.3.3), presumably through cleaving the kleisin subunit of Cohesin complex between sister chromatids (Nasmyth and Haering, 2009). However, both our study (Chapter 3.2.2-3.2.3 and 3.4.1) and another study (Urban, et al. 2014) strongly suggest that sister-chromatid cohesion is likely not conducted by the mitosis kleisin Rad21. Then what is the target of Separase during *Drosophila* meiosis? A potential candidate could be C(2)M/Mei-910, which also belongs to the kleisin family and is expressed in meiosis (Schleiffer, et al. 2003; Heidmann, et al. 2004). However, C(2)M had also been identified as one of the components of SC and it does not appear to have a role in sister-chromatid cohesion (Manheim and McKim, 2003; Heidmann, et al. 2004). Interestingly two proteins that are not related to any known Cohesin components, Ord and Solo, had been demonstrated to be essential for sister-chromatid cohesion during *Drosophila* meiosis (Bickel, et al. 1996; Yan, et al. 2010). In the absence of Ord, premature separation of sister chromatids at centromeric regions were observed in female oocytes, indicating Ord is responsible for centromeric sister-chromatid cohesion during meiosis (Bickel, et al. 2002). In addition, Solo was demonstrated to be essential for sister-chromatid cohesion in *Drosophila* (Yan, et al. 2010; Yan and McKee, 2013.). Furthermore, in male meiosis, Solo co-localizes with the common Cohesin backbone protein, SMC1, at centromeres and this co-localization is abolished after the knockdown of Shugoshin (Yan, et al. 2010). These discoveries imply that Solo could be a novel component for Cohesin complex that functions in *Drosophila* meiosis. This matches with our finding that the traditional Cohesin component, CAP and

Rad21, are not required during the process. It is yet unknown whether Ord or Solo are target(s) of Separase or not.

4.4 Pim may not be the only inhibitor of Separase in meiosis

Comparing to *pim* knockdown and/or Pim stabilization, it was found that *sse* knockdown generated the most efficient inactivation of Separase, since mitotic divisions were all arrested at very early stages during embryo development (Chapter 3.3.5 and Fig 6). Pim stabilization together with the knockdown of endogenous *pim* produced similar mitotic phenotypes comparing to *sse* knockdown (Chapter 3.6.3 and Fig 6). However, this double modification generated weaker meiotic phenotypes (Chapter 3.6.1) comparing to those seen in *sse* knockdown (Chapter 3.3.3). This indicates that in $pim^{RNAi5'}$-*GFP*-$pim^{\Delta dk}$ embryos the Separase activity during meiosis is not suppressed as much as that in *sse* knockdown. This could be caused by the incomplete elimination of endogenous Pim and/or the presence of another Separase inhibitory mechanism such as CycB-Cdk1 during meiosis. To test the latter possibility, the interaction between Separase and CycB need to be confirmed and studied in *Drosophila* meiosis first. Then the transgenic flies that expressed both stabilized Pim and modified version of Separase that resists the inhibition of CycB-Cdk1 should be generated. If CycB-Cdk1 does inhibit Separase during meiosis, then we expect that these transgenic flies would exhibit more similar meiotic defects compared to those detected in *sse* knockdown flies instead of $pim^{RNAi5'}$-*GFP*-$pim^{\Delta dk}$ flies.

In summary, our research demonstrates that Pim acts as an inhibitor for Separase in the meiotic sister chromatid separation pathway. The degree of abnormality generated during this pathway is positively related to the level of inhibitory effect exerted on Separase activity.

4.5 Polar body sister chromatid separation depends on Rad21 cleavage by Separase

After the formation of the polar body, the sister chromatid arms of each chromosome gradually separate as time increases. This process is independent from embryo development since it also occurs in the non-fertilized embryos (Chapter 3.1). Subsequent experiments demonstrated that both CAP and Rad21 are essential for centromeric sister-chromatid cohesion in the polar body (Chapter 3.2.4). Further analysis revealed that Rad21 is also responsible for the cohesion at the arm region (Chapter 3.4.2). These observations imply that sister-chromatid cohesion in the polar body is maintained by the Cohesin complex with Rad21 as its kleisin subunit. Since the knockdown of *sse* inhibits the separation of sister chromatid arms in the polar body, the arm cohesion is presumably released through Separase cleavage of Rad21 (Chapter 3.3.4 and 3.4.2). Furthermore, either *pim* knockdown or Pim stabilization leads to the blockage of sister chromatid separation in the polar body as seen in the knockdown of *sse* (Chapter 3.5.4 and 3.6.2). Therefore, Separase activity is regulated by both positive and inhibitory functions of Pim in the polar body. However, unlike meiosis, sister chromatid separation in the polar body is blocked by even the weakest alteration of Separase function through the knockdown of *pim* (Chapter 3.5.4). This implies that Separase activity is very critical for the separation of sister chromatid arms in the polar body. Hence, the Pim-Separase pathway could be the only regulatory mechanism involved in this process.

The centromeric regions of polar body sister chromatids always remain together after the separation of the arms (Chapter 3.1). Considering the fact that Shugoshin was detected at the centromeric regions of sister chromatids in the polar body (Moore, et al. 1998), it is hypothesized that Shugoshin protects centromeric Rad21 from Separase cleavage. If this hypothesis is correct, we would expect to observe completely separated

sister chromatids including the centromeric regions in the polar body after knockdown of *mei-S332* (*shugoshin* in *Drosopihla*). Overall, the mechanisms involved in sister chromatid separation in the polar body are similar to those found in mitosis.

4.6 Separase may have additional cellular functions other than the release of sister chromatids in syncytial mitosis

In *vtd* and *CAP* knockdowns, premature sister chromatid separation at centromeric regions was observed during metaphase of mitosis (Chapter 3.2.5). This observation is consistent with previous findings that both Rad21 and CAP are Cohesin components that are responsible for sister-chromatid cohesion in *Drosophila* mitosis (Vass, et al. 2003; Nasmyth and Haering, 2009). As described before, the embryonic mitotic phenotypes produced by modifications in the Pim-Separase pathway also match with the expectations generated based on the discoveries found in mitosis (Chapter 4.4). The only confusion was found in the mitotic phenotypes exhibited in *sse* and *vtd* double knockdown (Chapter 3.4.3). We expected that without the presence of Rad21, knockdown of *sse* will not generate any effects in mitosis and the mitotic phenotype exhibited in the double knockdown should be similar to that displayed in *vtd* single knockdown. The preliminary experimental results partially match with this expectation since after the double knockdown, the embryonic mitotic cycles exhibited the *vtd* knockdown phenotype that centromeric regions of sister chromatids separated prematurely at metaphase. However, unlike *vtd* single knockdown where the syncytial mitosis go through several cycles, mitosis in the *vtd* and *sse* double knockdown always arrests in the first or second division. Why is mitosis progression blocked even after the separation of sister chromatids? This implies that Separase has additional cellular functions other than just Rad21 cleavage during mitosis. It was known that Separase not only gets inhibited by CycB-Cdk1 but also

blocks the CycB-Cdk1 function during the mitosis of vertebrate cells (Gorr, et al. 2005). If this stays true in *Drosophila* mitosis, then without Separase, CycB-Cdk1 could be over activated and this will lead a failure to increase the tension of microtubules during the metaphase to anaphase transition (Shindo, et al. 2012). Therefore, although the cohesion between sister chromatids no longer exists, without the increase of microtubule tension triggered by CycB-Cdk1 inactivation, sister chromatids segregation is still not going to progress properly in mitosis.

4.7 The loss of arm cohesion did not occur until metaphase in embryonic mitotic cycles

During mitosis, both prophase pathway and anaphase pathway contribute to the release of sister-chromatid cohesion (Waizenegger, et al. 2000). The prophase pathway disassembles the Cohesin complex on the sister chromatid arms during prophase and prometaphase (Waizenegger, et al. 2000). Therefore, we expect that the arms of sister chromatids are separated before metaphase. However, according to our preliminary experimental results, sister chromatid arms can be either separated or unseparated during metaphase (Chapter 3.1). Furthermore, this arm separation seems to occur at the same time among all of the mitosis in a single embryo. This can be explained by either one of the following possibilities. One possible explanation is that the prophase pathway does not occur in the early embryonic mitotic cycles. The loss of cohesion at sister chromatid arm regions observed in metaphase is only caused by the abrupt activation of Separase just before the onset of anaphase (Yaakov, et al. 2012). Another possibility is that although prophase happens, the loss of Cohesin complex during the prophase pathway is not enough to trigger the separation of sister chromatid arms. Furthermore, it is also not enough to tiger sister chromatid separation in the case of a prolongued mitotic arrest caused by *sse* knockdown (Chapter 3.3.5). This matches with the previous finding that the

prophase pathway leads to the disassociation of most, but not all, of the Cohesin complexes on sister chromatid arms (Waizenegger, et al. 2000; Nishiyama, et al. 2013). These remaining Cohesin complexes are able to hold the sister chromatid arms together until presumably anaphase onset. To determine which hypothesis is correct, embryos could be stained with antibodies that against one or more Cohesin component(s). If the prophase pathway does occur during early embryonic mitotic cycles, we expect to observe obvious decrease in the concentration of Cohesin complex along the sister chromatid arms from prophase to metaphase.

4.8 Number of crossovers may affect the separation of sister chromatid arms after the resolution of chiasmata during meiosis

During meiosis, the cohesion between sister chromatid arms is released after metaphase I in order to allow the proper segregation of homologous chromosomes (Kudo, et al. 2006). We expected that the sister chromatid arms of each homologous chromosome would separate from each other after the release of arm cohesion (Fig 4). However, it was observed that the arm regions of sister chromatids were either separated or unseparated after metaphase I (Fig 5). Furthermore, the time of the arm region separation is not predictable. They could separate as early as anaphase I where the sister chromatid arm cohesion is just released or stay together until metaphase II just before the separation of sister chromatids. These observations do not match with the expectation (Fig 5).

A potential explanation for these observations could lay in the number of crossovers formed between homologous chromatids. If there is only one crossover point, then the exchangeable region of homologous chromatid starts from the point of crossover to the terminal of the arm. As shown in Fig 24A, after the exchange, the original sister

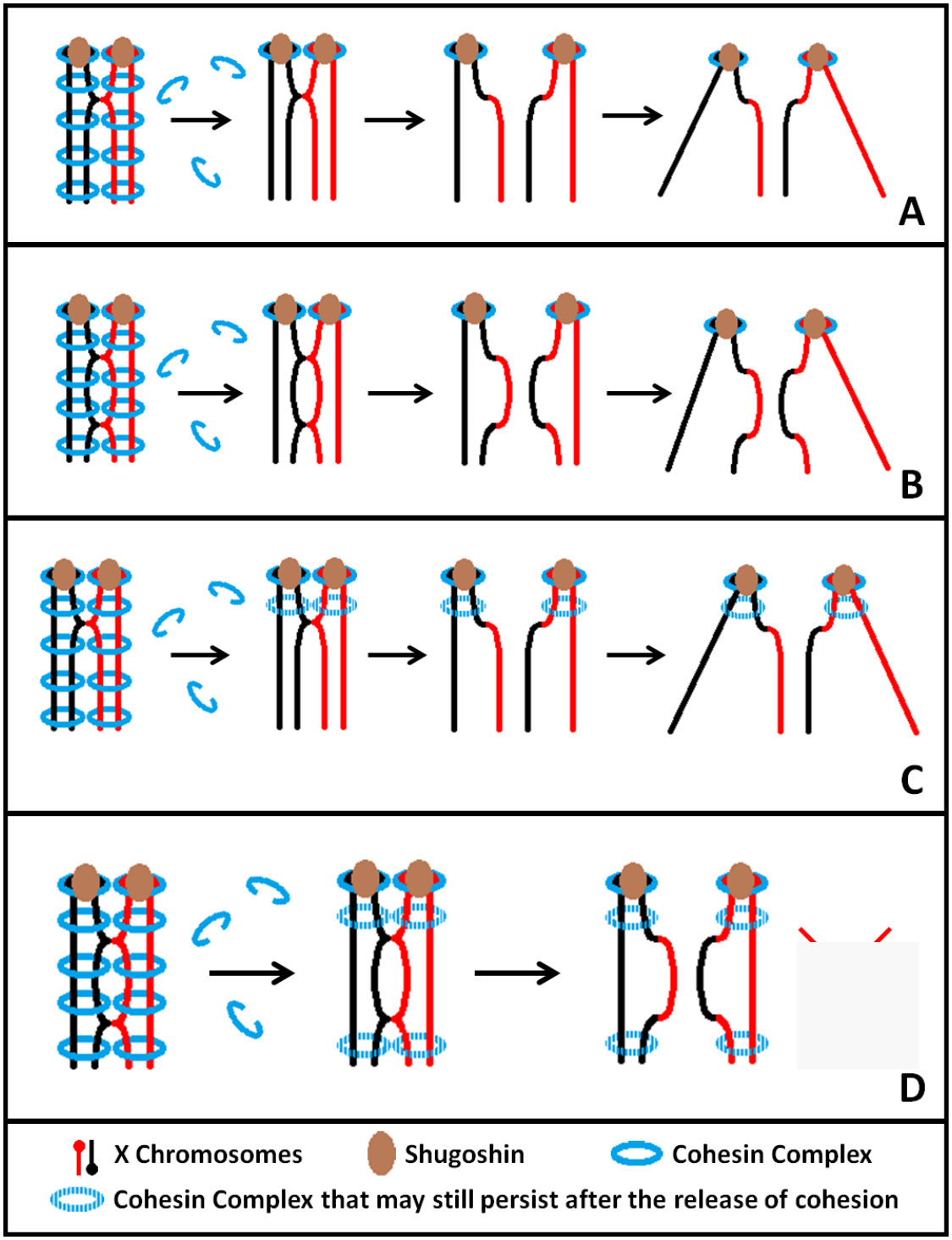

Fig 24. Introduction of the segregation of homologous chromosome with either one (A and C) or two (B and D) crossovers.
(X chromosomes that only have chromosome arms on one side are displayed in this figure as an example. For convenience, microtubules and the changes in chromosome orientation caused by the stretching force of microtubules shown in Fig 4 were not exhibited in this figure).

chromatids (having the same color in the figure), from the crossover point to the end of the arm, now become non-sister chromatids that also known as homologous chromatids. However, at this point, these homologous chromatids are still bound to each other by Cohesin complex. In this case, after the segregation of homologous chromosomes triggered by the disassembly of Cohesin complex, the arm region of sister chromatids will be completely separated from each other and drift randomly in the cytoplasm (Fig 24A). However, if there are two crossovers on the same side of chromosomes, then the exchangeable homologous sister chromatid regions are restricted between the two crossover sites (Fig 24B). Hence, the terminals of sister chromatids are not affected by crossovers and still remain close together. This orientation of sister chromatids with unseparated arms, in theory, could be maintained after the segregation of homologous chromosomes. Nonetheless, since the cohesion force at the arm region has already been lost at this stage, sister chromatid arms are more likely to drift apart from each other instead of staying together (Fig 24B). Therefore, it is hypothesized that after the separation of homologous chromosomes, there are still residual amounts of Cohesin complex left between sister chromatid arms (Fig 24C and 24D). This hypothesis seems go against the already established model that sister chromatid arm cohesion has to be released for the resolution of chiasmata and proper segregation of homologous chromosomes (Kudo, et al. 2006). However, the resolution of chiasmata just requires removal of the cohesion between the exchanged chromatid region but not along the entire sister chromatid arm region (Fig 24C and 24D). Hence it is possible that the cohesion between the terminals of sister chromatids still exists after the resolution of chiasmata in the situation where two crossovers were formed (Fig 24D). However, the terminals have

to be separated for chiasmata resolution when there is only one crossover along the entire chromatid arm (Fig 24C).

In sum, it is hypothesised that the separation of sister chromatid arms after the resolution of chiasmata may depend on two things. One is the number of crossovers formed on the same side of homologous chromosomes. The other is the Cohesin complex remaining on the sister chromatid arms that do not interfere the separation of homologous chromosomes. Nonetheless, this model is based on assumptions and can not explain why the arm cohesion is only released at the cross over regions but not all along the sister chromatid arms. To test whether this model is correct, it is best to immuno-stain the Cohesin complex and observe its localization after metaphase I. However, it is not known yet whether the regular Cohesin complex components are required for the sister-chromatid cohesion during *Drosophila* meiosis (Chapter 4.1.1). Therefore, the priority should be given to the investigation of the protein that is responsible for meiotic sister-chromatid cohesion.

4.9 Conclusion

In our research, we demonstrated that Separase is required for the proper separation of homologous chromosomes and sister chromatids during *Drosophila* meiosis. This activity of Separase is inhibited by Pim and, possibly, CycB. However the Separase substrate that is responsible for sister-chromatid cohesion during meiosis still remains unknown. No evidence was found to support the idea that meiotic sister-chromatid cohesion is maintained by the mitotic kleisin Rad21 or the common Cohesin component CAP (SMC3). This further brings the importance of the Cohesin complex during meiosis into question. It is also revealed that in the polar body, sister-chromatid cohesion is maintained by Rad21 that presumably acts as the kleisin subunit of the Cohesin complex. This cohesion is able to be released by Separase that is regulated by both positive and inhibitory functions of Pim.

REFERENCES

- Adams, M.D. et al. 2000. The genome sequence of Drosophila melanogaster. Science, Vol 287, Issue 5461, 2185-2195.

- Anderson, D.E. et al. 2002. Condensin and cohesin display different arm conformations with characteristic hinge angles. Journal of Cell Biology, Vol. 156, Issue 3, 419-424.

- Batiha, O. 2013. Regulation of the Anaphase Promoting Complex/Cyclosome in Drosophila female meiosis. PhD thesis, University of Windsor.

- Bickel, S.E. et al. 1996. Identification of ORD, a Drosophila protein essential for sister-chromatid cohesion. EMBO Journal, Vol 15, Issue 6, 1451-1459.

- Bickel, S.E. et al. 2002. The sister-chromatid cohesion protein ORD is required for chiasma maintenance in Drosophila oocytes. Current Biology, Vol 12, Issue 11, 925-929.

- Brand, A.H. and Perrimon, N. 1993. Targeted Gene-Expression as a Means of Altering Cell Fates and Generating Dominant Phenotypes. Development, Vol 118, Issue 2, 401-415.

- Buonomo, S.B.C. et al. 2000. Disjunction of homologous chromosomes in meiosis I depends on proteolytic cleavage of themeiotic cohesin Rec8 by separin. Cell, Vol 103, Issue 3, 387-398.

- Ciosk, R. et al. 1998. An ESP1/PDS1 complex regulates loss of sister-chromatid cohesion at the metaphase to anaphase transition in yeast. Cell, Vol 93, Issue 6, 1067-1076.

- CohenFix, O. et al. 1996. Anaphase initiation in Saccharomyces cerevisiae is controlled by the APC-dependent degradation of the anaphase inhibitor Pds1p. Genes & Development, Vol 10, Issue 24, 3081-3093.

- Dernburg, A.F. Chapter 2: In situ hybridization to somatic chromosomes. In Sullivan, W., Ashburner, M. and Hawley R.S. (Ed.) Drosophila Protocols, 2000, 30-41.

- Dhaliwal, R.K. 2011. Roles of Cyclin A and Cyclin B in Drosophila female meiosis. MSc. thesis, University of Windsor.

- Eichinger, C.S. et al. 2013. Disengaging the Smc3/kleisin interface releases cohesin from Drosophila chromosomes during interphase and mitosis. EMBO Journal, Vol 32, Issue 5, 656-665.

- Foe, V.E. et al. 1993. Mitosis and Morphogenesis in the Drosophila Embryo: Point and Counterpoint . In: Bate, M. and Martinez Arias, A. (Ed.), the development of Drosophila melanogaster. Cold Spring Harbor Laboratories: Long Island NY, 149-300.

- Fraune, J. et al. 2012. The mammalian synaptonemal complex: Protein components, assembly and role in meioticrecombination. Experimental Cell Research, Vol 318, Issue 12, 1340-1346.

- Gandhi, R. et al. 2006. Human Wapl is a cohesin-binding protein that promotes sister-chromatid resolution in mitotic prophase. Current Biology, Vol 16, Issue 24, 2406-2417.

- Gerlich, D. et al. 2006. Live-cell imaging reveals a stable cohesin-chromatin interaction after but not before DNA replication. Current Biology, Vol 16, Issue 15, 1571-1578.

- Gorr, I.H. et al. 2005. Mutual inhibition of separase and Cdk1 by two-step complex formation. Molecular Cell, Vol 19, Issue 1, 135-141.

- Guacci, V. et al. 1997. A Direct Link between Sister-chromatid cohesion and Chromosome Condensation Revealed through the Analysis of MCD1 in S. cerevisiae. Cell, Vol. 91, Issue1, 47-57.

- Gutierrez-Caballero, C. et al. 2012. Shugoshins: from protectors of cohesion to versatile adaptors at the centromere. Trends in Genetics, Vol 28, Issue 7, 351-360.

- Haering, C.H. et al. 2002. Molecular architecture of SMC proteins and the yeast cohesin complex. Molecular Cell, Vol. 9, Issue 4, 773-788.

- Haering, C.H. et al. 2004. Structure and stability of cohesin's Smc1-kleisin interaction. Molecular Cell, Vol 15, Issue 6, 951-964.

- Hagting, A. et al. 2002. Human securin proteolysis is controlled by the spindle checkpoint and reveals when the APC/C switches from activation by Cdc20 to Cdh1. Journal of Cell Biology, Vol 157, Issue 7, 1125-1137.

- Hauf, S. et al. 2005. Dissociation of cohesin from chromosome arms and loss of arm cohesion during early mitosis depends on phosphorylation of SA2. PLOS Biology, Vol 3, Issue 3, 419-432.

- Heidmann, D. et al. 2004. The Drosophila meiotic kleisin C(2)M functions before the meiotic divisions. Chromosoma, Vol 113, Issue 4, 177-187.

- Heifetz, Y. et al. 2001. Ovulation triggers activation of Drosophila oocytes. Developmental Biology, Vol 234, Issue 2, 416-424.

- Hellmuth, S. et al. 2014. PP2A delays APC/C-dependent degradation of separase-associated but not free securin. EMBO Journal, Vol 33, Issue 10, 1134-1147.

- Herzig, A. et al. 2002. Proteolytic cleavage of the THR subunit during anaphase limits Drosophila separase function. Genes & Development, Vol 16, Issue 18, 2443-2454.

- Heyting, C. 1996. Synaptonemal complexes: Structure and function. Current Opinion in Cell Biology, Vol 8, Issue 3, 389-396.

- Holland, A.J. and Taylor, S.S. 2006. Cyclin-B1-mediated inhibition of excess separase is required for timely chromosome disjunction. Journal of Cell Science, Vol 119, Issue 16, 3325-3336.

- Holland, A.J. et al. 2007. Protein phosphatase 2A and separase form a complex regulated by separase autocleavage. Journal of Biological Chemistry, Vol 282, Issue 34, 24623-24632.

- Hong, A. et al. 2003. The p27 (cip/kip) ortholog dacapo maintains the Drosophila oocyte in prophase of meiosis I. Development, Vol 130, Issue 7, 1235-1242.

- Horner, V.L. and Wolfner, M.F. 2008. Mechanical stimulation by osmotic and hydrostatic pressure activates Drosophila oocytes invitro in a calcium-dependent manner. Developmental Biology, Vol 316, Issue 1, 100-109.

- Hornig, N.C.D. et al. 2002. The dual mechanism of separase regulation by securin. Current Biology, Vol 13, Issue 12, 973-982.

- Hornig, N.C.D. and Uhlmann, F. 2004. Preferential cleavage of chromatin-bound cohesin after targeted phosphorylation by Polo-like kinase. EMBO Journal, Vol 23, Issue 15, 3144-3153.

- Hsieh, T. and Brutlag, D. 1979. Sequence and sequence variation within the 1.688g/cm^3 satellite DNA of Drosophila-melanogaster. Journal of molecular biology, Vol 135, Issue 2, 465-481.

- Jacobs, H.W. et al. 2001. A complex degradation signal in Cyclin A required for G_1 arrest, and a C-terminal region for mitosis. EMBO Journal, Vol 20, Issue 10, 2376-2386.

- Jager, H. et al. 2001. Drosophila separase is required for sister chromatid separation and binds to PIM and THR. Genes & Development, Vol 15, Issue 19, 2572-2584.

- Jallepalli, P.V. and Lengauer, C. 2001. Chromosome segregation and cancer: Cutting through the mystery. Nature Reviews Cancer, Vol. 1, Issue 2, 109-117.

- Jang, J.K. et al. 2003. Relationship of DNA double-strand break to synapsis in Drosophila. Journal of Cell Science, Vol 116, Issue 15, 3069-3077.

- Ji, J.Y. et al. 2005. Genetic interactions between Cdk1-CyclinB and the separase complex in Drosophila. Development, Vol 132, Issue 8, 1875-1884.

- Katis, V.L. et al. 2010. Rec8 Phosphorylation by Casein Kinase 1 and Cdc7-Dbf4 Kinase Regulates Cohesin Cleavage by Separase during Meiosis. Developmental Cell, Vol 18, Issue 3, 397-409.

- Kitajima, T.S. et al. 2004. The conserved kinetochore protein shugoshin protects centromeric cohesion during meiosis. Nature, Vol 427, Issue 6974, 510-517.

- Kitajima, T.S. et al. 2006. Shugoshin collaborates with protein phosphatase 2A to protect cohesin. Nature, Vol 441, Issue 7089, 46-52.

- Kudo, N.R. et al. 2006. Resolution of chiasmata in oocytes requires separase-mediated proteolysis. Cell, Vol 126, Issue 1, 135-146.

- Kulemzina, I. et al. 2012. Cohesin rings devoid of Scc3 and Pds5 maintain their stable association with the DNA. Plos Genetics, Vol. 8, Issue 8, e1002856.

- Lake, C.M. and Hawley, R.S. 2012. The Molecular Control of Meiotic Chromosomal Behavior: Events in Early Meiotic Prophase in Drosophila Oocytes. Annual Review of Physioogy, Vol 74, 425-451.

- Leismann, O. et al. 2000. Degradation of Drosophila PIM regulates sister chromatid separation during mitosis. Genes & Development, Vol 14, Issue 17, 2192-2205.

- Leismann, O. and Lehner, C.F. 2003. Drosophila securin destruction involves a D-box and a KEN-box and promotes anaphase inparallel with cyclin A degradation. Journal of Cell Science, Vol 116, Issue 12, 2453-2460.

- Losada, A. et al. 2000. Identification and characterization of SA/Scc3p subunits in the Xenopus and human cohesin complexes. Journal of Cell Biology, Vol 150, Issue 3, 405-416.

- Manheim, E.A. and McKim, K.S. 2003. The synaptonemal complex component C(2)M regulates meiotic crossing over in Drosophila. Current Biology, Vol 13, Issue 4, 276-285.

- Mazumdar, A. and Mazumdar, M. 2002. How one becomes many: blastoderm cellularization in Drosophila melanogaster. Bioessays, Vol 24, Issue 11, 1012-1022.

- McGuire, S.E. et al. 2004. Gene expression systems in Drosophila: a synthesis of time and space. Trends in Genetics, Vol 20, Issue 8, 384-391.

- McKee, B.D. 2004. Homologous pairing and chromosome dynamics in meiosis and mitosis. Biochimica et Biophysica Acta-gene Structure and Expression, Vol. 1677, Issue 1-3, 165-180.

- Mehrotra, S. and McKim, K.S. 2006. Temporal analysis of meiotic DNA double-strand break formation and repair in Drosophilafemales. PLOS Genetics, Vol 2, Issue 11, 1883-1897.

- Michaelis, C. et al. 1997. Cohesins: Chromosomal proteins that prevent premature separation of sister chromatids. Cell, Vol. 91, Issue 1, 35-45.

- Molnar, M. et al. 1995. The Rec8 gene of Schizosaccharomyces-Pombe is involved in linear element of formation, chromosome-pairing and sister-chromatid cohesion during meiosis. Genetics, Vol. 141, Issue 1, 61-73.

- Moore, D.P. et al. 1998. The cohesion protein MEI-S332 localizes to condensed meiotic and mitotic centromeres until sister chromatids separate. Journal of Cell Biology, Vol 140, Issue 5, 1003-1012.

- Nasmyth, K. 2001. Disseminating the genome: Joining, resolving and separating sister chromatids during mitosis and meiosis. Annual Review of Genetics, Vol.35, 673-745.

- Nasmyth, K. 2002. Segregating sister genomes: the molecular biology of chromosome separation. Science, Vol 297, Issue 5581, 559-565.

- Nasmyth, K. and Haering, C.H. 2009. Cohesin: Its roles and mechanisms. Annual Review of Genetics, Vol. 43, 525-558.

- Nishivama, T. et al. 2010. Sororin Mediates Sister-chromatid cohesion by Antagonizing Wapl. Cell, Vol 143, Issue 5, 737-749.

- Nishiyama, T. et al. 2013. Aurora B and Cdk1 mediate Wapl activation and release of acetylated cohesin from chromosomes by phosphorylating Sororin. Proceedings of the National Academy of Sciences of the United States of America, Vol 110, Issue 33, 13404-13409.

- Oliveira, R.A. et al. 2010. Cohesin cleavage and Cdk inhibition trigger formation of daughter nuclei. Nature Cell Biology, Vol 12, Issue 2, 185-193.

- Page, A.W. and Orr-Weaver, T.L. 1997a. Stopping and starting the meiotic cell cycle. Current Opinion in Genetics & Development, Vol 7, Issue 1, 23-31.

- Page, A.W. and Orr-Weaver, T.L. 1997b. Activation of the meiotic divisions in Drosophila oocytes. Developmental Biology, Vol 183, Issue 2, 195-207.

- Pesin, J.A. and Orr-Weaver, T.L. 2007. Developmental role and regulation of cortex, a meiosis-specific anaphase-promoting complex/cyclosome activatior. PLOS Genetics, Vol 3, Issue 11, 2208-2220.

- Peters, J.M. 2002. The anaphase-promoting complex: proteolysis in mitosis and beyond. Molecular Cell, Vol 9, Issue 5, 931-943.

- Petronczki, M. et al. 2003. Un menage a quatre: The molecular biology of chromosome segregation in meiosis. Cell, Vol 112, Issue 4, 423-440.

- Riparbelli, M.G. and Callaini, G. 2005. The meiotic spindle of the Drosophila oocyte: the role of centrosomin and the central aster. Journal of Cell Science, Vol 118, Issue 13, 2827-2836.

- Sakuno, T. and Watanabe, Y. 2009. Studies of meiosis disclose distinct roles of cohesion in the core centromere and pericentromeric regions. Chromosome Research, Vol 17, Issue 2, 239-249.

- Schleiffer, A. et al. 2003. Kleisins: A superfamily of bacterial and eukaryotic SMC protein partners. Molecular Cell, Vol 11, Issue 3, 571-575.

- Schmekel, K. and Daneholt, B. 1995. The central region of the synaptonemal complex revealed in 3 dimensions. Trends in Cell Biology, Vol 5, Issue 6, 239-242.

- Shindo, N. et al. 2012. Separase sensor reveals dual roles for separase coordinating Cohesin cleavage and Cdk1 inhibition. Developmental Cell, Vol 23, Issue 1, 112-123.

- Sigrist, S. et al. 1995. Exit from mitosis is regulated by Drosophila Fizzy and the sequential destruction of Cyclin-A, Cyclin-B and Cyclin-B3. EMBO Journal, Vol 14, Issue 19, 4827-4838.

- Stemmann, O. et al. 2001. Dual inhibition of sister chromatid separation at metaphase. Cell, Vol 107, Issue 6, 715-726.

- Stiffler, L.A. et al. 1999. Cyclin A and B functions in the early Drosophila embryo. Development, Vol 126, Issue 23, 5505-5513.

- Stratmann, R. and Lehner, C.F. 1996. Separation of sister chromatids in mitosis requires the Drosophila pimples product, a protein degraded after the metaphase anaphase transition. Cell, Vol 84, Issue 1, 25-35.

- Swan, A. and Schupbach, T. 2005. Drosophila female meiosis and embryonic syncytial mitosis use specialized Cks and CDC20 proteins for cyclin destruction. Cell Cycle, Vol 4, Issue 10, 1332-1334.

- Swan, A. and Schupbach, T. 2007. The Cdc20(Fzy)/Cdh1-related protein, Cort, cooperates with Fzy in cyclin destruction and anaphase progression in meiosis I and II in Drosophila. Development, Vol 134, Issue 5, 891-899.

- Tavosanis, G. et al. 1997. Essential role for gamma-tubulin in the acentriolar female meiotic spindle of Drosophila. EMBO Journal, Vol 16, Issue 8, 1809-1819.

- Telenius, H. et al. 1992. Degenerate oligonucleotide-primed PCR - general amplification of target DNA by a single degenerate primer. Genomics, Vol 13, Issue 3, 718-725.

- Tessie M.Ng, et al. 2009. Pericentromeric sister-chromatid cohesion promotes kinetochore biorientation. Molecular Biology of the Cell, Vol. 20, Issue 17, 3818-3827.

- Uhlmann, F. et al. 2000. Cleavage of cohesin by the CD clan protease separin triggers anaphase in yeast. Cell, Vol 103, Issue 3, 375-386.

- Urban, E. et al. 2014. The Cohesin Subunit Rad21 is Required for Synaptonemal Complex Maintenance, but not Sister-chromatid cohesion, during Drosophila Female Meiosis. PLOS Genetics, Vol 10, Issue 8, e1004540.

- Vass, S. et al. 2003. Depletion of Drad21/Scc1 in Drosophila cells leads to instability of the Cohesin Complex and disruption of mitotic progression. Current Biology, Vol 13, Issue 3, 208-218.

- Visintin, R. et al. 1997. CDC20 and CDH1: A family of substrate-specific activators of APC-dependent proteolysis. Science, Vol 278, Issue 5337, 460-463.

- Waizenegger, I.C. et al. 2000. Two distinct pathways remove mammalian cohesin from chromosome arms in prophase and from centromeres in anaphase. Cell, Vol 103, Issue 3, 399-410.

- Waizenegger, I.C. et al. 2002. Regulation of human separase by securin binding and autocleavage. Current Biology, Vol 12, Issue 16, 1368-1378.

- Wang, C. et al. 1994. Genetics of Nanos Localization in Drosophila. Developmental Dynamics, Vol 199, Issue 2, 103-115.

- Warren, W.D. et al. 2000. Drad21, a Drosophila rad21 homologue expressed in S-phase cells. Gene, Vol 250, Issue 1-2, 77-84.

- Yaakov, G. et al. 2012. Separase Biosensor Reveals that Cohesin Cleavage Timing Depends on Phosphatase PP2A(Cdc55) Regulation. Developmental Cell, Vol 23, Issue 1, 124-136.

- Yan, R.H. et al. 2010. SOLO: a meiotic protein required for centromere cohesion, coorientation and SMC1 localization in Drosophila melanogaster. Journal of Cell Biology, Vol 188, Issue 3, 335-349.

- Yan R.H. and McKee, B.D. 2013. The cohesion protein SOLO associates with SMC1 and is required for synapsis, recombination, homolog bias and cohesion and pairing of centromeres in Drosophila meiosis. PLOS Genetics, Vol 9, Issue 7, e1003637.

- Zhang, J. et al. 2014. Molecular mechanisms of homologous chromosome pairing and segregation in plants. Journal of Genetics and Genomics, Vol 41, Issue 3, 117-123.

- Zou, H. et al. 1999. Identification of a vertebrate sister-chromatid separation inhibitor involved in transformation and tumorigenesis. Science, Vol 285, Issue 5426, 418-422.

APPENDIX A: COPYRIGHT PERMISSION

from: Andrew Swan <aswan@uwindsor.ca>

to: guoz@uwingmail.uwindsor.ca

date: Wed, Jan 21, 2015 at 1:35 PM

subject: copyright permission

Dear Zhihao,

A part of the pending publication:

"Distinct Roles for Securin, Separase and the cohesin complex in female meiosis, polar body formation and syncytial mitotic divisions of Drosophila"

is found in the result part (Chapter 3) of the master's thesis of Zhi Hao Guo. As the supervisor and the corresponding author of the publication, I give the permission to Zhi Hao Guo, as one of the authors, to use the information of our publication in his master's thesis.

-
Andrew Swan
Associate Professor
Department of Biological Sciences
Room 302 Biology Bldg.
University of Windsor
Windsor, ON N9B 3P4
Canada
(519) 253 3000 ext. 2730

VITA AUCTORIS

NAME:	Zhi Hao Guo
PLACE OF BIRTH:	Nanjing, China
YEAR OF BIRTH:	1988
EDUCATION:	B.Sc. in Biology and Biotechnology [H] University of Windsor Windsor, Ontario 2010
	M.Sc. in Biological Sciences University of Windsor, Windsor, Ontario 2014